5-2011

IN-WHEEL COUPLED SUSPENISON AND DRIVE SYSTEM FOR ATTITUDE CONTROL AND VEHICLE PROPULSION

Robert Clippard
Clemson University, robert.clippard@gmail.com

IN-WHEEL COUPLED SUSPENSION AND DRIVE SYSTEM FOR ATTITUDE CONTROL AND VEHICLE PROPULSION

A Dissertation
Presented to
the Graduate School of
Clemson University

In Partial Fulfillment
of the Requirements for the Degree
Doctor of Philosophy
Automotive Engineering

---

by
Robert Morris Clippard
May 2011

Accepted by:
Dr. John Ziegert, Committee Chair
Dr. Paul Venhovens
Dr. Ardalan Vahidi
Dr. Todd Hubing

Abstract

The automotive marketplace is a volatile and dynamic system driven by consumer desires, marketing, fuel prices, technology, and legislation. Recently many of these factors have culminated in a common effort to encourage hybrid and electric vehicle development. The technology for electric vehicles has finally found enough maturity to be implemented into consumer based vehicles from hybrid SUVs to high performance sports cars. This expansion in available propulsion systems and vehicle architectures has spurred research and development into new and novel approaches for propulsion as well as systems to provide increased ride comfort.

This work presents a dual electric motor drive system that incorporates a mechanism that allows not only longitudinal actuation of the vehicle, but also low frequency vertical actuation of the vehicle. The system is able to achieve this by coupling two motors per wheel and combining them with a new kinematic mechanism that facilitates dual degree of freedom actuation with coupled motors. By utilizing two motors coupled together to actuate the two degrees of freedom, more efficient utilization of resources is possible. Rather than having a motor that provides longitudinal motion and another that provides vertical actuation, the system uses two motors coupled together to provide both. When one degree of freedom doesn't require actuation, the motors can be utilized to provide higher performance in the other degree of freedom.

This system is designed, modeled, and actually converted into a prototype design throughout the entirety of this work. Initial conceptual modeling and performance metric definition occurs in a kinematic analysis of a basic mechanism. This is then developed into a more complex three dimensional model, and finally converted into physical hardware. In parallel to the hardware development, the controller that allows the system to operate is also explored. From actuating a single degree of freedom to a linearized coupling algorithm that allows both degrees of freedom to be controlled independently and simultaneously, the control system evolves into a functioning system.

Dedication

Dedicated to my loving family and friends, without their support I could not pursue my dreams.

In loving memory of my father

Table of Contents

Table of Figures

Introduction

This work presents a novel design for a coupled dual in-wheel electric drive and suspension system. The coupled dual motor drive design allows for the system to actuate the rotational degree of freedom of the wheel for both braking and acceleration as well as the vertical degree of freedom of the suspension in order to provide attitude control of the vehicle body. While there are systems in place to provide both modes of actuation such as the Michelin active wheel; none of the current systems couple the actuators together to take full advantage of their available power. In the proposed system, both motors can be utilized to actuate a single degree of freedom, thus providing an improved system response; or they can be utilized to provide actuation for both DOFs simultaneously when the single DOF demands are reduced. As an added advantage the motors have the ability to be utilized for regeneration during braking, damping, and also during vertical actuation with the appropriate controls and hardware.

The system is conceptualized around the recent influx of city based vehicles, small, lightweight cars that can take advantage of hybrid and electric drive technology, and can be used efficiently and effectively in densely populated metropolitan centers. These smaller vehicles don't have the physical space for the large crash absorption zones that exist in many modern vehicles. The packaging of the drive system also removes valuable interior space from designers. The system proposed here moves the propulsion system inside the dead space that exists inside a wheel. It also moves the

majority of the power plant weight to the four corners of the vehicle were it can be shed during accidents reducing the kinetic energy that puts the passengers at risk.

The dual electric drive and suspension, or DEDS, supplies a new method for propulsion and attitude control in vehicles. It reduces the interior space that is consumed by present propulsion technology opening the door for designers to explore an entirely new approach to a vehicle platform. Consumers of these vehicles will be able to take advantage of extended range, a reduction in fuel consumption, and an increase in stability due to the addition of attitude control and regeneration technology.

In order for this system to be feasible, it had to be built upon current technological advances that have made fully electric and hybrid electric vehicles feasible for production. The dual electric drive and suspension utilizes advances from electric motors and drives, drive and suspension controls, regeneration systems from electric vehicles, and also attitude control methods that have been researched for increases in vehicle stability and dynamics. Each of these branches of technological advancement was required for the system's successful conceptualization, design, development, and testing.

Both the simulation model and the hardware were created in parallel to ensure that the model closely represents a system that is physically feasible with available parts while also serving as a hypothetical test bench to evaluate design tradeoffs and potential performance goals. The vehicle that the system is designed for is purely conceptual in

nature and tips the scales at 900kg. A semi-trailing arm rear suspension was chosen for packaging of the drives in the rear of the vehicle. A leading arm suspension has been explored to ensure that the system can be applied to a steering axle, but only in a packaging sense. The steering axle configuration was not explored dynamically. What follows is an exploration of the conceptualization of the device, the technology on which the system relies, and then the modeling and implementation of the system in a quarter vehicle model.

1 System Description

Electric drive systems and force generating suspensions are not new concepts. There are many cases in which one or both systems have been employed in consumer vehicles to provide lower fuel consumption and/or increased ride comfort. However, these systems are typically applied independently and not in a coupled package like the one described here. Some may argue that Michelin's active wheel is a coupled package, but it utilizes two independent actuators to provide the vertical and rotational actuation separately while being packaged into a single assembly that fits inside the wheel. The dual electric drive and suspension, DEDS provides both the longitudinal actuation of the vehicle as well as the vertical actuation of the suspension utilizing the same two electric motors to actuate both degrees of freedom.

There are many benefits to utilizing two actuators in a single coupled system. The first benefit is that the two motors can be smaller, lighter, and lower cost when they are utilized in the coupled system than if they are sized to actuate individual DOFs. Another major benefit from this combined utilization of the motors allows for optimization of the drive system to provide vertical actuation when the torque demand for rotational actuation is reduced during less than extreme operating conditions. The actuators can also be utilized for regeneration, thus extending the range of fully electric vehicles and reducing the impact of the vertical actuation power consumption that is typical of active style suspensions. The DEDS has the potential to regenerate power during two different

operations. During braking, both motors can be utilized as generators to slow the vehicle and recharge the system. Also during normal driving the electric motors can replace or supplement the damper by extracting some of the energy contained in the relative velocity of the vehicle body mass and the wheel mass. A three dimensional conceptual model of the system is shown in Figure 1-1.

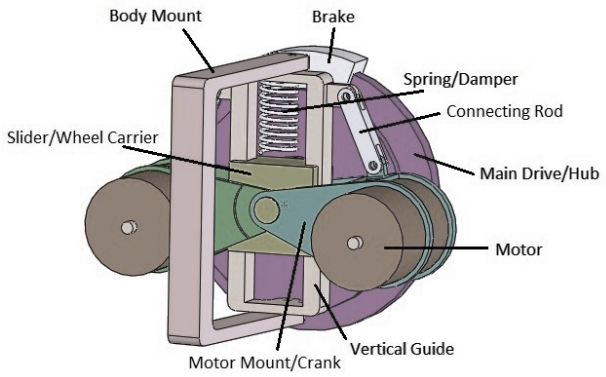

Figure 1-1 Linear guide DEDS system prototype design

1.1 System Layout

The system consists of a vertical guide that constrains the motion of the wheel carrier relative to the vehicle body. The motor mounts attach both motors to the wheel carrier and provide a pivot for the connecting rods to the vehicle body. The two motor mounts allow the motors to pivot around the center of the wheel carrier. This provides a constant drive tension or gear engagement depending on what drive connection mechanism is utilized. The motors are constrained from simply rotating around the main drive gear by the two connecting rod links that connect them to the vehicle body. The motors are also connected to the wheel via the main drive gear. This main drive

gear is free to spin around the wheel carrier and is connected directly to the wheel and tire assembly.

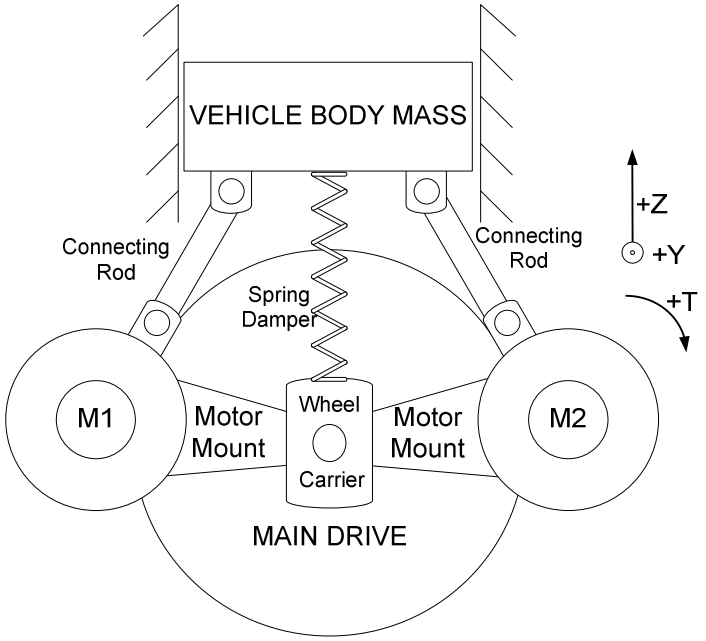

Figure 1-2 Mechanism layout

The planar kinematic layout is shown in Figure 1-2. In the three dimensional model the wheel center is shown as a slider moving along a linear guide. When the system is converted to the planar mechanism the wheel center was connected to the ground and the vehicle body became constrained by a slider mechanism. This was done to simulate the system actuating the mass of the vehicle while the wheel was on the ground. The two degrees of freedom of the planar kinematic model are the rotation of the main drive and the vertical position of the vehicle body. The basic mechanism is recognizable as a dual slider-crank mechanism with two cranks (motor mounts) and two connecting rods connected to a single slider (vehicle body). Their positions are coupled and driven

by either motor's position around the main drive gear. Since the drive gear is free to rotate the vertical position of the vehicle body can be found by using the difference in the two motors rotational position β_{M1} and β_{M2}. This difference is then multiplied by a constant of mechanical advantage C_{lift}. C_{lift} is a product of the mechanism geometry and can be adjusted by changing the connection locations of the connecting rods. Unlike the vertical degree of freedom, the rotational degree of freedom is driven by the average velocity of the two motors ω_{M1} and ω_{M2} multiplied by the gear ratio between the motors and the main drive system *n*. These relationships are described in equations (1.1) and (1.2).

$$Z_{Vehicle} = C_{lift}(\beta_{M1} - \beta_{M2}) \tag{1.1}$$

$$\omega_{drive} = n\left(\frac{\omega_{M1} + \omega_{M2}}{2}\right) \tag{1.2}$$

Of course during dynamic operations the concern is not focused on absolute position of the system but rather the relative position, velocity, and acceleration between the vehicle body and the wheel carrier along with the rotational velocity and torque on the main drive gear. As such the relationships in equations (1.1) and (1.2) can be expanded to include the torque of each motor and their relationship with the actuation force and wheel torque. Equation (1.3) represents the actuation force of the suspension which is a product of the difference in torques between the two motors and B_{lift}; where B_{lift} is a function of both design and vertical position. Equation (1.4) represents the resulting

torque on the wheel as a product of the sum of the torques of the two motors and the gear ratio between the motors and the main drive gear.

$$F_a = B_{lift}(T_{M1} - T_{M2}) \tag{1.3}$$

$$T_W = n(T_{M1} + T_{M2}) \tag{1.4}$$

The spring supports the entire body weight when the body is in the nominal ride height position. In order to actuate the vehicle mass vertically, F_a must be nonzero. If F_a is a positive force the distance between the wheel center and the vehicle mass is lengthened, and if it is negative the length will decrease. For the rotational degree of freedom to be excited the torque T_w must be nonzero. A positive torque will results in acceleration or a constant velocity while a negative torque will exert a braking effort on the wheel.

1.2 Modes of Operation

Using these simple relationships the system's operation can be described. As a coupled vehicle suspension and drive the DEDS must be able to fulfill the roles of both independent systems. In a drive capacity the overall goals are to accelerate the vehicle up to speed, maintain a constant velocity, and decelerate the vehicle back to rest. As a suspension system the DEDS must be able to locate the wheel relative to the vehicle, maintain adequate tire to road forces, isolate the vehicle from road disturbances, and maintain itself inside a working space defined by design. In addition to these suspension

roles, this system is designed to allow for attitude control of the vehicle body by controlling the vertical position of individual wheels to provide a mechanism for controlling squat and dive during braking and acceleration as well as roll when cornering.

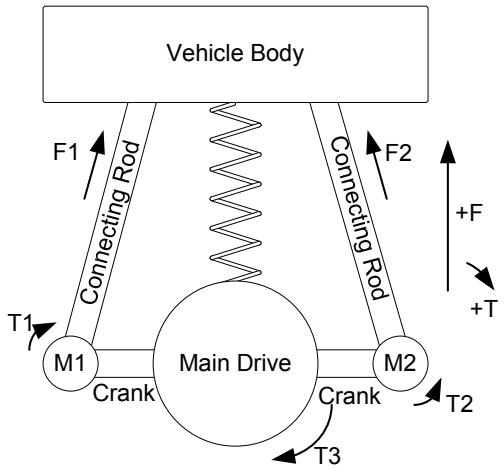

Figure 1-3 Vertical Actuation

When it is desired for the vehicle to accelerate or maintain a constant velocity the DEDS system must apply a net positive torque to the main drive wheel. While this operation has the ability to utilize the maximum torque available from both motors to obtain maximum acceleration and deceleration, in many cases there will be additional torque available for actuating the suspension vertically. For small vertical displacements it is possible for $T_1$and T_2 to both be positive but having different magnitudes. When larger vertical actuations are required it becomes necessary for one motor to apply an opposing torque. Figure 1-3 represents the system when the actuation is working to

extend the suspension. M_1 applies the torque needed to maintain the net drive torque on the main drive. To accomplish this, it must apply additional torque to overcome the braking torque being applied by M_2. In order to compress the suspension the roles of the two motors would be reversed.

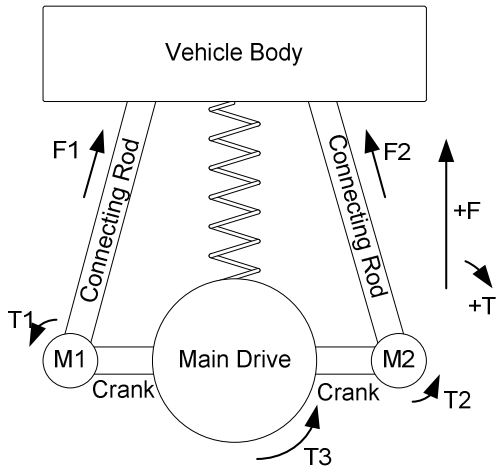

Figure 1-4 Braking Actuation

Similarly, when the vehicle is undergoing a braking maneuver it is possible to actuate the suspension vertically as shown in Figure 1-4. During braking maneuvers the primary motor provides additional braking torque which can be utilized for energy regeneration. The actuating motor then provides a small difference in braking torque for vertical actuation, or in the case of large actuations to counteract the dive of a braking maneuver it can provide a drive torque to push the suspension. The primary motor is defined by the direction of acceleration as well as the desired direction of travel. The roles of each motor for each operating condition can be seen in Table 1-1.

Direction of Acceleration	Direction of Actuation	Motor 1 Role	Motor 2 Role
Positive	Compression	Actuating	Primary
Positive	Extension	Primary	Actuating
Negative (Braking)	Compression	Primary	Actuating
Negative (Braking)	Extension	Actuating	Primary

Table 1-1 Motor Roles

The final mode of operation for the DEDS system is when the wheel is actuating solely in the vertical direction. In a four wheel vehicle this could be useful for isolating large disturbances or for large attitude control maneuvers. The motors in this case utilize equal but opposing torques to apply a net torque of zero to the wheel but still provide the actuation to the suspension. In order to actuate the system vertically in extension M_1 applies a positive torque and M_2 a negative torque of equal magnitude. Compression of the suspension requires a reversal of roles of the motors.

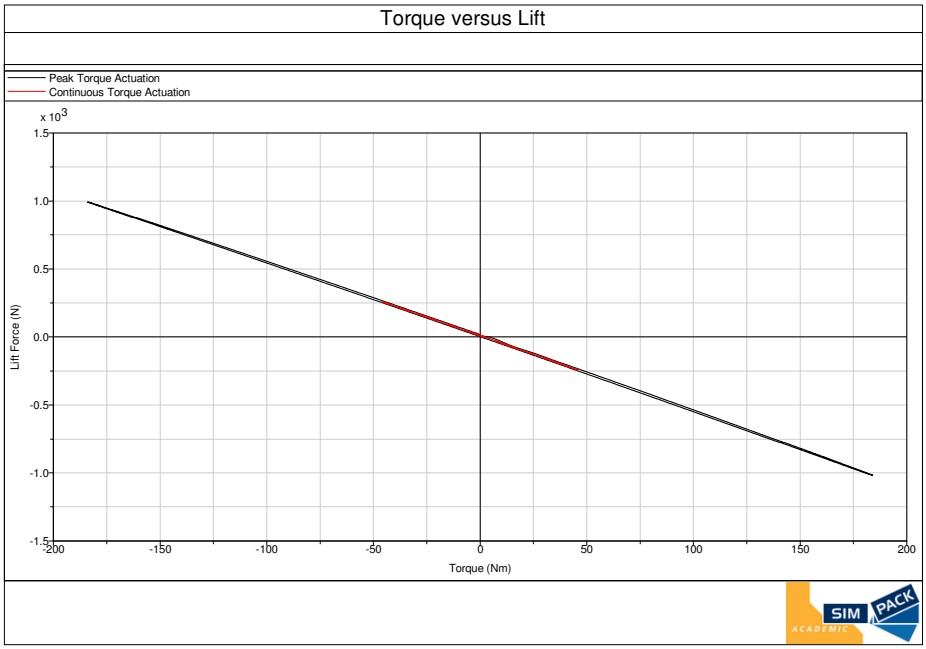

Figure 1-5 Lift Force versus Motor Torque

When operating the system in the vertical degree of freedom the torque of the motors provides a lift force in addition to the spring. Figure 1-5 shows vertical actuation force versus the torque of the motors for what is considered the nominal location of the connecting rods. When operating at a maximum steady state torque the system can provide up to 350 N of additional vertical force in both the positive and negative direction. This additional force allows the system to assist the spring and change the ride height by removing or adding additional down force. When even larger actuation forces are needed the motors can be driven for short periods of time with even higher currents and up to 1kN of additional force can be supplied. B_{lift} from equation (1.3) is equivalent to the slope of the line in Figure 1-5. If the connecting rods are moved

closer to the motor mount pivot, the vertical forces are increased but the available travel is reduced. If they are moved further away from the motor mount pivot the mechanical advantage is reduced so the vertical forces are reduced, but the available travel is increased.

1.3 Variations in Design

This system has many different approaches that can be utilized to obtain the same results. There are several different variations that will be explored. A symmetrical layout like the one that has already been explored, an asymmetrical design that is more conducive to hardware implementation, and a steering design that would need to be utilized to allow all four wheels to be actuated. The location of the motors can also be switched from in wheel to outside of the wheel depending on packaging requirements. The numerous designs lend credence to the system's ability to be utilized for many different applications.

The symmetrical design is the most basic format for the system. The wheel position is constrained by a linear slide mechanism. This is not typically utilized in a vehicle suspension system due to the loads involved and the application environment. However in a simulation environment the symmetric layout offers many benefits. It is easy to design, modify, and control. The control algorithm only has to handle the nonlinearity of the vertical force generated as the motors rotate around the wheel carrier.

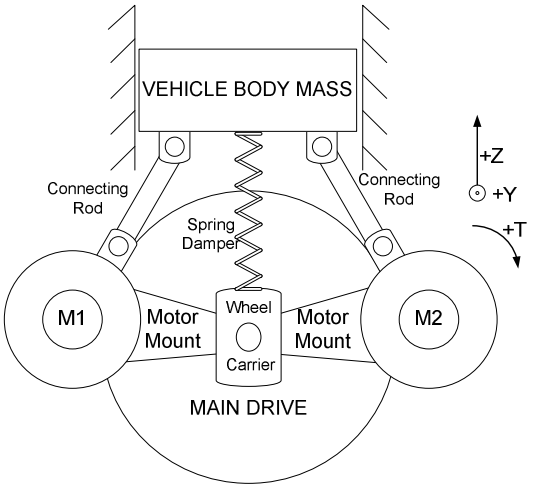

Figure 1-6 Symmetrical Drive Configuration

The asymmetric design utilizes components and layouts that are more conducive to an automotive suspension. A trailing arm style suspension was selected to locate the wheel carrier for the prototype DEDS system described later in this dissertation. This causes the wheel to travel in an arc rather than a linear path like that in the symmetric design. This arc causes asymmetry through the range of travel of the suspension system. This asymmetry can introduce more complexity into the control algorithm.

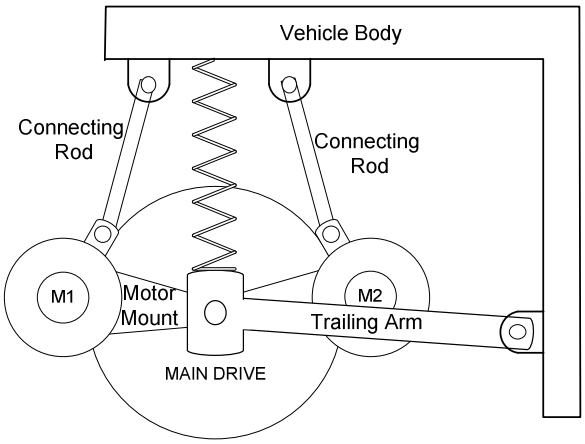

Figure 1-7 Asymmetrical Drive Configuration

Application of the system to only the non-steering axle results in a dramatically diminished return on investment. In order to fully exploit the advantages of such a system, it needs to be implemented at each wheel. Packaging in a steering configuration is more complex; however it can be accomplished as shown in Figure 1-8. Several options for including the steering were explored and packaging studies were performed to ensure feasibility. However for initial development and testing, it was decided to prototype the DEDS system for a non-steered axle to reduce prototyping costs and to enable focus to be placed on development of a control system and testing of system performance.

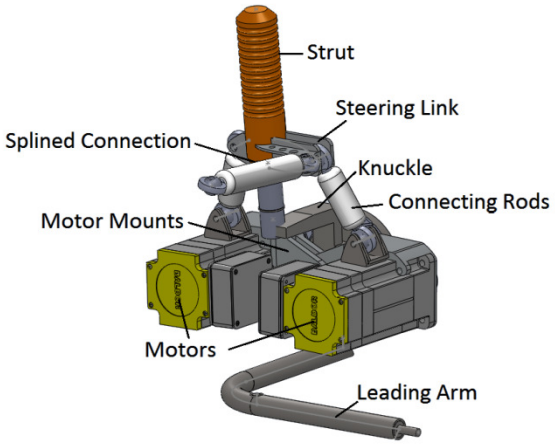

Figure 1-8 Potential front axle implementation of the DEDS system

When utilizing the electric motors it is possible to locate them in the wheel or to pull them back outside of the wheel. The main advantage to locating the motors outside of the wheel is the ability to utilize larger motors than those that would fit inside the wheel. The location of the motors will also impact the overall vehicle dynamics and depending on performance goals it could be beneficial to have more centrally located mass. This location adds the complexity of an additional mechanism to transmit the power out to the suspension or the additional design complexity of offsetting the wheel so far from the drive mechanism. Locating the motors in the wheel increases the packaging complexity, but provides the benefit that the system in its entirety is located within the wheel well. The mass is moved out to the corners of the vehicle and is located as low as possible. The inside of the wheel layout also has the advantage of increased air flow over the motors as the wheels move and generates turbulence inside the wheel well.

Finally, it is possible to explore additional methods for connecting the motors to the actual wheel carrier to transmit the power to the wheel. Initial exploration into gear, toothed belt, and chains led to the conclusion that a toothed belt would be utilized for the hardware in the prototype. Gears would need to be enclosed for adequate lubrication and this would be difficult to achieve due to the motors pivoting around the wheel carrier. Exposed gears would be difficult to lubricate and keep clean in the vehicles operating environment. A chain could be utilized, but was ruled out due to noise and longevity concerns. In other vehicular applications chains have been found to stretch and their gears wear causing problems with their operation. A toothed belt was selected as the best option for the operating environment as well as loading conditions.

A semi-trailing arm vehicle suspension layout was chosen to represent the rear passenger side of a vehicle for the quarter vehicle model. The motors are located inside the wheel and connected to the hub via a toothed drive belt. All of the locating and steady state load carrying is performed by the semi-trailing arm and a coilover shock. The coilover shock reduces the packaging space required, provides easily adjustable damping and spring rates, and can even have the damping disabled and be utilized solely as a coil spring carrier. While this layout proves to be asymmetric by design, the designed travel of the vehicle suspension allows the system to operate in a nearly linear, symmetric region.

2 Background and Motivation

The DEDS system provides a solution for multiple different functional goals. It is able to actuate the wheel rotationally, and thus the vehicle longitudinally. There is also vertical actuation to provide attitude control. The dual motors can also provide braking forces in order to slow and stop the vehicle, while capturing that energy for later reuse. On top of all of this it also functions as the suspension and provides all of that functionality as well. Of course some of these roles that the DEDS provides are commonplace in a vehicle, some are just penetrating the market, and others are still mainly academic with very few examples of commercial application to date. As such, the DEDS draws on several different arenas of technology and research.

The DEDS system is built around a vehicular suspension system. These systems are designed to locate the tire, provide vibration isolation, and also to maintain tire to road contact. Many different approaches to suspensions have been researched, tested, and implemented in various vehicles [1-6]. Various designs from rigidly mounting the axle and tires to the vehicle in order to increase load capacity and reduce system complexity, to five bar linkages with electronically controlled dampers and air springs can be found in vehicles on and off the road. The design of the suspension system usually has to deal with the packaging space and the intended environment in which the system will operate. High performance sports cars for example tend to have more complex multi-link suspensions in order to provide predictable, controlled tire motion with the

opportunity for substantial adjustability to suit driving conditions. This is accomplished by sacrificing simplicity, cost, and packaging space. Heavy trucks tend to have more simplistic systems that optimize load capacity over driver comfort. Typical passenger cars are generally a tradeoff between the two extremes with packaging and cost of manufacturing and assembly also being considered along with the functional requirements.

With the large range of operating conditions that a vehicle will encounter throughout its lifecycle, it is difficult to design and build a suspension system that is optimal for any one set of conditions, much less all of them. Road conditions, loading conditions, driver input, and weather all have an impact on a suspension's ability to perform its roles. Engineers and researchers have explored various methods to optimize a suspension for varying operating conditions. Variable rate springs and dampers are common passive elements used to broaden the tuned operating space of suspensions. Semi-active and fully active suspensions have been explored and implemented as methods for improving the flexibility of a suspension. Semi-active systems can be classified by their lower power consumption and the lack of ability to generate a force on a suspension independent of the systems motion [7]. These systems generally consist of variable dampers that adjust the damping ratio by either mechanical or electrical means, however some systems rely on low power actuators to adjust suspension geometry [8, 9]. Magneto-rheological shock absorbers are one of the prominent methods for accomplishing semi-active suspension implementations [7, 10, 11]. These dampers

utilize a magnetically excited fluid that changes its viscosity in a magnetic field. This allows the piston to be converted into a piston with an electro magnet. As the magnetic field around the piston is varied, the fluid traveling through the piston changes viscosity, and thus the damping rate is adjusted. Since the magnetic field is local to the piston, the power consumption is reduced. This design and other semi-active suspension designs, help to broaden the flexibility of the suspension but they are still very limited [12, 13].

Fully-active suspension systems have the ability to actuate the suspension independent of the relative velocity of the components [14]. Several researchers have found that active suspensions don't really offer a large improvement in general ride performance, but instead their application strength is in their ability to adjust the ride performance for differing road and handling requirements [15, 16]. These systems utilize more power, but are able to provide much greater flexibility to the suspension system. The force generation in active suspensions is implemented in many different ways. Air springs, hydraulic springs, variable geometry, and electrically driven linear drives are a few of the methods that have been explored [15, 17-20].More research has been spent on the actual control of the systems, rather than the method of implementation. Fuzzy logic controls have been explored by many as a method to allow the active system to dynamically adjust to the operating conditions [21]. Others have explored optimal controls and varying feedback methods to try and allow the system to have a preview of the upcoming disturbances to reduce the response time [22-25]. With the addition of

fully active suspensions, limitations on the improvement in operation of the systems have been found. The added complexity, cost, and weight of these systems can be difficult to justify when they only reduce the vertical RMS acceleration by 11% [15].

Of course, vehicles also experience heave, roll, and pitch due to road and driver inputs. Semi-active and fully-active suspension systems tend to be utilized to provide additional ride comfort, road handling, and/or maintain the suspension working space. Combating heave caused by road inputs, roll during steering maneuvers, or pitch during acceleration and braking is another aspect of additional actuation that some systems provide. Control of the heave, pitch, and roll of a vehicle is referred to as attitude control. Attitude control is an exercise in improving vehicle stability. During steering maneuvers vehicles experience weight transfer towards the outside of the turn. This shift in weight causes the vehicles to roll to the outside of a corner causing the load experienced by the outer wheels to increase while the inner wheel loads decrease. Anti-roll control is a form of attitude control that combats this occurrence. Anti-roll control improves the stability of a vehicle and the cornering performance by using force generation to combat the deflection of the outer suspension systems thus reducing or preventing the weight shift to the outside tires [26]. Anti-dive control works in much the same way as anti-roll control, but for acceleration and braking maneuvers.

In order to achieve the actuation necessary for attitude control many different variations of control and hardware are utilized. Using variable dampers it is possible to

achieve an increase in vibration isolation as well as reduce the amount of roll during cornering maneuvers [27, 28]. They applied fuzzy logic to control four magneto-rhelogical dampers in a vehicle with modified ground-hook and ski-hook algorithms to control both vibration and attitude of a vehicle. Others have explored using hydraulic actuators attached to the passive anti-roll bar to prevent roll in vehicles [26]. These designs have actually seen production in vehicles like the Citroën Xantia. The Xantia has hydraulic actuators attached to the anti-roll bars that allow the vehicle to have a soft ride during normal operation, but then a very stiff feel during steering maneuvers and in this case no body roll at all. Jiangtao [29]explored theoretically the amount of attitude control that can be accomplished with a bicycle model and ILQ and LQ control algorithms, and found that the ILQ algorithm was an improvement over LQ control strategies. Many approach attitude control utilizing a full vehicle model [30-33]. Full exploration of attitude control requires a full vehicle model. Pitch and heave can be realized in a bicycle model, but the addition of roll requires the remainder of the vehicle. Control approaches for full vehicle control range from optimal PID loops to LQR skyhook systems. In all of the development cases for controls, the method of feedback is an important assumption. Some of the simulations utilized full state feedback, others used off axis accelerometers and calculated the moments, and still others used more advanced sensor networks or observers. The DEDS is explored as a quarter vehicle model, so the ability to provide attitude control is demonstrated by showing that the system is capable of actuating vertically as well as rotationally. The vertical position

control applied is not meant to represent or replace any of the more complex, and complete attitude control systems that would be utilized in a full vehicle.

The DEDS doesn't only fill the roles of the suspension system; it also propels the vehicle. Recently, electrically powered vehicles have begun to find homes in consumer's driveways and garages. Rising fuel prices coupled with the reduction in air quality in urban environments and the popularity of being eco-friendly have set the stage for an explosion in alternatively fueled vehicles and newer more efficient platforms. Whether these vehicles are mild hybrid vehicles which depend mainly on the IC engine for propulsion with an electric boost, or fully electric vehicles which rely solely on an electric motor for propulsion, these vehicles have found not only a niche in the market but also governmental backing.

Hybrid vehicle technology has progressed rapidly over the previous few years. The hybrid moniker doesn't only apply to conventional vehicles with the addition of an electric assist drive, but also to vehicles which utilize multiple fuel sources. For the purposes here hybrid vehicles refers to hybrid-electric vehicles which utilize an electric motor for some if not all of the propulsion of the vehicle. Hybrid electric vehicles typically utilize two configurations, parallel and series.

A parallel hybrid consists of both an internal combustion engine and an electrical motor both of which are connected to provide locomotive power to the vehicle. There are several different methods in which the two drive systems can be utilized. In some cases

the electric motor is connected to one axle, and the IC engine is connected to the other. This is known as a parallel through the road hybrid vehicle [34-36]. It is also possible to combine the electric and IC motors through a gearbox that allows both to drive the same axle. Some designs also incorporate the electric motor as a starter/alternator/booster in which case the electric motor can provide a small assist when starting from a stop while also fulfilling the roles of the starter and/or alternator. This type of system allows the vehicle to turn off the IC engine when stopped to reduce idle fuel consumption. Of course there are many other configurations that can be dreamed up and only a few of the more prominent solutions have been touched here.

Series vehicles do not connect the IC engine to provide locomotive power to the vehicle. They utilize only electric motors to propel the vehicle and the IC engine is used as a generator to run the motors and/or charge the batteries. This is the type of system that lends itself to the DEDS hardware. Series hybrids are geared towards urban driving styles and excel in conditions that are wrought with stop and go conditions [37]. The efficiency of the series hybrid is worse than that of the parallel hybrid during other operating conditions due to the inflexibility of the architecture.

Fully electric vehicles are also beginning to find a home in the marketplace. Mainly as city based vehicles and novelty status based vehicles, several different small production models have found their way to consumer's garages. The Nissan Leaf, Chevy Volt, and Tesla Roadster are just a couple vehicles that rely completely on electric motors for

propulsion. These vehicles utilize a battery pack and in some cases, a bank of ultra-capacitors to store the energy for the electric motors. The range is limited by driving style and the amount of on-board storage that is available; however it can be extended by utilizing regeneration methods for both braking and suspension. The application of regeneration was up until recently not as common commercially as hybrid vehicle technology, but the benefits are now being realized to further improve hybrid vehicle efficiency.

Both hybrid and electric vehicles rely heavily on energy management and control solutions. Many of these control strategies rely on the SOC of the battery pack and ultra-capacitor if applicable [38-40]. They monitor the state of charge and adjust the control strategy to optimize energy efficiency and emissions. Of course the type and quantity of storage in the vehicle also plays a role in the control strategy [41]. Plug in hybrids have the opportunity to rebuild the SOC during periods of recharging. Hybrids without the ability to plug in and recharge have to try to optimize electrical motor usage while maintaining the SOC throughout the driving cycle. Imai [42] trys to maintain a SOC of 50-55% in the Canter HEV in order to take advantage of braking regeneration. During braking regeneration the SOC is allowed to climb above these limits, but the generation from the motor only maintains these lower limits. This allows the system to be more prepared for the influx of regenerated energy so that it is not wasted and expelled as heat due to fully charged batteries.

The addition of electrical drives also requires revisiting efficiency analysis and fuel consumption. Tradition evaluation techniques relate the amount of fuel burned in the IC engine to the distance traveled. Fully electric vehicles still utilize fuel in the form of electricity, but traditional evaluation does not have a method to compare electrical energy consumption with fossil fuel consumption. Hybrid electric vehicles still rely on traditional methods, but with the increase in plug-in available vehicles new measurement standards are necessary. Wen [43] worked on a method to determine efficiency of hybrid vehicles by evaluating current accepted driving cycles and generating hybrid micro-trip cycles that evaluate hybrid vehicles. Imai [42] considers total energy efficiency by considering the total efficiency of the fuel. Considering generation, transportation, and utilization efficiencies hybrid, electric, and IC vehicles can be compared on a level field.

Of course hybrid-electric and fully electric vehicles see a wealth of research, development and testing in control algorithms to improve efficiency, performance, and stability [27, 38, 44]. Options to designers and control engineers continually expand as all wheel independent drive systems that allow for individual wheel torque vectoring and regeneration reach maturity [45]. Motor and drive technology are ever expanding and higher power systems evolve almost continuously [39, 44, 46]. These advances in technology continue to push hybrid and electric vehicles deeper into the consumer marketplace

Fully electric vehicles are still plagued with range limitations and longer recharge times. Energy regeneration has the ability to increase the available range for electric vehicles, and increase the efficiency of hybrid vehicles. Many different approaches to regeneration have been studied ranging from mechanical regeneration through the use of flywheels and hydraulics to electrical regeneration through the use of generators and/or drive motors[47-51]. For the purposes here only electrical regeneration will be explored. Two different modes of regeneration are of importance in the DEDS system, vertical damping and braking. Both of these have been explored in an effort to enhance the performance of both hybrid-electric and fully electric vehicles.

Regeneration of the suspension is based upon recapturing the kinetic energy that is dissipated in the damper of a passive suspension. This kinetic energy is a product of the suspension velocity, or the relative velocity of the wheel carrier and the vehicle body, and the desired damping force. The quick estimate of the amount of power available for potential damping regeneration is defined by equation (2.1). The actual amount of power that can be captured from the suspension is dependent on many variables such as the ratio of unsprung mass to sprung mass, the damping ration, and the control strategy. This is only the available power and the actual amount that can be captured will depend on the efficiency of the hardware implementation. The total power available from suspension based regeneration is also a product of the road roughness. Smoother roads will require less damping force while rougher roads will require more.

The more damping force that is required the more power that can be collected from the system.

$$P_{SusRegen} = F_{damper} \times V_{suspension} \tag{2.1}$$

The damping force in a typical suspension system is generated by a hydraulic damper. In these types of systems $P_{SusRegen}$ is converted into heat. The heat is then dissipated into the air by the body of the damper. During higher performance driving that leads to rapid and long term cycling of the suspension, the damper's ability to dissipate the heat reduces and lowers the damping rate of the suspension and thus degrades the performance. This heat is wasted energy and as such is a potential source for regeneration. There is potential for regeneration through thermo-electronic means, but the thermal gradient necessary to produce electricity is only present during higher performance driving during which the dampers' performance has been reduced. A method presented by Kawamoto [52, 52] proposes that the damper be replaced by an electro-mechanical actuator that allows for both suspension actuation as well as damping with energy regeneration. They found that the system could operate in a regeneration region, but that the control gains required were different between the active suspension and regeneration operating modes.

Others have explored the actual potential for regeneration through the suspension. Ignoring the physical implementation the limits of regeneration can be explored. The maximum amount of energy dissipated through a conventional damper can be

evaluated and thus becomes the baseline for the maximum amount of regeneration energy. One difficulty of this approach is that a conventional damper doesn't have the ability to be tuned for varying operating conditions. A regeneration based system can vary the damping force to provide a time varying damper and also to optimize the power regeneration for given driving conditions. Montazeri-Gh [50] found that on a smooth road up to 35% of the energy that was available for regeneration through braking was able to be pulled from a suspension regeneration algorithm. So if a system could utilize braking and damping regeneration, an additional 35% of the regenerated power could be pulled from the suspension. Of course on rougher roads or conditions with less braking, even more of the regenerated energy could be supplied by the suspension.

Braking regeneration provides the majority of the potential energy that is available to extend the range of electric and hybrid-electric vehicles in most conditions. In a friction based braking system a friction pad is clamped against a rotating surface and the friction slows the rotation of the wheel and thus the vehicle. As the clamping force is increased the amount of friction increases and the vehicles slows. This system has several problems. The first is that both the friction pad and the surface it clamps on are consumable. The second is that the friction generates heat; as the heat builds up it can lead to brake fade and an overall reduction in system effectiveness. Finally, the end result is the same as for a damper, a lot of energy is wasted as heat instead of being utilized to propel the vehicle or drive the accessories. The energy available for braking

regeneration is directly related to the kinetic energy of the moving vehicle (2.2). Without braking, the vehicle deceleration is caused by aerodynamic drag, rolling resistance, and gravitational forces (when not on a level road).

$$P_{BrakeRegen} = U_e - U_{aero} - U_{rolling} - U_{gravitational} \tag{2.2}$$

Electric regeneration based braking systems are not without their own faults. Their efficiency is highly defined by the algorithm which controls their operation and the implementation hardware. In highly active braking conditions that utilize little electrical propulsion the system could reach a full charge, at which time the regeneration energy would have to be converted to heat and dissipated instead of stored in the batteries. Of course electrical brake regeneration allows antilock braking without having to add additional actuators to the system. Due to the increased amount of energy available, substantially more work has been focused on braking regeneration [50, 51, 53, 54].

Many forms of electric braking regeneration rely on the drive motor to act as a generator. This utilizes the back EMF of the motor to recharge the batteries. However, the back EMF of a motor typically has a nominal voltage that is less than the batteries that it is trying to recharge [53]. Thus a regenerative braking system relies on a charge booster of some sort to be able to recharge the batteries. These charge cycles are also short in duration and generate large amounts of current which can damage battery packs [55]. Ultra-capacitors have been explored as a method to reduce the necessary battery capacity which reduces the weight and cost, reduce the discrete high current

charge conditions that damage batteries, and also to buffer the high current demands placed on a battery by high acceleration maneuvers.

It has been shown by Ming-Ji [53] that a simple regeneration system can extend a purely electrical vehicles range by 16.2%. More complex systems like those explored by Apter [51] found that regeneration of 40-60% is possible in a battery system which could dramatically increase the range of a vehicle when used in urban settings where braking cycles are common. These limits however, were found utilizing a 100% efficiency which is unrealistic, but they do provide an upper limit of the energy that is available and can be scaled by an effective efficiency to determine the actual amount of energy that could be replaced in the battery pack. Delgado and Guo [56, 57] both found that approximately 30% of the energy utilized to propel a vehicle in urban settings could be recaptured through braking.

Combining both suspension and braking regeneration could significantly extend the range of an electric vehicle. They could also be utilized to improve the efficiency of hybrid vehicles by providing additional options for power generation. Studies have found that braking regeneration can recapture up to 60% of the energy expanded to propel a vehicle, with 30-40% being more realistic and realizable. Suspension regeneration has the ability to add an additional 12% of the energy used to propel the vehicle back to the battery. This sets the stage for either electric or hybrid vehicles to experience an increase of efficiency and range.

So a system such as the DEDS stands to provide a mechanism for extending the range of a vehicle by capturing energy that is typically expelled as heat in both the damper and the brakes. The controls and sensors for attitude based control of a vehicle have been explored and developed for both bicycle and full vehicle models. Electrical propulsion systems are not new and unproven in passenger vehicles. Since the technology exists that would allow a fully developed systems such as the DEDS to be commercially viable, it is a reasonable leap to explore the system to see if the design has merit.

3 System Modeling

Modeling of complex systems can take many different forms. The complexity of the model tends to increase as desired fidelity increases. Complex systems start with simplified models that make several assumptions in order to gain rapid, low fidelity access to the system's performance. It is important to understand the assumptions that are necessary to facilitate the simplified models. The additional complexity of higher fidelity models doesn't rule out assumptions. In many cases the more complex the model becomes, the more assumptions are required. The DEDS system modeling started with a planar single degree of freedom quarter vehicle model. As the data was analyzed and parts, layout, and general performance parameters became more apparent the model became more complex. The planar single DOF model became a planar two DOF model that represented not only the vertical position of the sprung mass, but also the rotation of the tire and wheel assembly. From these two models, more complex multi-body dynamic models were formed that incorporated prototype hardware designed parts and multiple dimensions.

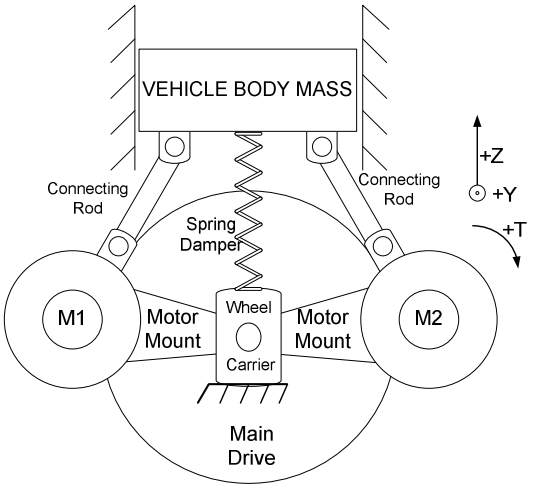

Figure 3-1 Planar representation of a simplified DEDS suspension

3.1 Planar Mechanism Modeling

Simple planar mechanism modeling has the ability to provide general mechanism results in very little time. The goal behind performing planar analysis on the DEDS system was to determine initial performance levels and to also remove some uncertainty in initial component sizing and placement. A two degree of freedom model was generated to explore the vertical position of the sprung mass and also the rotational actuation of the tire and wheel assembly. This model provided the data needed to determine initial component placement of the connecting rods as well as the sizing of the motors.

The constrained model can be seen in Figure 3-1. The vehicle body can be treated as though it is constrained to purely vertical motion by the use of a frictionless slider mechanism. The hub center becomes the origin of the system and is mounted to the ground reference frame. This means that the system can essentially pull on the ground

in order to actuate the vehicle body. In a real system this assumption would be invalid. Two motor mounts are also mounted to the ground mount and allowed to rotate about the mount in the XZ plane. The motor center is mounted to the other side of each respective mount. This combination of motor mount and motor causes the actual pinion gear to travel in a radius around the drive gear maintaining the belt tension. Attached to each motor mount is an upper link (connecting rod) that connects the motor to the vehicle mass. These two links are what allow the motors to push and pull on the vehicle mass enabling the vertical actuation. The initial modeling of the system assumed that a simple ideal gear system would be utilized to transmit the power of the motors. The drive gear was modeled as being centered on the hub and allowed to rotate but the inertia of the gear, wheel, and tire are neglected since the concern was to find appropriate vertical actuation forces. The model was quickly modified to incorporate an equivalent inertia for the wheel and gear system that represented the quarter vehicle model.

This simplified model can be broken down into its independent parts and a quick evaluation of the statics of the system can be evaluated. The vehicle body is represented as a quarter mass of the vehicle. The vehicle body is constrained by a slider mechanism. The forces were summed for both the X and Z direction and resulted in equations (3.1) and (3.5). F_{LU} and F_{RU} will provide the active suspension actuation while F_S is the passive suspension force generated by the spring and damper. Because the mass is constrained by a slider, equation (3.1) can be set to zero. For purely vertical

actuation the X component of F_{LU} and F_{RU} should cancel each other in this symmetrical mechanism. If there is an asymmetrical design these forces would not be equal and F_{slider} would no longer be zero. The spring force, F_s, is composed of the static load of the vehicles mass summed with the force generated by the spring when the body position is different than the steady state as shown in equation (3.4). The force from the damper is neglected as the analysis is done at steady state.

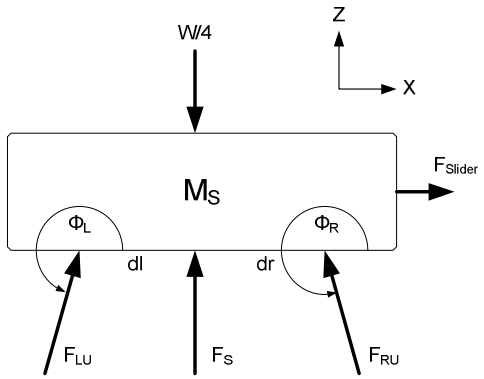

Figure 3-2 FBD of Vehicle Body

$$\sum F_X = F_{Slider} + F_{LU}\sin\phi_L - F_{RU}\sin\phi_R \tag{3.1}$$

$$\sum F_Z = M_s a_z = F_S - \frac{W}{4} + F_{LU}\cos\phi_L + F_{RU}\cos\phi_R \tag{3.2}$$

$$F_s = \frac{w}{4} + k(z_{sprung} - z_{unsprung}) + \cancel{c(\dot{z}_{sprung} - \dot{z}_{unsprung})} \tag{3.3}$$

$$F_s = \frac{w}{4} + k\Delta z_{sprung} \tag{3.4}$$

$$\sum F_z = k\Delta z_{sprung} + F_{LU}\cos\phi_L + F_{RU}\cos\phi_R \tag{3.5}$$

In this analysis the tire has been attached to the ground reference system creating a 2 DOF system; the vertical motion of the vehicle body and the rotation of the tire. The wheel and main drive gear are modeled as a single body. This body sees the forces from the two motor mounts, the spring and damper, and the two pinion gears. Due to the mechanism symmetry, ϑ_{ML} and ϑ_{MR} are equal. The equations can be simplified by considering the motor mount forces F_L and F_R as their X and Z components. Similarly the pinion gear forces F_{GL} and F_{GR} can be separated into a normal force and a tangential force. Equations (3.8) and (3.9) represent the summation of forces in the X and Z direction. Since the body is connected to the ground reference frame both of the equations can be set to 0.

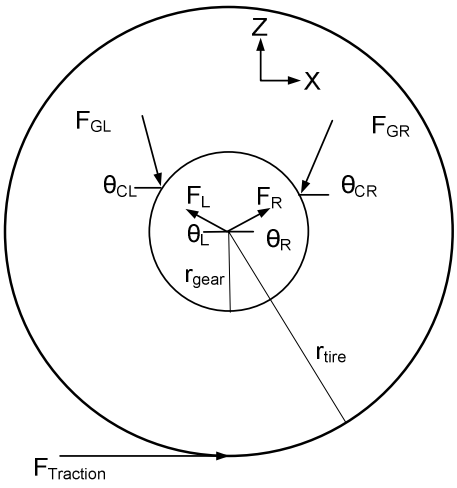

Figure 3-3 FBD of Wheel and Main Drive

$$\sum M_o = F_{Traction} \times r_{tire} + \left(F_{GLT} - F_{GRT}\right) r_{Gear} \tag{3.6}$$

$$\sum F_X = ma_X = 0 = F_R \sin\theta_R - F_L \sin\theta_L - F_{GR} \sin\theta_{CR} + F_{GL} \sin\theta_{CL} - F_{Traction} \quad (3.7)$$

$$\sum F_X = 0 = F_{RX} - F_{LX} - F_{GR} \sin\theta_{CR} + F_{GL} \sin\theta_{CL} - F_{Traction} \quad (3.8)$$

$$\sum F_Z = 0 = -F_{Spring} + F_{LZ} + F_{RZ} + F_{GL} \cos\theta_{CL} + F_{GR} \cos\theta_{CR} \quad (3.9)$$

The right and left linkages are mirror images of one another. As such the analysis here will only focus on the right side of the mechanism (see Figure 3-4). S_Z represents the suspension length. This will actually be a measured quantity in the system as it is very easy to measure with sensors, a string potentiometer could be utilized but the angular difference in position of the two motors can also be used. U_R, R_U, and R_L are constants of the design. For any value of S_Z it is possible to solve for both θ_R and ϕ_R. It is also possible to solve for the angular velocities of the upper link and motor mount given a vertical speed of the body since the vector loop equations (3.11) and (3.12) can be differentiated to obtain the velocity equations (3.13) and (3.14) where ω_{RL} and ω_{RU} are the angular velocities of the lower link (motor mount) and the upper link (connecting rod) respectively.

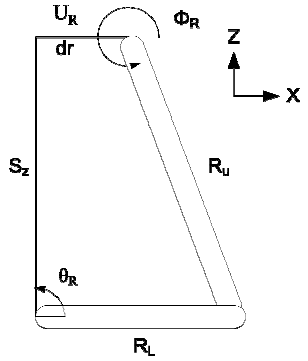

Figure 3-4 Kinematic Layout of Right Mechanism

$$\vec{U}_R + \vec{R}_U + \vec{R}_L = \vec{S}_Z \tag{3.10}$$

$$R_U \cos\phi_R + R_L \sin\theta_R = S_Z \tag{3.11}$$

$$U_r + R_U \sin\phi_R + R_L \cos\theta_R = 0 \tag{3.12}$$

$$\cancel{U}^{0}_{r} + R_U \omega_{RU} \sin\phi_R + R_L \omega_{RL} \cos\theta_R = 0 \tag{3.13}$$

$$R_U \omega_{RU} \cos\phi_R + R_L \omega_{RL} \sin\theta_R = \dot{S}_Z \tag{3.14}$$

The kinematic analysis allows for the angles of both the motor mount and the upper support link to be found if the body position, S_z, is specified. Using these angles it is possible to calculate the component values of the link force on the motor and pinion body. F_{RU} is broken down into its X and Z components. The contact forces of the pinion drives on the motors are considered to be ideal, where the normal force is neglected and all meshing forces are used to drive the wheel. These forces are then used to solve equations (3.18) and(3.19).

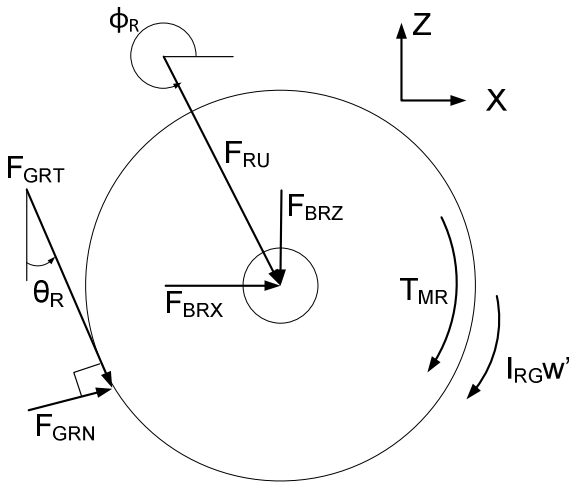

Figure 3-5 Right Motor and Pinion FBD

$$\sum F_x = \cancel{F_{GRN}\cos\theta_{CR}} + F_{GRT}\sin\theta_{CR} + F_{BR}\sin\phi_R + F_{RU}\sin\phi_R \quad (3.15)$$

$$\sum F_Z = \cancel{F_{GRN}\sin\theta_{CR}} - F_{GRT}\cos\theta_{CR} - F_{BR}\sin\phi_R - F_{RU}\cos\phi_R \quad (3.16)$$

$$\sum M = F_{GRT} \times r_{PinionGear} + T_{MR} \quad (3.17)$$

$$\sum F_x = F_{GRT}\sin\theta_{CR} + F_{BRX} + F_{RU}\sin\phi_R \quad (3.18)$$

$$\sum F_Z = -F_{GRT}\cos\theta_{CR} - F_{BRZ} - F_{RU}\cos\phi_R \quad (3.19)$$

The right motor mount is the last piece of this puzzle (Figure 3-6). Summing the forces in the X and Z directions results in equations (3.21) and (3.22) respectively. These two equations allow for a solution for the right side of the mechanism. The left portion of the mechanism is a mirror image of the right. As such the equations are very similar with the main difference being the angles found in the kinematic solution.

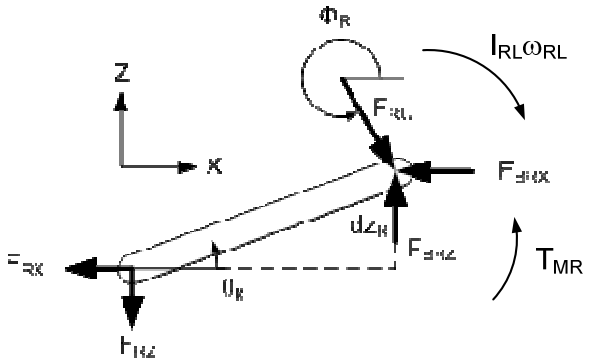

Figure 3-6 Right Lower Link FBD

$$\sum M = F_{RU} L_L - F_{BRX} dz_R - F_{BRZ} dx_R - T_{MR} \tag{3.20}$$

$$\sum F_x = F_{RU} \sin\phi_R - F_{RX} - F_{BRX} \tag{3.21}$$

$$\sum F_Z = F_{BRZ} - F_{RU} \cos\phi_R - F_{RZ} \tag{3.22}$$

Since the left side is fully symmetric to the right, the equations are extremely similar and the full derivation can be found in Appendix B. It is possible to build a matrix using equations (3.1), (3.5), (3.6), (3.17), (3.18), (3.19), (3.20),(3.21), (3.22), and the left hand equivalent equations for equations (3.17) through (3.22). Using this solution matrix for both the left and right side of the mechanism leaves 17 unknowns with two inputs and two outputs. It is possible to arrange the equations so that the vertical displacement from the nominal ride height position (Δz) and traction force ($F_{Traction}$) are the outputs while the motor torques (T_{MR} and T_{ML}) are inputs (3.23). Sometimes it will be desired to solve for the motor torques dependent on the tractive force and vertical displacement

desired. In this case the equations can be rearranged and the matrix rewritten to solve for the torque of both motors (3.24).

(3.23)

$$\begin{bmatrix} 1 & \sin\phi_L & -\sin\phi_R & 0 & 0 & 0 & 0 & 0 & 0 & 0 & 0 & 0 & 0 & 0 & 0 \\ 0 & \cos\phi_L & \cos\phi_R & k & 0 & 0 & 0 & 0 & 0 & 0 & 0 & 0 & 0 & 0 & 0 \\ 0 & 0 & 0 & 0 & r_{Tire} & r_{Gear} & -r_{Gear} & 0 & 0 & 0 & 0 & 0 & 0 & 0 & 0 \\ 0 & 0 & 0 & 0 & 0 & 0 & r_{PG} & 0 & 0 & 0 & 0 & 0 & 0 & 0 & 0 \\ 0 & 0 & \sin\phi_R & 0 & 0 & 0 & \cos\theta_{CR} & 1 & 0 & 0 & 0 & 0 & 0 & 0 & 0 \\ 0 & 0 & -\cos\phi_R & 0 & 0 & 0 & \sin\theta_{CR} & 0 & -1 & 0 & 0 & 0 & 0 & 0 & 0 \\ 0 & 0 & L_L & 0 & 0 & 0 & 0 & -dz_R & -dx_R & 0 & 0 & 0 & 0 & 0 & 0 \\ 0 & 0 & \sin\phi_R & 0 & 0 & 0 & 0 & -1 & 0 & 0 & 0 & 0 & 0 & -1 & 0 \\ 0 & 0 & -\cos\phi_R & 0 & 0 & 0 & 0 & 0 & 1 & 0 & 0 & 0 & 0 & 0 & -1 \\ 0 & 0 & 0 & 0 & 0 & r_{PG} & 0 & 0 & 0 & 0 & 0 & 0 & 0 & 0 & 0 \\ 0 & -\sin\phi_L & 0 & 0 & 0 & -\cos\theta_{CL} & 0 & 0 & 0 & -1 & 0 & 0 & 0 & 0 & 0 \\ 0 & -\cos\phi_L & 0 & 0 & 0 & \sin\theta_{CL} & 0 & 0 & 0 & 0 & -1 & 0 & 0 & 0 & 0 \\ 0 & -L_L & 0 & 0 & 0 & 0 & 0 & 0 & 0 & dz_L & dx_L & 0 & 0 & 0 & 0 \\ 0 & -\sin\phi_L & 0 & 0 & 0 & 0 & 0 & 0 & 0 & 1 & 0 & 1 & 0 & 0 & 0 \\ 0 & -\cos\phi_L & 0 & 0 & 0 & 0 & 0 & 0 & 0 & 0 & 1 & 0 & -1 & 0 & 0 \end{bmatrix} \begin{bmatrix} F_{Slider} \\ F_{LU} \\ F_{RU} \\ \Delta z \\ F_{Traction} \\ F_{GLT} \\ F_{GRT} \\ F_{BRX} \\ F_{BRZ} \\ F_{BLX} \\ F_{BLZ} \\ F_{LX} \\ F_{LZ} \\ F_{RX} \\ F_{RZ} \end{bmatrix} = \begin{bmatrix} 0 \\ 0 \\ 0 \\ -T_{MR} \\ 0 \\ 0 \\ T_{MR} \\ 0 \\ 0 \\ T_{ML} \\ 0 \\ 0 \\ -T_{ML} \\ 0 \\ 0 \end{bmatrix}$$

(3.24)

$$\begin{bmatrix}
1 & \sin\phi_L & -\sin\phi_R & 0 & 0 & 0 & 0 & 0 & 0 & 0 & 0 & 0 & 0 & 0 & 0 \\
0 & -\frac{\cos\phi_L}{k} & -\frac{\cos\phi_R}{k} & 0 & 0 & 0 & 0 & 0 & 0 & 0 & 0 & 0 & 0 & 0 & 0 \\
0 & 0 & 0 & 0 & 0 & \frac{r_{Gear}}{r_{Tire}} & \frac{-r_{Gear}}{r_{Tire}} & 0 & 0 & 0 & 0 & 0 & 0 & 0 & 0 \\
0 & 0 & 0 & 1 & 0 & 0 & r_{PG} & 0 & 0 & 0 & 0 & 0 & 0 & 0 & 0 \\
0 & 0 & \sin\phi_R & 0 & 0 & 0 & \cos\theta_{CR} & 1 & 0 & 0 & 0 & 0 & 0 & 0 & 0 \\
0 & 0 & -\cos\phi_R & 0 & 0 & 0 & \sin\theta_{CR} & 0 & -1 & 0 & 0 & 0 & 0 & 0 & 0 \\
0 & 0 & L_L & -1 & 0 & 0 & 0 & -dz_R & -dx_R & 0 & 0 & 0 & 0 & 0 & 0 \\
0 & 0 & \sin\phi_R & 0 & 0 & 0 & 0 & -1 & 0 & 0 & 0 & 0 & 0 & -1 & 0 \\
0 & 0 & -\cos\phi_R & 0 & 0 & 0 & 0 & 0 & 1 & 0 & 0 & 0 & 0 & 0 & -1 \\
0 & 0 & 0 & 0 & -1 & r_{PG} & 0 & 0 & 0 & 0 & 0 & 0 & 0 & 0 & 0 \\
0 & -\sin\phi_L & 0 & 0 & 0 & -\cos\theta_{CL} & 0 & 0 & 0 & -1 & 0 & 0 & 0 & 0 & 0 \\
0 & -\cos\phi_L & 0 & 0 & 0 & \sin\theta_{CL} & 0 & 0 & 0 & 0 & -1 & 0 & 0 & 0 & 0 \\
0 & -L_L & 0 & 0 & 1 & 0 & 0 & 0 & 0 & dz_L & dx_L & 0 & 0 & 0 & 0 \\
0 & -\sin\phi_L & 0 & 0 & 0 & 0 & 0 & 0 & 0 & 1 & 0 & 1 & 0 & 0 & 0 \\
0 & -\cos\phi_L & 0 & 0 & 0 & 0 & 0 & 0 & 0 & 0 & 1 & 0 & -1 & 0 & 0
\end{bmatrix}
\begin{bmatrix}
F_{Slider} \\ F_{LU} \\ F_{RU} \\ T_{MR} \\ T_{ML} \\ F_{GLT} \\ F_{GRT} \\ F_{BRX} \\ F_{BRZ} \\ F_{BLX} \\ F_{BLZ} \\ F_{LX} \\ F_{LZ} \\ F_{RX} \\ F_{RZ}
\end{bmatrix}
=
\begin{bmatrix}
0 \\ \Delta z \\ -F_{Traction} \\ 0 \\ 0 \\ 0 \\ 0 \\ 0 \\ 0 \\ 0 \\ 0 \\ 0 \\ 0 \\ 0 \\ 0
\end{bmatrix}$$

Variable	Value	Units
M_S	380	kg
U_L, U_R	0.07	m
L_U, R_u	0.19	m
L_L, R_L	0.16	m
S_Z	0.268	m
r_{tire}	0.3	m
$r_{PinionGear}$	0.01248	m
$r_{DriveGear}$	0.1194	m
K	33,000	N/m

Table 3-1 Kinematic Modeling Constants

Using this model it is possible to perform initial motor sizing, drive sizing, and determine initial loading conditions for the components. This kinematic planar model was executed in Matlab. The values shown in Table 3-1 for mass (M_s), spring stiffness (k), and the tire radius (r_{tire}) all came from an initial design of a small compact vehicle. The lower links or motor mounts were determined by looking into available wheel sizes and a choice was made to try to fit the entire DEDS system inside a 16 inch wheel. The upper links or connecting rods (L_U and R_U) were determined by considering compact cars on the market and measuring some of the suspensions and hard points to determine

the amount of space available. The same is true for the separation distance on the connecting rods (U_L and U_R). These assumptions plus a goal maximum velocity of over 120kph provided enough constraints that potential gear systems could be considered. A gear ratio of 9.567:1 was initially selected. This maintained the electric motor at lower rpm ranges with only using 1061 rpm at 120kph. With motors available with 3000rpm maximum radial velocities, there was some room to adjust the gear ratio to gain the appropriate longitudinal performance.

Using the values from Table 3-1, it was possible to determine what size motors would be required to actuate the suspension model. The relationship between torque differential and displacement can be seen in Figure 3-7. The system is nonlinear due to the change in mechanical advantage that occurs as the motors rotate around the main drive gear. In compression the spring requires additional force to compress so that compression actuation requires more torque than the extension travel. The actual suspension is proposed to have a travel of 130mm with 60mm in jounce and 70mm in rebound. In this layout it would require motors each capable of just over 50Nm of steady state torque to have the ability to actuate the suspension from one extreme of travel to the other. Several different length cranks were evaluated as well. As the length of the crank is extended the amount of torque necessary to deflect the suspension reduces. As the length of the crank is increased, the location of the force moved further out, but the gear ratio didn't change. In the actual hardware the relationship between the wheel center to motor pinion length and the upper connecting rod mounting location have a

larger impact on displacement versus torque than the crank length. Another goal of the modeling was to determine how much force a system such as this one would be capable of generating while actuating the suspension.

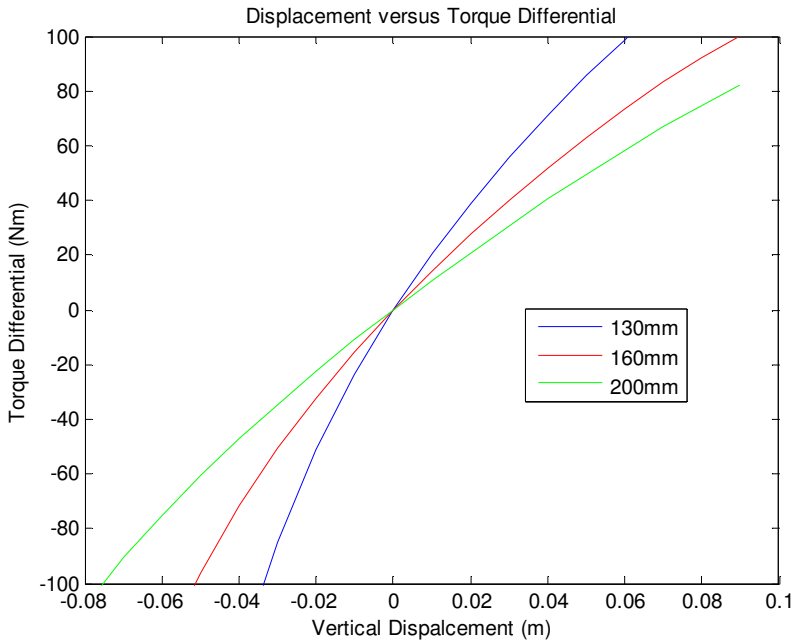

Figure 3-7 Kinematic analysis of motor torque versus vertical displacement of the vehicle body

Figure 3-8 shows force in the connecting rods as a function of the primary motor torque. As the system operates in jounce the force in the connecting rods is nonlinear. This is caused by the compression of the spring coupled with the mechanical advantage of the crank portion of the mechanism. This causes the connecting rods to experience a larger load and increased force. Over the range of torque that can be applied by the design motors, the connecting rods experience a peak load of just under 4kN. During rebound travel the DEDS mechanism doesn't need to compress the spring, but it has to be able to

support the additional load from decompressing the spring. The maximum travel is reached with only 2kN of force in each connecting rod.

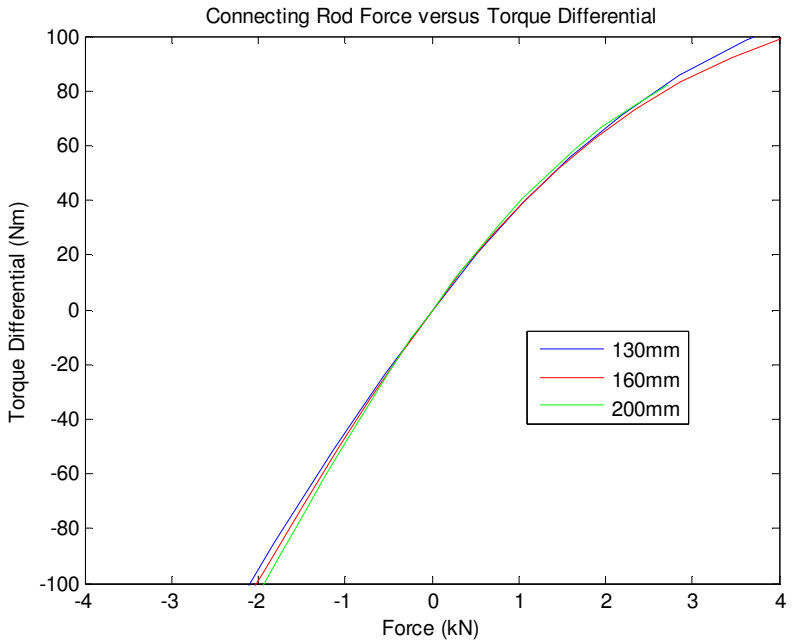

Figure 3-8 Kinematic analysis of motor torque versus force in the connecting rods for a varying lower link length

The planar kinematic model provided the initial desired sizing of the system. It showed that the system would be able to actuate the vehicle body throughout the range of motion with motors capable of provide 50Nm of steady state torque. It also provided some initial loading conditions for all of the components that helped facilitate the solid modeling and design of the three dimensional system. With satisfactory results obtained through the kinematic analysis, the next step was to generate a 3D model that consisted of a design that was feasible for implementation on a vehicle.

3.2 Hardware Design

The goal of the design is to have hardware that is ready to be implemented into a test vehicle. In an effort to reduce prototyping costs and to reduce the complexity of the initial data analysis and control design, it was decided to explore the application of a DEDS system to the rear of a vehicle. The design began by exploring the amount of room available for such a system in a small vehicle. Certainly a vehicle could be designed with a system such as this in mind, but a goal of the design is to be able to implement this system in existing body structures. After evaluating the available space for the suspension and wheel in several compact vehicles it was determined that a trailing arm style suspension would be a good base to start with.

A semi-trailing arm provided room for the mechanism to tuck inside the wheel without the interference of any control linkages. The semi-trailing arm can also be designed to facilitate camber change throughout the range of travel which is desirable for cornering performance. It is also a proven system that has been implemented in many vehicles, although it has been neglected with the recent move to multilink or twist-beam rear suspensions in front wheel drive vehicles. Simplification of future modeling required that two sets of hardware be designed. One design would be the passive suspension and vehicle body that would serve as a benchmark in simulation that the DEDS system could be measured against. The second design would be built upon the passive system to maintain identical camber and toe curves versus travel.

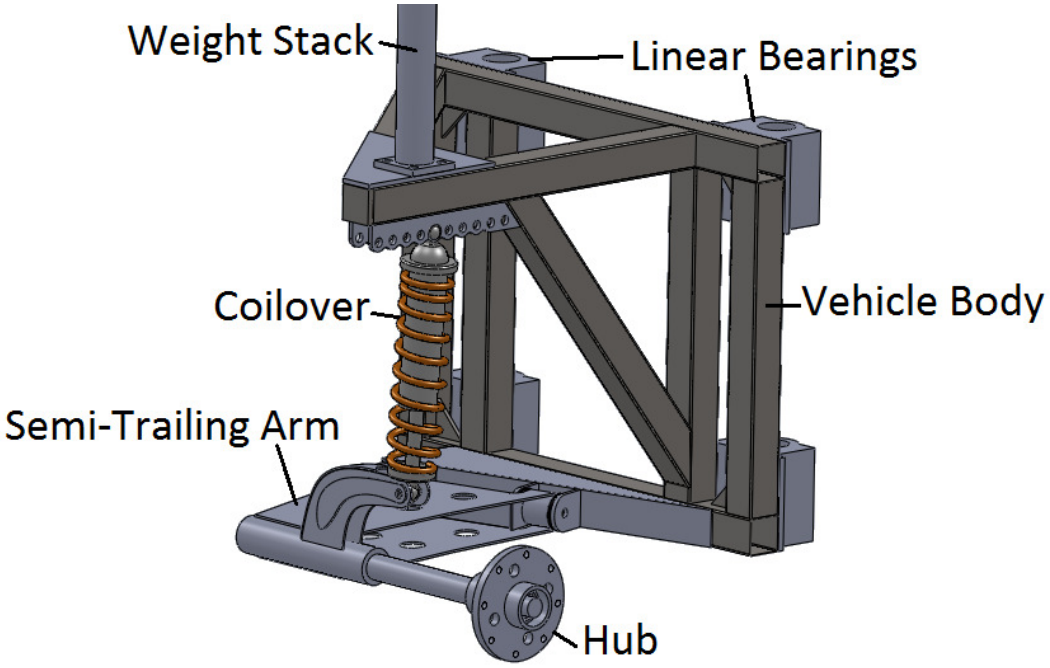

Figure 3-9 Passive suspension design and test vehicle

The passive system consists of a semi-trailing arm, a custom hub, a commercially available coilover shock assembly, and a quarter vehicle test structure (Figure 3-9). The trailing arm is designed with 1/8" thick steel formed into a box structure. The shaft leading to the hub is designed to allow the mounting of the motors. Two polyurethane bushings are used to provide the rotational degree of freedom for the suspension arm. They also provide a mechanism for helping to absorb some of the energy from any potential longitudinal and lateral disturbances. The weight of the vehicle is supported by a coilover assembly. The coilover was selected due to its small footprint and adjustability. The vehicle body test structure was designed to support both the passive and DEDS equipped suspension. Four linear bearings are used to constrain the vehicle

body to vertical motion. On the top of the vehicle structure is a rod to support weights to determine the system's response to varying load conditions.

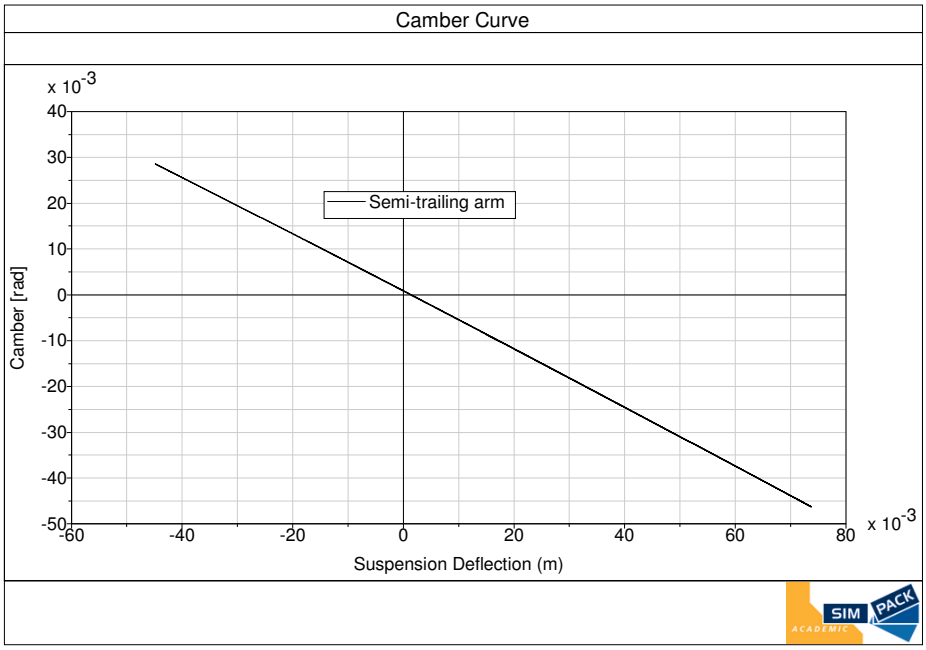

Figure 3-10 Semi-trailing arm camber curve

The semi trailing arm provides a mechanism for controlling camber throughout the range of travel. In this setup the semi-trailing arm was designed to provide negative camber as the vehicle suspension experienced jounce. Figure 3-10 shows the camber with respect to the suspension deflection. The design also causes the wheel to experience a positive camber condition when the suspension is excited in rebound. The system also experiences a change in the toe angle of the wheel. Around equilibrium the tire experiences a slight bit of toe out which is undesirable in a passenger vehicle. As it travels the wheel returns to toe-in. The design generates a range of +/- 0.004 radians

of toe over the entire 130mm of travel. The trailing arm could be modified to bias the toe angle to modify the operation so that the wheel is always experiencing toe-in, but this complicated the manufacturing of the prototype so the change was not incorporated as full vehicle dynamics are not explored.

Figure 3-11 Semi-trailing arm toe versus suspension deflection

The passive system provided acceptable kinematics and left room for the addition of the DEDS system. The first step in designing the actual hardware for the DEDS was to select a motor capable of driving the system. In order to facilitate rapid control a low inertia ac servo motor was selected. The power that was found during kinematic analysis earlier was not possible within the research budget, so a slightly underpowered pair of motors was selected. Baldor BSM100N-2150AA motors were selected. These motors fit

the requirements for fitting inside a 16 inch wheel, rapid control possibility, price, and they have a matched drive and resistive brake available. These motors individually are capable of 23Nm of steady state torque and 92Nm of peak torque for a period of 3 seconds. The drives match the motor in terms of supply current and time limits. A timing belt was selected as a method for transmitting the power from the motors to the main drive. Toothed drive belts are conducive to harsh operating environments, require no lubrication, and are fairly quiet. This required that the motor mounts have adjustability to tension the belt.

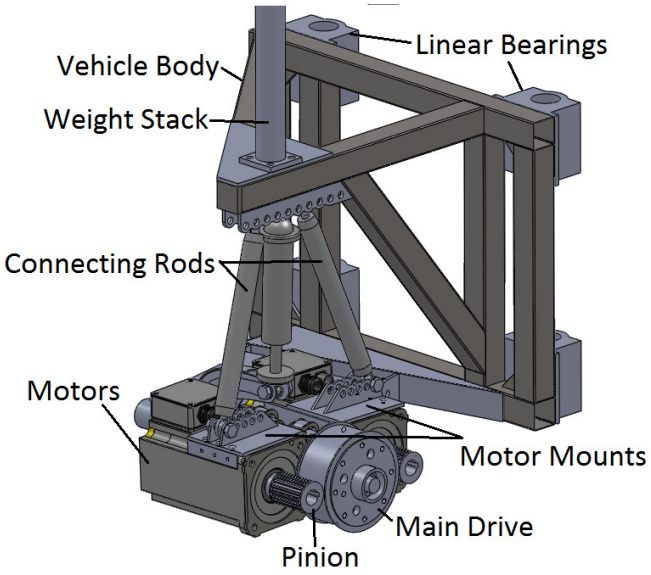

Figure 3-12 DEDS Hardware model with vehicle body attached

Figure 3-12 shows the full vehicle test system with the DEDS installed. The passive system is the base and the DEDS hardware installs directly to the existing structure. The DEDS consists of the two motors and their motor mounts (cranks). It also has a main

drive pulley that attaches to the hubs and two connecting rods to complete the mechanism. The connecting rods are designed to use spherical rod ends on both sides to cope with any misalignment. The drive belt is not shown in Figure 3-12 so that the drive pulleys and motors are more visible. The timing belt system required a modification to the gear ratio. Commercially available pulleys and belts required that the system be changed to a 2.82 final drive ratio. Since this design is built directly around the passive system it experiences the same camber and toe kinematics. The idea behind the design was to use as few custom parts as possible to reduce cost and development time. The hub uses commercially available automotive grade bearings and seals. The only custom parts are the hub, motor mounts, connecting rods, and trailing arm.

The two most complex parts are the motor mounts. The toothed belt requires a large amount of tension. The motors must pivot around the main drive pulley to maintain the tension. There is also a concern about belt alignment to maintain optimal operating conditions for the belt. A simple method was incorporated into the mounts to provide the adjustment. Four identical belt tensioners were built and added to a motor cage. These tensioners utilize a bolt to push the motor away from the central pivot. This tensions the belt and positively holds the tension. Clamping bolts were then utilized to lock down the mechanism and prevent any changes due to vibrations. The use of these mounts allow for the pinions to be moved over 15mm each. This provides adequate belt preload and leaves room for any adjusting out any stretching that may occur. The

system pivots about the hub utilizing bronze bushings. There is very little angular change in this system and the bronze bearings fit the load profile and the packaging requirements.

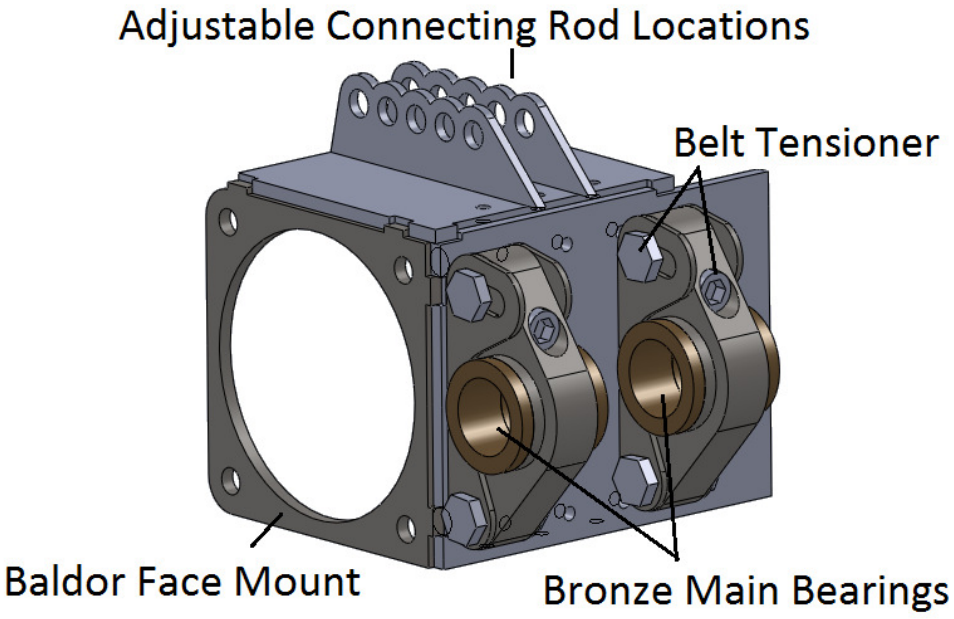

Figure 3-13 M1 motor mount with tensioning mechanism and main pivot bearings

This three dimensional model facilitated the use of multi-body software. Through solid modeling it was possible to ensure clearance of moving parts, specify parts and assemblies for manufacturing, and to obtain masses and inertias for the individual parts to facilitate increased accuracy in the multi-body model. The final hardware assembly was built directly from the solid model. This produced a system without any collisions and with the correct kinematics to match the simulation models.

3.3 Multi-body Dynamic Modeling

The multi-body dynamic modeling utilizing Simpack® software simplifies the modeling process for complex dynamic systems. The software accounts for the dynamic properties of each individual piece based on the design shown in section 0 and provides accurate results for forces, torques, and response to inputs. The forces and torques for each part and joint in the Simpack® simulation are then used to complete/verify the structural design of the components. The response to inputs in the simulation allows for control design and simulation. So in this sense the multi-body model provides two important functions for the design of the overall system. The first is to help ensure that individual components of the suspension/drive system can withstand the forces applied to them. The second is that it provides a low cost, rapid development platform for a system controller. The following will focus first on the actual setup of the model and then the co-simulation between Simpack® and Simulink®.

3.3.1 Model Setup

The Simpack® modeling software uses several building blocks to generate a model. The initial reference is what is referred to as *Isys*. *Isys* is the inertial reference frame for the entire model, essentially the ground. Bodies are the next largest of the building blocks used in Simpack®. A body represents an individual part in Simpack®. It contains the 3D geometry, mass and inertia properties, and also connection points known as markers. Each body can have one and only one joint. A joint is a method of attachment to

another body or *Isys*. These joints can take many forms, from a single degree of freedom to a six degree of freedom connection and are represented in a block diagram by an arrow. The direction of the arrow is important because it defines the 'to' and 'from' bodies. This means that the reference frame for the degrees of freedom associated with the joint will be with respect to the 'from' body's reference frame. All other connections must be made in the form of constraints. Constraints are exactly what they sound like. Each constraint can constrain a connection in up to six DOFs and are represented by a capacitor or damper symbol. In this model constraints are used to define the drive system. They represent a torque to torque coupling between the pinions and drive gear. The torque to torque constraint model in software also constrains the angular position of the respective bodies to represent a gear interaction without any engagement dynamics. This means that the pinions are driven with torque T_p and the drive gear is driven with the pinion torque multiplied by a gear ratio (n_g) as shown in equation(3.25). All other dynamics of the actual coupling system are neglected. The last major modeling element used in this model is a force element. These are the springs, dampers, and time excitations via external forces.

$$T_d = n_g T_P \tag{3.25}$$

The model begins with a simple block diagram to layout the actual model that will be built in Simpack®. The block diagram for the system utilized here can be seen in figure

3-14. In this model the longitudinal degree of freedom of the vehicle is removed from the model, but the tire can still spin to represent the longitudinal DOF.

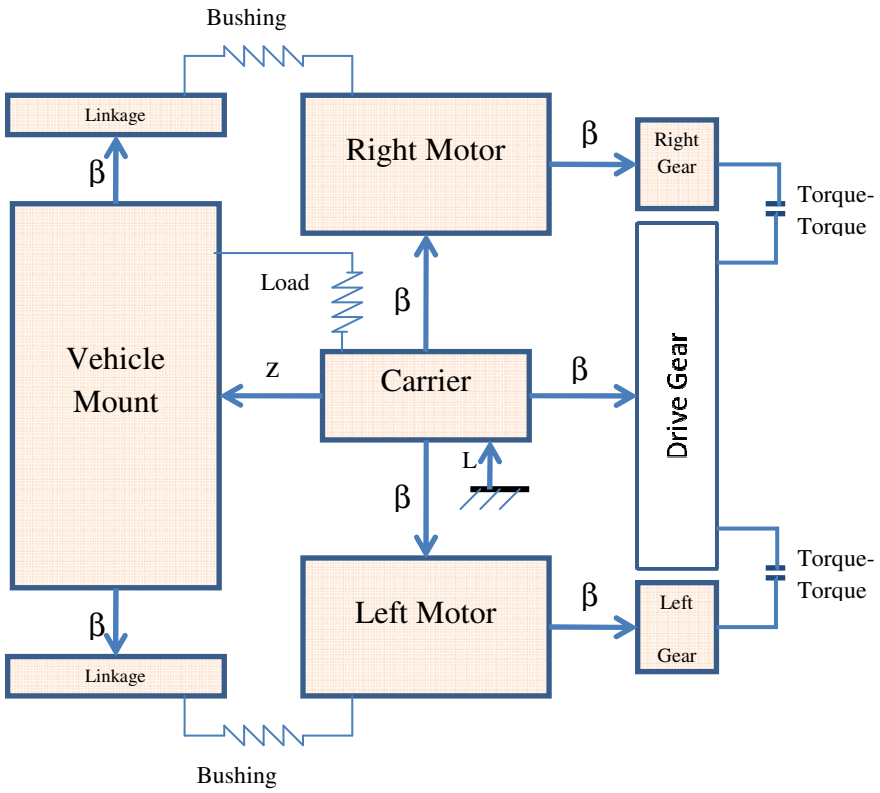

Figure 3-14 Simpack® Block Diagram

With the block diagram finished, the model can be built in Simpack. The bodies for each part are imported via a CAD interface that allows the correct 3D shape to be represented. Direct import from CAD software allows the physical shape of the part to be represented in the software aesthetically, but having the actual design files allows for each part to have appropriate mass and inertial properties defined in the simulation.

The joints and constraints can then be added to ensure proper kinematic functionality of the model.

3.3.2 Tire Modeling

Tires are very complex and difficult to accurately model. In the multi-body modeling environment it is possible to model the tire in several different ways. The initial tire was modeled as a massless point follower with a spring and damper (Figure 3-15) coupled with a reflected inertia that represented the quarter vehicle. The tire stiffness is represented by K_t and the damping is represented by C_t. Typically K_t will be an order of magnitude higher than the suspension stiffness [6]. This simple tire model neglects all rolling dynamics making it invalid for longitudinal and lateral system testing. Simulations requiring the system to accelerate on a road surface will require a more complex tire model.

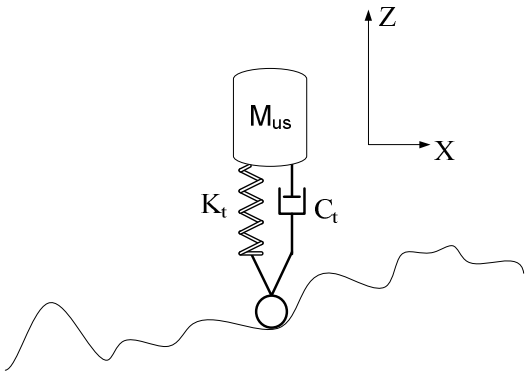

Figure 3-15 Massless point follower tire model

A widely accepted model for basic tire dynamics is the Pacejka similarity model [58]. This model represents the lateral and longitudinal slip characteristics of a tire allowing it to be utilized for simulations that require tire contact with road while moving. There are many other suitable models that could be used during these simulations. Pacejka, Oosten, Hall, and many others are continually working to develop more accurate tire models [59-62]. The similarity model is one of several that was readily implemented in Simpack. The software also has available the Pacejka Magic Formula model, HSRI, Delft MT/Swift, and the RMOD-K tire models. The similarity model was chosen for its simplicity as well as ease of implementation in the modeling environment.

4 System Dynamics

As a coupled system, the DEDS needs to fulfill the roles of both the vehicle drivetrain and the suspension. The drivetrain requires the system to be able to accelerate the vehicle, maintain a constant velocity, and to decelerate the system. As a suspension the basic purpose of the DEDS are to locate the tire, maintain tire to road contact, maintain suspension working space, control the attitude of the vehicle body relative to the ground, and to isolate the sprung mass from road disturbances. Due to the coupling of the two smaller actuators, the DEDS utilizes tradeoffs to try and maximize the performance of the overall system. It is important to evaluate the impact of the hardware on the passive system performance, as well as to determine the single degree of freedom performance that is available. Considering these extremes of actuation in both directions, the system can be treated as a single degree of freedom system and individual system analysis and controls can be developed.

4.1 Longitudinal Dynamics

The DEDS system provides maximum longitudinal performance when both motors are utilized with the same torque direction and magnitude. During this operation the two motors can be treated as one for the generation of longitudinal force, and since the mechanism is almost symmetric there is almost no vertical actuation. The main variables in longitudinal performance are tire size (r_{tire}), gear ratio (n), and motor torque (T_m) assuming the vehicle properties remain constant.

$$F_{drive} = n(T_{m1} + T_{m2})r_{tire} \tag{4.1}$$

The force imparted at the contact patch is given by equation(4.1). The full hardware model was simulated in Simpack over a track surface with a Pacejka tire model and aerodynamic drag and rolling resistance. The results are shown in Figure 4-1and Figure 4-2 for three different torque levels. The peak torque of the available hardware was applied and achieved a performance of 0-100kph and back to 0 in under 15 seconds. That is an acceleration of over 13m/s^2, which is only feasible because there is unlimited friction in this model. The motors and drives will not support this length of time at these currents, but for short bursts under 3 seconds, the motors could support improved performance. The design torque found from the planar kinematic model that would achieve full vertical actuation was applied. This 50Nm torque achieved the same goal in just over 25 seconds with an average acceleration of 7.2 m/s^2. The steady state torque from the available hardware was able to finish in just over 56 seconds with an average acceleration of 3.4m/s^2. Of course the motors that are chosen for the hardware are not actively cooled; with the addition of active cooling they could sustain higher torques for longer periods of time. Also, in a production environment, quantity would be on the side of the builder and custom gear ratios could be utilized to tune performance.

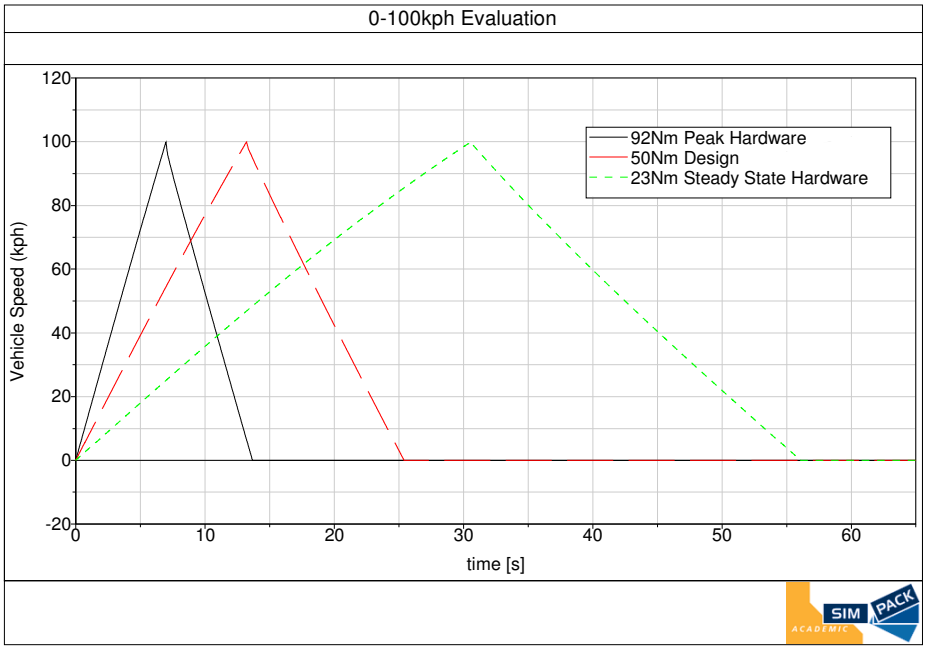

Figure 4-1 0-100kph-0 simulation results including rolling resistance and aerodynamic drag of the quarter vehicle software model

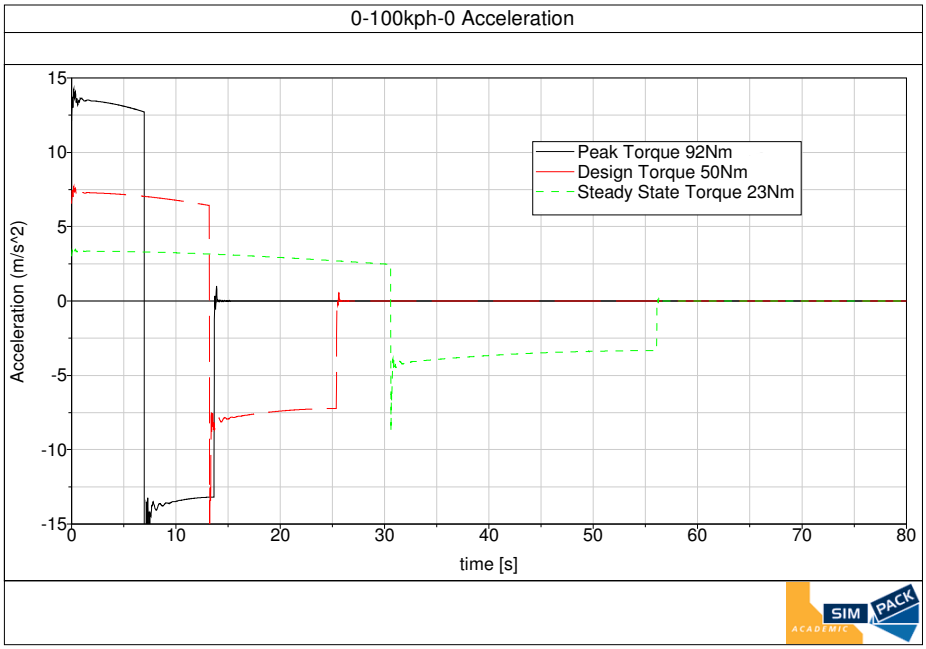

Figure 4-2 0-100kph-0 Acceleration data including rolling resistance and aerodynamic drag of the quarter vehicle software model

4.2 Vertical Dynamics

The physical suspension design is a semi-trailing arm and a coilover shock. The semi-trailing arm provides the physical locating of the wheel while the coilover provides the passive weight carrying capacity as well as a minimum level of damping. Evaluating a suspension design can take many different forms ranging from simple two degree of freedom models, to shaker tables, to subjective evaluation. Due to the desire to relate the DEDS configuration to a purely passive system, the two degree of freedom models are surpassed for multi-body dynamic models of the actual hardware design. Shaker tables are not only utilized to test the hardware, but are also modeled in the simulation system. Subjective testing is left for the future when a fully vehicle implementation is

possible. To keep both models similar, the mass of the DEDS system was added to the test structure for the passive system to emulate a conventional drive configuration. Both systems utilize the same damper and spring configuration as well as tire model values.

The passive suspension model and the non-actuated hardware will be tested by exciting them vertically with two different styles of road inputs. Regular road inputs such as constant frequency sinusoidal displacements and swept frequency sinusoidal displacements are used to evaluate the basic configuration's vertical response. Further simulation and testing occurs with the application of random road inputs. These inputs vary from a smooth runway to a gravel road as defined by the Society for Automotive Engineers. Irregular inputs are used to evaluate the comfort of the system similar to that which would be seen by a passenger and a vehicle equipped with such a system. The idea behind these tests is to determine the impact of the additional hardware on the overall dynamics of the vehicle system.

4.2.1 Response to Regular Road Inputs

A suspension system can be measured by its ability to isolate the sprung mass, operate within the suspension design space, and by road holding [6]. In many instances initial evaluation of these performance metrics is considered by ignoring the physical suspension layout and only considering a two mass system with the appropriate springs and dampers. Since a three dimensional model has already been generated, the full

multi-body models of both the passive suspension and a non-actuated DEDS system will be evaluated.

$$Transmissibility = z_s / z_r \tag{4.2}$$

The isolation performance of a suspension system can be evaluated by looking at the transmissibility ratio between the road vertical disturbance (input) and the vertical deflection of the sprung mass (output) seen in equation (4.2). Where z_s represents the vertical displacement of the sprung mass from its equilibrium position and z_r represents the vertical displacement of the road input. Figure 4-3 shows the transmissibility ratio for a quarter vehicle model with and without the DEDS hardware when actuated with a swept sinusoidal signal from 0.01Hz to 25Hz. The body natural frequency is excited between 1 and 2Hz as would be expected of the suspension, but the DEDS configuration lowers the body frequency from a typical layout. The passive system without the DEDS system attached filters out the wheel natural frequency. The additional coupling of the DEDS hardware without control or actuation generates an additional mode around 7Hz which is undesirable. The addition of the mass and inertia of the motors coupled to the drive cause these shifts in vertical response.

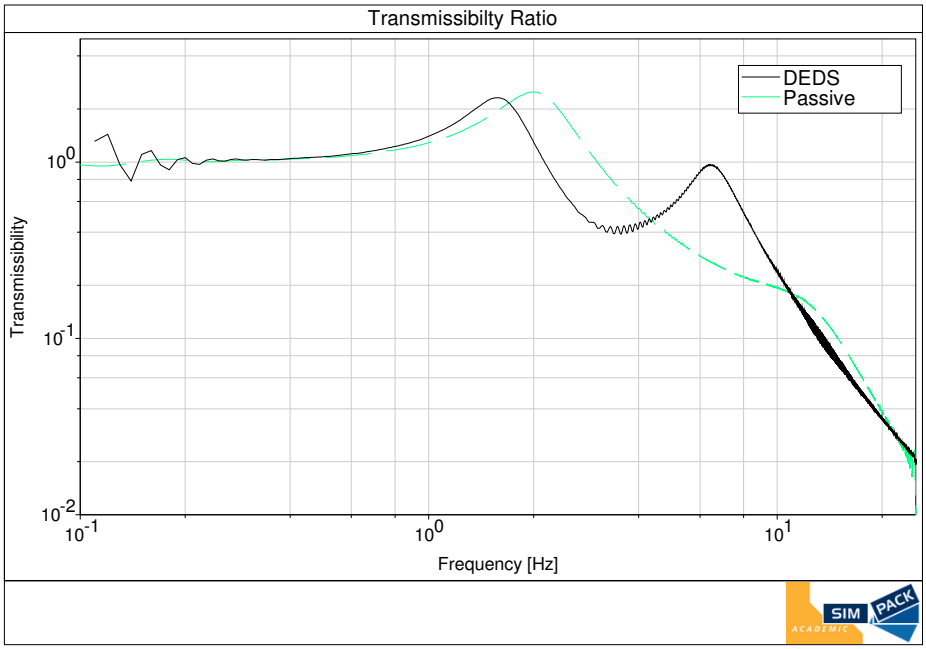

Figure 4-3 Transmissibility ratio as a function of frequency for a quarter vehicle software model with and without the DEDS hardware installed system.

The suspension travel ratio (STR) helps designers to determine the packaging space required to facilitate the vehicle suspension. It is defined as the ratio of the suspension's deflection to the vertical road input. The location of bump and rebound stops can be determined by looking at the necessary "rattle space" and then moving further so as to prevent the suspension from reaching its mechanical limits. The STR can also be useful in damper design as many modern dampers and springs are progressive rate systems. The location of the transition between different damping rates can be determined in part by evaluating the suspension's travel over a varying frequency. Figure 4-4 shows the trailing arm suspension systems STR versus frequency for a passive configuration and also with the non-actuated DEDS hardware in place. Again the

motors are not actuated for this simulation and only the dynamic impact of the design is evaluated. As was the case with the transmissibility the DEDS shifts the body mode to a lower frequency and it also accentuates a higher frequency mode around the 6Hz range. Above 8Hz the addition of the DEDS reduces the STR. The DEDS system also reduces the suspension's ability to filter out lower frequency disturbances and tracks the road input more than a passive system below 0.25Hz.

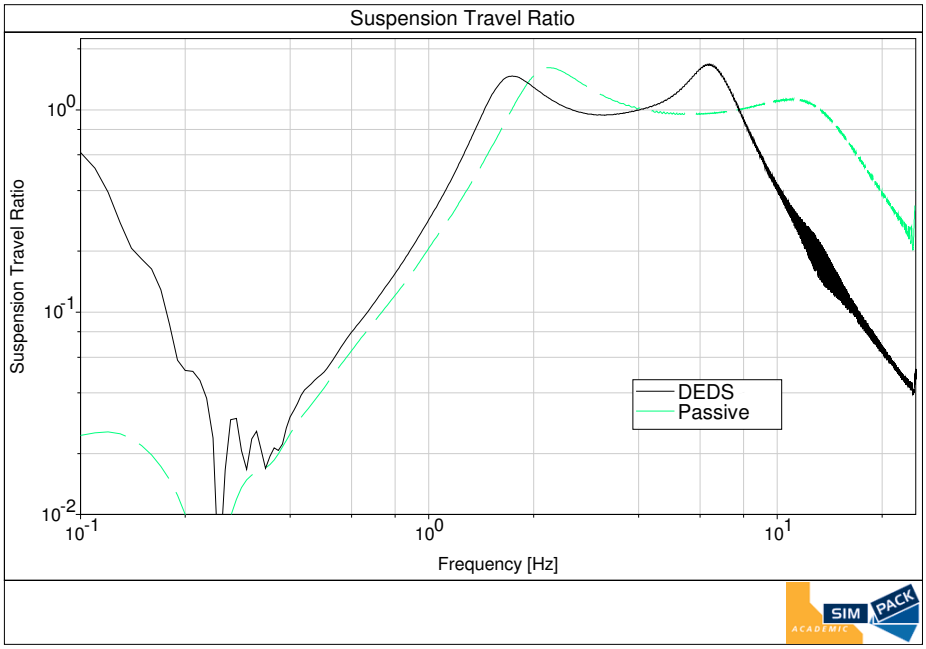

Figure 4-4 Suspension deflection ratio as a function of frequency for a quarter vehicle suspension software model with and without the DEDS hardware installed

A very important aspect of a vehicle suspension system is its ability to maintain adequate tire to road forces to facilitate any maneuvers that are necessary to maintain the vehicle's desired trajectory. This is evaluated by considering the road holding ability

of the system. This is defined as the maximum tire deflection divided by the road displacement for a given input. Figure 4-5 shows the road holding of a system with and without the DEDS hardware excited over a range of frequencies from 0.01-25Hz. At lower frequencies the DEDS hardware has little effect on the ability of the system to maintain sufficient road forces, but at the lowered wheel hop frequency the system experiences a reduction in road holding ability over a system without the DEDS linkages in place. The same shift and amplification can be found in systems with an increased unsprung mass to sprung mass ratio. The additional mass of the motors is not purely unsprung but does increase the effective unsprung mass.

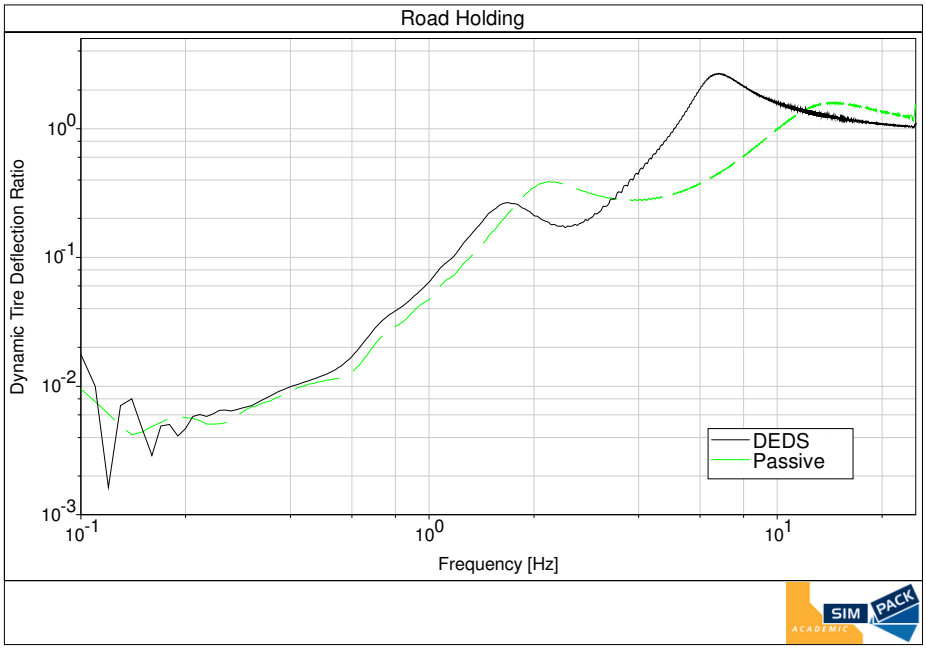

Figure 4-5 Road holding as a function of frequency for a quarter vehicle software model with and without the DEDS hardware installed

Each of these evaluations has an impact on the overall system performance. The transmissibility ratio relates directly to passenger comfort by evaluating the isolation ability of the suspension. The STR not only helps to define the packaging requirements, but also evaluates the ability of the system to recover to a neutral position after a disturbance. A system with this ability doesn't experience packing, which is where a suspension which experiences repeated disturbance inputs is pushed closer and closer to its physical travel limits and eventually will reach them without adequate time to recover to a neutral position. The road holding ability is arguably the most important aspect of a suspension system. Without adequate road holding the vehicle becomes unsafe for operation. Even with these three metrics to evaluate a suspension, only a small portion of what a suspension system is required to accomplish is evaluated here. These metrics ignore the reliability of the hardware and also don't take into account any of the lateral and longitudinal handling characteristics of the entire vehicle system. They also ignore pitch, heave, and roll.

4.2.2 Response to Irregular Road Inputs

Roads are not perfect sinusoidal signals like those used earlier to test the isolation, deflection, and road holding performance. There are many different road surfaces and the condition of these road surfaces vary with material, quality of construction, use, and maintenance. The Society of Automotive Engineers and ISO have come up with two remarkably similar descriptions for the condition of a road with respect to vertical disturbances. Both systems rely on the spatial frequency and the power spectral density

to classify the road surface roughness. Spatial frequency is utilized as it is independent of the velocity traveled. For the purposes here, the SAE definition of road surface roughness will be utilized. It was found by [63] and [6] that the road surface roughness as classified by SAE could be approximated by (4.3). $S_g(\Omega)$ is the spatial power spectral density of the vertical road displacement. C_{sp} and N are road dependent constants and Ω is the spatial frequency in cycles/m.

$$S_g(\Omega) = C_{sp}\Omega^{-N} \tag{4.3}$$

Evaluation of the passive system and the addition of the DEDS linkages take place using three different road profiles as defined by (4.3) and Table 4-1. Using these inputs on a quarter vehicle model, neglects the pitch, roll, and wheelbase filtering that can occur in larger models. They do however give a method for evaluating the ride comfort of the simplified model using ISO 2631 reduced comfort boundaries. These boundaries are proposed exposure limits to vertical and longitudinal accelerations over a wide range of frequencies.

Table 4-1 Road description values for calculating the spatial PSD[6]**.**

Description	N	C_{sp}
Smooth Runway	3.8	$4.3\text{x}10^{-11}$
Smooth Highway	2.1	$4.8\text{x}10^{-7}$
Gravel Road	2.1	$4.4\text{x}10^{-6}$

In building a road profile from the prescribed spatial PSD estimation, the length of the road is important. A base length of 2km was chosen as the measured section of road to be compared to the road spatial PSD description. The longest wavelength of excitement described in the SAE and ISO road classifications is 100m. The 2km base length provides more than adequate distance for the appropriate sampling to obtain these low frequencies. It also provides reasonable vertical displacements over the range of frequencies of concern. When the base length is shortened the vertical displacements must be increased to contain the same power levels. Likewise when the base length is extended the vertical displacements must be reduced or the power levels with not match with the SAE description. In some cases simulations require longer road profiles and those are built by placing the base road back to back until the appropriate length is built.

4.2.2.1 Vertical Comfort Performance

The three roads described in Table 4-1 are utilized to drive the simulation and the actual hardware on a single post shaker. Evaluation of both the models and the actual hardware over the three different road cycles results is performed by analyzing the frequency response over the entire test range. Rather than considering road handling and suspension deflection the irregular road responses are evaluated using ISO comfort criteria. The ISO comfort criterion utilizes exposure limits to RMS vertical and longitudinal accelerations over a range of frequencies and times. Higher RMS accelerations are tolerable over short durations while lower RMS accelerations are

acceptable over a longer time range. The ISO comfort criteria define several different curves for different exposure times. For the purposes of exploring system performance, the damping and spring rate are defined as those available on the prototype hardware and have not been fully optimized based on system performance. The coilover has several discrete damping rates and as such a reasonable rate was chosen. The damping rate provides a minimum performance level for the suspension in the situations where all of the motor power is required for rotational actuation.

When a smooth highway road profile was applied to the passive system, the system exceeded the proposed limits at the two and half hour exposure time at 7Hz and 11Hz. The addition of the DEDS linkages and motors degraded the overall performance and actually exceeded the ISO one hour exposure limit at 7Hz. This is without any actuation of the motors to try and improve system performance. Both systems utilized the same spring and damper settings as a common element in the analysis. The systems performed similarly on the remaining two road profiles.

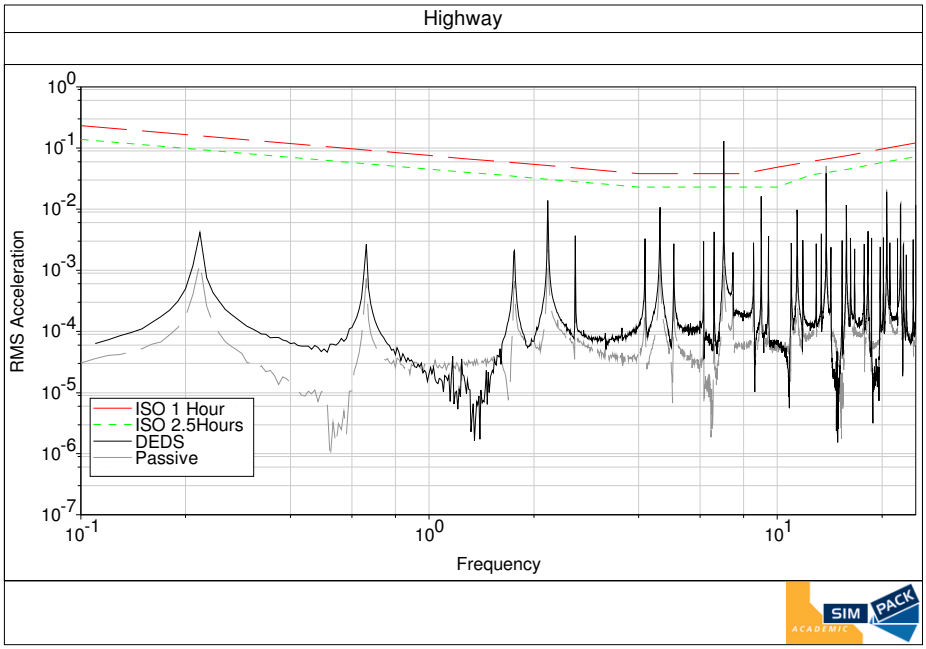

Figure 4-6 ISO 2631 evaluation of both the passive and DEDS hardware equipped software model

This method of testing is only viable for the quarter vehicle model as it ignores pitch, roll, and heave. There is also no accounting for additional spring and damper systems that can be used to describe the seats or any cabin isolation that could be used in a full vehicle. They do show that the addition of the DEDS linkages and motor inertias degrades the vertical dynamics of the system, but they do not have a large impact on the ride comfort that could be seen by the passengers. Certainly, a vehicle suspension should be able to remain below the eight hour ISO comfort curve for a smooth highway, and with an optimized spring and damper combination either of these two systems could reach that level.

4.2.3 Vertical Actuation

Of course the DEDS system wasn't created to be attached to an existing suspension system and not be actuated. The longitudinal actuation was already explored in section 4.1. Here the vertical actuation performance of the system will be explored. As equations (1.3) and (1.4) show, if torques of equal magnitude and opposite direction are applied to the planar mechanism, the system will actuate solely in the vertical degree of freedom. To explore the system's coupling between the two degrees of freedom and its ability to actuate the actual hardware model vertically, a simple system that applies torques that oppose each other is explored. When the system is actuated at the steady state torque values available by the selected prototype hardware of 23Nm, it was possible to actuate the vehicle body vertically by a peak of 20mm. This occurs at the body frequency of 1.65 Hz. Beyond this the response of the sprung mass falls off drastically. As the torque was increased towards the peak level, the amount of displacement that could be forced was also increased. Also, when the damper was removed from the system, such as would be the case if the DEDS system was to replace the mechanical damper, the system actuated to the physical limits of the hardware and the response did not fall off immediately after the earlier body frequency.

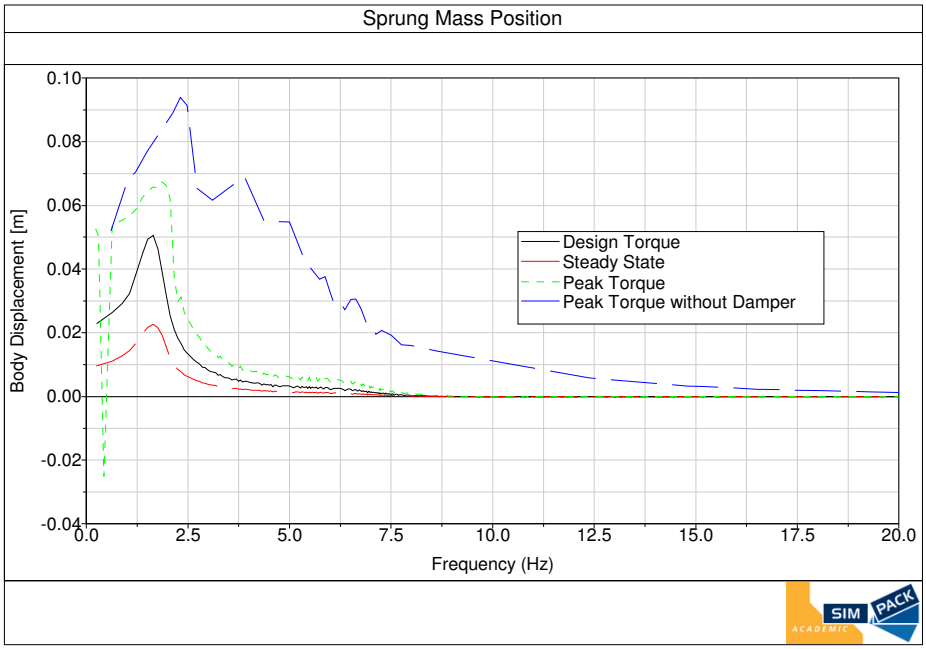

Figure 4-7 Sprung mass vertical actuation versus frequency of the quarter vehicle software model

Of course the system operates between the unsprung mass and sprung mass, so one cannot be actuated without impacting the other. Figure 4-8 shows the response of the unsprung mass when the actuation is applied. The system causes the tire to deflect and the unsprung mass to move around its steady state location.

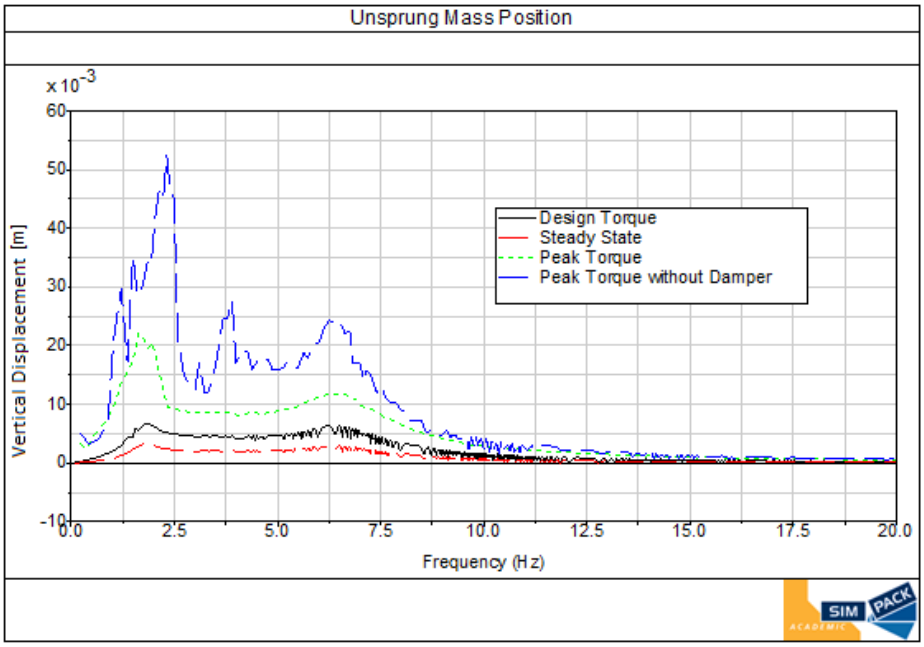

Figure 4-8 Vertical actuation of the unsprung mass with respect to actuation velocity of the quarter vehicle software model

Since the system is coupled and what is represented here is the actual hardware design in a multi-body simulation environment, these simulations also provided information into the asymmetry of the design. Ideally, when both motors are provided equal magnitude torques with opposing directions there will be no rotation of the wheel assembly. In these simulations the wheel vertical dynamics are represented as a massless point-follower. The wheel and tire itself are left free to rotate with no drag of the actual road contact to slow them down and without the additional inertia that was used previously to simulate the quarter vehicle model. During vertical actuation the rotational degree of freedom was actuated to a peak velocity of only 1.5rad/sec. This coupling is considered excessive, but only occurs when the wheel has no drag or loading

conditions. A more reasonable evaluation of the coupling will occur when the system is tested in its entirety and a more complex tire model is utilized.

The DEDS system impacts the ability of the suspension to perform the role of vibration isolation and its ability to maintain the same working space when compared to a passive suspension of similar design. It did however improve road holding at lower frequencies and reduced the wheel hop mode magnitude with respect to handling, at the cost of additional higher frequency degradation. The coupled system, when actuated independently in each degree of freedom showed minimal cross coupling between vertical and rotational degrees of freedom for the models explored. The actuated system also displayed the potential to improve the overall system dynamics through the use of actuation assuming that an appropriate control system could be applied.

5 Energy Regeneration

A reason for the push to hybrid electric and electric vehicles is to reduce fuel consumption. Fully electric vehicles have limited ranges due to the lack of energy storage density in batteries and capacitors. Hybrid vehicles utilize smaller storage units and can be forced to operate at inefficient levels in order to recharge the batteries to take full advantage of the electric drives. In order to extend the range and overall flexibility of vehicles with electric drives many have turned to various regeneration methods to recapture energy back from the vehicle system. The most popular method of regeneration is braking. There are also methods to recapture energy from dampers and thermal gradients that exist in vehicles, but they operate at much lower power levels than the brakes.

5.1 Braking Regeneration

Braking regeneration is a popular method for extending the range of electrically powered vehicles due to the amount of energy available and the simplicity of implementation. Generally in regenerative braking systems the electric drive motor can be switched from a drive configuration to a generator configuration. This equates to the addition of a small amount of additional electronics and controls and the existing hardware can recharge the batteries. The other reason that braking regeneration is so

popular is the shear amount of energy that is available to recapture. The kinetic energy of a vehicle in motion is very significant and with the appropriate system a good portion of this energy can be captured.

In a perfect world with no friction or drag, all of the energy that is expended to accelerate a vehicle would be available for regeneration during deceleration, and it could be captured by a system with 100% efficiency. Of course there are frictional losses, aerodynamic drag, rolling resistance, and regeneration inefficiencies that negate the perfect no net use energy vehicle. Braking regeneration only occurs during braking maneuvers. During braking, the amount of energy that is available for regeneration can be found by considering the change in kinetic energy and the drag forces. The change in kinetic energy minus the energy consumed by aerodynamic drag, rolling resistance, and frictional loses is the upper limit of available regenerative energy. In order to calculate the amount of energy used for propulsion and the amount used for braking over the three simulation driving cycles, the drive force is found. F_{drive} can be found using equations (5.1) - (5.3). If F_{drive} is positive then the system is consuming energy, and when it is negative the brakes are being utilized. The power utilized by the system can be found using equation(5.4). When P_{drive} is positive the system is consuming power, and when it is negative the brakes are engaged. This provides a way to find the energy that is available for regeneration. Using these equations it is possible to obtain an upper limit of available energy which would then be reduced by the efficiency of the regeneration hardware and control strategy as well as unaccounted frictional loses.

$$F_{drive} = ma + F_{aero} + F_{rolling} \tag{5.1}$$

$$F_{aero} = \frac{1}{2}\rho v^2 A C_D \tag{5.2}$$

$$F_{rolling} = c_r N_f \tag{5.3}$$

$$P_{drive} = F_{drive} \times v_{vehicle} \tag{5.4}$$

Variable	Description	Value	Units
m	¼ Vehicle mass	254	kg
ρ	Density of air	1.2041	kg/m^3
A	¼ Frontal area	0.5	m^2
C_D	Drag coefficient	0.33	
c_r	Rolling resistance coefficient	0.013	

Table 5-1 Longitudinal data for a quarter vehicle model

Using the values for basic city vehicle as shown in Table 5-1 it is possible to determine the maximum amount of energy that is available for braking regeneration for varying velocities and stopping conditions. Even though the amount of power versus braking force can be calculated, it is more realistic to utilize the aforementioned driving cycles to obtain the energy available. This method provides not only the power available for regeneration but also the power utilized by the system for propulsion. These are the same cycles that will be utilized to evaluate the DEDS system later. Figure 5-1 shows the power consumption of the model described in Table 5-1. Positive power indicates that the vehicle is consuming energy to perform the maneuver; negative power represents

energy that must be dissipated through the braking system. The worst case for braking regeneration is when a vehicle is operated in a highway environment with few braking operations. The two urban driving cycles experience numerous braking operations and are more suited for regenerative braking. The two urban driving cycles have the potential to regenerate over 30% of the energy consumed to propel the vehicle as shown in Table 5-2. The highway cycle on the other hand only has the potential for 5.9% regeneration from braking.

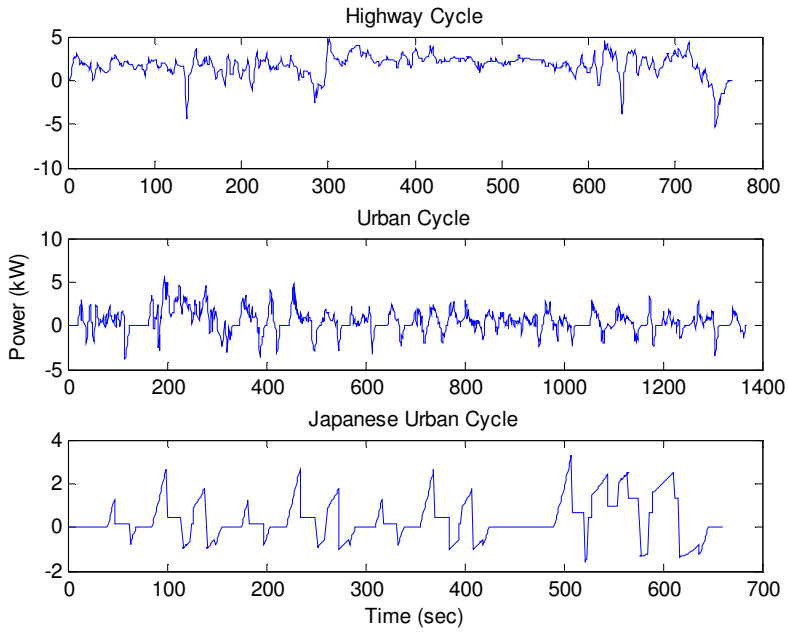

Figure 5-1 Driving cycle power consumption

Driving Cycle	Energy Consumed (kJ)	Braking Energy (kJ)
Urban Cycle	1,001.6	304.6
Japanese Urban Cycle	326.4	111.8
Highway Cycle	1,427.8	84.8

Table 5-2 Energy utilization for individual driving cycles of a quarter vehicle model

Braking systems consume a large quantity of energy and converts it to heat in order to slow and stop a vehicle. When these friction-based systems are replaced with other forms of braking, significant amounts of power are available for capture. With the appropriate controls and hardware the system's range should experience significant extension during urban operation. It was found that when operating at 100% efficiency, upwards of 30% of the energy consumed to propel the vehicle was available for regeneration. This falls short of the 40-60% that was found by Apter [51]. Of course braking regeneration can only occur during braking conditions, so it is important to also explore the available energy that can be found continuously in the damper of the suspension.

5.2 Damper Regeneration

It is possible to replace the damper with a system that performs the role of the damper while converting the energy into electrical energy instead of heat. This type of system provides a way to add continuous energy generation to a vehicle while it is moving. A

suspension damper functions by generating a force opposite to the relative velocity of its end connections(5.5). This force is typically generated by passing oil through small orifices in a piston inside the damper body. As the fluid is forced through these holes energy is absorbed from the system and converted to heat. The DEDS system, like several others ([50, 52]) has the ability to remove energy from the system and convert it to electrical energy which can then be used to provide locomotion or additional vertical actuation.

$$F_{damper} = v_{damper} c \tag{5.5}$$

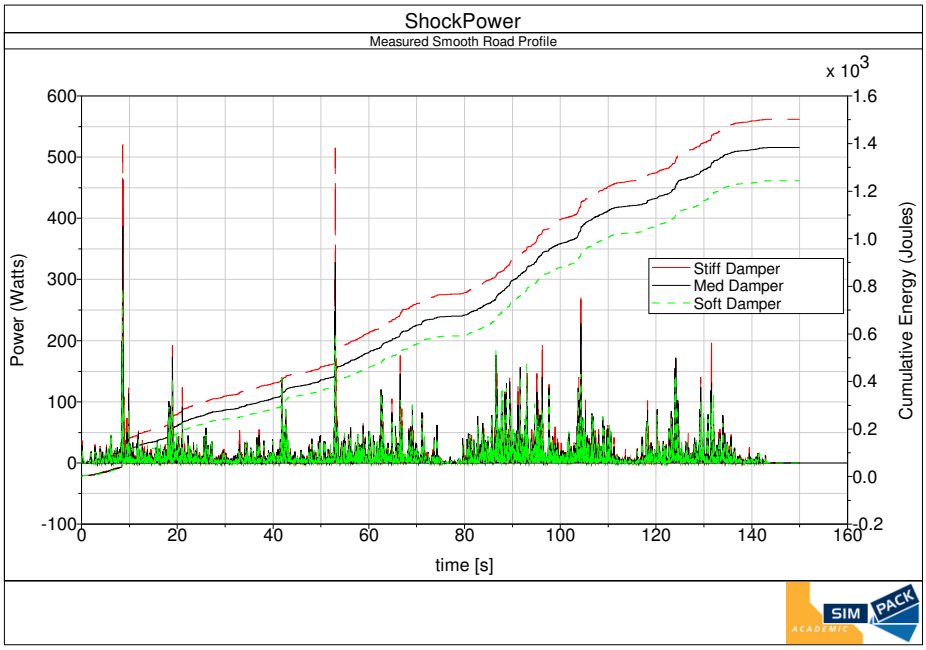

Figure 5-2 Energy consumed by a damper during a short smooth road simulation

There are many variables in determining the amount of energy that could potentially be recaptured from a suspension system. Any variable which impacts the ability of the

suspension to perform its functions impacts the ability of the system to provide power for regeneration. In order to narrow this down only a few variables will be explored. The damping ratio, the road surface roughness, and the ratio of unsprung mass to the sprung mass of the system all impact the amount of energy available for regeneration. The damping ratio and mass ratio are under direct control of the suspension designer. The road surface roughness is independent of the actual vehicle design, but does influence design as it pertains to the operating conditions that the vehicle design will encounter. If the system is viewed as a power generation plant, the damper is the generator, the road surface is the actual driving force, and the mass ratio affects the transmission between the two.

With the damper acting as a generator it is important to see how varying the size of the damper affects the amount of power that is captured. The amount of energy consumed by the damper in a passive suspension system over a real-measured road rated as smooth is shown in Figure 5-2. As the damping rate is increased there is an increase in the energy that can be harvested from the system. 1.5kJ of energy were harvested by the damper to be converted into heat over 150 seconds. If this energy capture rate was applied over the urban driving cycle explored earlier, 20.475kJ could be recaptured over the length of road. This equates to just over 11% of the energy that was available for braking regeneration. If it is applied to the highway driving cycle, damper regeneration could account for an additional 10.4% of available power for a smooth road profile. This is lower than the urban driving cycle due to the length of the simulation and amount of

power consumed to propel a vehicle at higher rates of speed. Of course the damper isn't just in place to generate power from vibrations; its main purpose is to improve the vertical dynamics of the suspension system. The regeneration levels presented here are for passive damper rates. It is possible to have a system that optimizes the damping rate to improve ride quality, or power regeneration. The two will not always be complimentary, so there is a tradeoff associated with tuning for one or the other[50].

Figure 5-3 illustrates that the roughness of the road surface has a large impact on the available energy. During conditions such as those found on high quality highways and runways as defined by SAE, there is very little available energy. However when the conditions degrade the amount of energy that can be captured increases dramatically. This is very promising as the road conditions in many large cities are very poor and a city based vehicle design could potentially see significant regeneration energy from the damper system. A highway with gravel as classified by SAE has the ability to provide 10 watts of regeneration power for the given quarter vehicle model when discrete disturbances are neglected. This regeneration potential will increase with the addition of the discrete disturbances that exist in road surfaces.

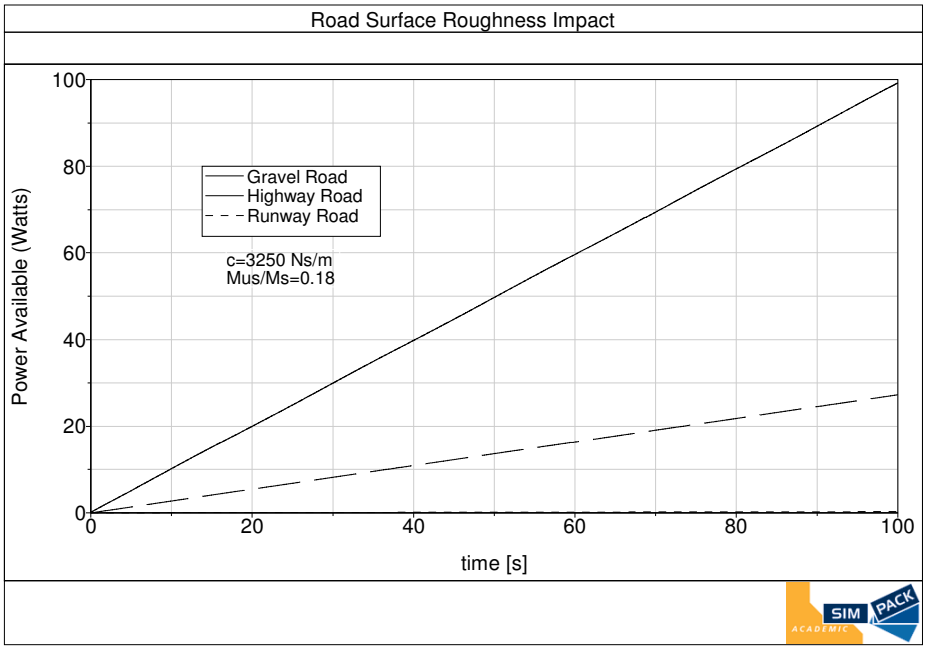

Figure 5-3 Impact of road surface roughness on available regeneration power in a suspension using a 3250 Ns/m damper

The DEDS system moves the mass of the drive system out from the vehicle chassis to inside the wheels. The hardware configuration increases effective unsprung mass and as such has the ability to significantly adjust the ratio of unsprung to sprung mass. This is due to the dynamics of the road to unsprung mass interface, or the tire. Increasing the unsprung to sprung mass ratio has a positive effect on damping regeneration; however it is not good for ride quality. Figure 5-4 shows the regeneration potential for a highway with gravel road surface for varying unsprung to sprung mass ratios. A typical passenger vehicle has a very low ratio, while systems with hub-centric drives and solid axles tend to have higher ratios. As the ratio of unsprung mass to sprung mass is increased the

trend is for the potential energy from a damper system to increase as well. The DEDS system has an equivalent unsprung/sprung mass ratio of around 0.18.

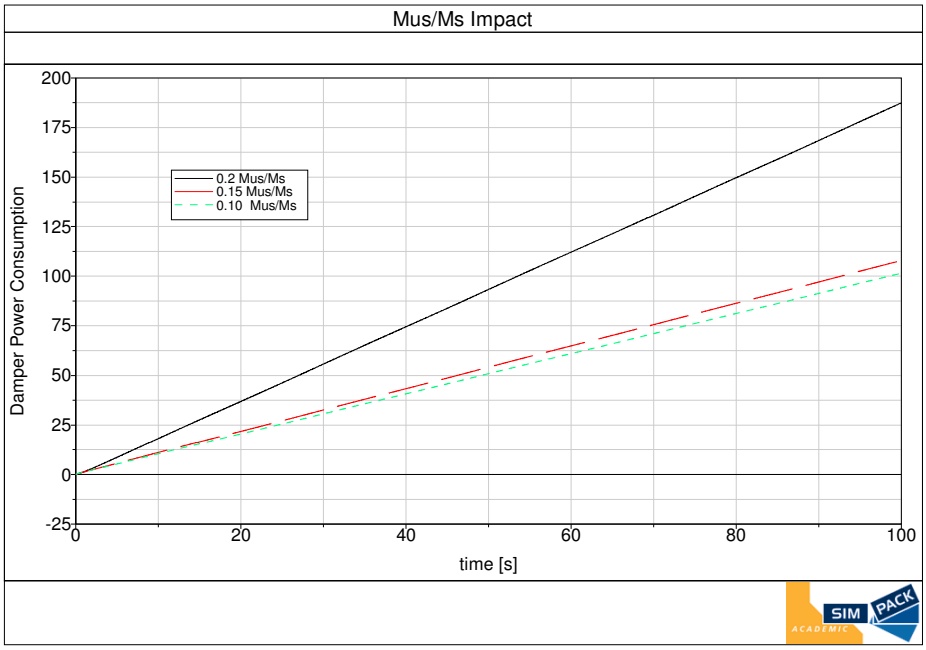

Figure 5-4 Impact of the mass ratio on energy regeneration through damping.

So as the unsprung mass increases and the sprung mass decreases, a vehicle experiences an increase in the M_{us}/M_s ratio. By moving the motors to the area inside the wheel, and directly connecting them to both the vehicle body and the wheel carrier the DEDS system reduces the sprung mass and increases the equivalent unsprung mass. The hardware configuration does not move all of the motor mass to become part of the unsprung mass. Instead a portion of the motors weight can be considered to be sprung and the rest is considered unsprung. Typically in suspension modeling, half of the connecting linkages are considered to be sprung and the other half unsprung. In the

case of the DEDS, the percentage is dependent on the mechanical layout. As the connecting rod location is adjusted on the motor mount, the equivalent unsprung mass is adjusted. The DEDS also provides the potential for a variable damping rate that could be utilized to optimize the regeneration performance based on the current operating conditions.

Overall, the braking regeneration shows the potential for 223 watts during city driving, while the damper has the potential to contribute over 15 watts. This equates to the ability to capture over 6.7% of the energy that is available through braking through the dampers. Unfortunately, this amounts to only 2% of the total energy used to propel the vehicle. Regenerative dampers have not gained traction in the marketplace due to these lower power opportunities. The DEDS system incorporates the ability to provide both forms of regeneration from a single piece of hardware, which could significantly increase the range and efficiency of an electric or hybrid vehicle, and also makes the system more attractive from a marketing viewpoint.

6 Control Development

The previous chapters have presented the system and its dynamics without any control system in place. The two degrees of freedom can be actuated independently as based loosely on the initial modeling equations (1.3) and (1.4). With the clear distinction between the two modes of operation, the control system was developed in steps. First the longitudinal control system was developed. For this system the torques were assumed to be equal in both magnitude and direction essentially acting as a single large actuator. Next the vertical deflection controller was developed. This controller applied the torques with equal magnitudes but opposing directions. Finally the two were brought together to form a coupled controller that allows for the independent control of both the rotation of the wheel and the vertical position of the vehicle body.

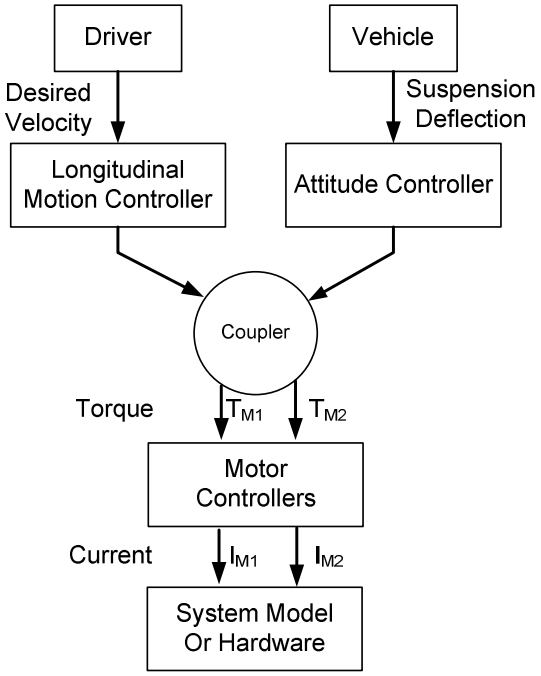

Figure 6-1 DEDS control architecture

The main architecture (Figure 6-1) utilizes two input models. In a full vehicle attitude control system there will be an algorithm that calculates the desired deflection of the individual wheels of the suspension system to create the desired vehicle attitude. Absent a full vehicle model and an attitude controller, a basic algorithm was employed to determine the vertical actuation desired based on the longitudinal acceleration of the model. The commanded acceleration multiplied by a constant provides the desired deflection for the system. The constant was determined by trial and error until a reasonable commanded deflection was obtained for varying acceleration levels. Since the model is of a rear suspension, positive accelerations results in an extension of the suspension to represent a system combating squat. Under braking operations, the

system compresses the suspension to simulate a trying to fight dive with a rear axle in a full vehicle. The driver would typically use a throttle and brake to control the longitudinal velocity of the vehicle. In the control development and testing, the driver is replaced with a desired velocity profile. This simple algorithm enabled the vertical wheel control to be tested for typical driving cycles that contain regions of acceleration and deceleration. While this simple algorithm does not consider lateral dynamics and roll control, such a system would also entail vertical commands to each wheel. Therefore, testing of the system for pitch control will demonstrate the basic functionality of the DEDS for full vehicle attitude control.

These two blocks supply the inputs to the control system. Two independent single degree of freedom controllers are utilized to drive the system to the appropriate desired state. The longitudinal controller is a PI controller that uses the desired wheel velocity in rad/sec and the actual measured wheel velocity in rad/sec to determine a control effort. The vertical controller is also a PI controller, but it uses the desired deflection in mm and the measured suspension deflection to determine the control effort. These two control signals are then combined in the coupler block to calculate the desired motor torques of the two motors.

6.1 Longitudinal Control

The longitudinal motion of the system actually relates directly back to rotational control of the wheel's velocity. In order to control the rotation of the wheel, the controller uses

rotational velocity feedback from the system. There are several ways to obtain this data. In simulation the wheel rotational velocity is available as a feedback signal. The hardware implementation does not include this signal. The rotational velocity of the wheel can be calculated by using(6.1). The wheel velocity is the average motor velocity multiplied by the gear ratio. From this it is easy to calculate the vehicle velocity by multiplying by the rolling radius of the tire. The motors utilized to drive the system include a built-in encoder that provides the motor's velocity. The input signal to the controller is a desired rotational velocity.

$$\omega_{tire} = n\frac{\omega_{M1} + \omega_{M2}}{2} \tag{6.1}$$

The longitudinal controller is represented in Figure 6-2. Here the integral term is used to reduce steady state error in the event of constant desired velocity such as cruise control or steady state driving conditions. The simplest controller that would provide the desired system response was chosen. A purely proportional controller resulted in an excess of steady state error. In purely longitudinal control, the controller applies torques of equal magnitude and direction to the motors. The motors receive the same torque so that the load is split between motors and the actuation is purely longitudinal. The motor torque model divides the desired torque of the controller in half and supplies this as the desired torques to the plant. The reason the controller is tuned to command the entire desired torque is to simplify integration into the couple architecture.

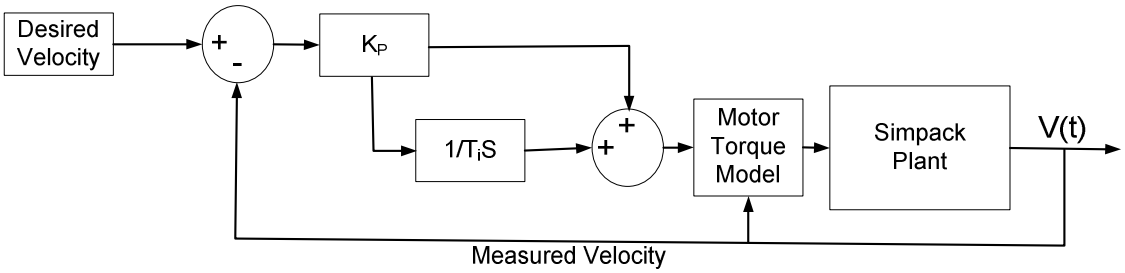

Figure 6-2 Longitudinal PI Controller

This controller was utilized with two different models. The first model was built with the unsprung mass connected to the ground reference as described in 3.3.1. Without the tire connection to ground, the model neglected rolling resistance, aerodynamic drag, and the actual acceleration of a vehicle in the longitudinal plane. To combat these shortcomings in the model the inertia of the tire was increased to represent the equivalent reflected inertia of a ¼ vehicle according to equation(6.2). The mass of the ¼ vehicle is represented by *m* and the radius of the tire is *r*. This is obtained by setting the translational kinetic energy of the vehicle equal to the rotational kinetic energy of the equivalent wheel. The velocity at the perimeter of the tire is equal to the linear velocity of the vehicle. This neglects tire deflection and dynamics, but is a good approximation for initial simulation and control development.

$$I_{equiv} = 4m\pi^2 r^2 \tag{6.2}$$

The second system is also described in chapter 3. The tire model was converted from a massless point follower setup to a Pacejka similarity model and the vehicle system was allowed to move on a simulated test track. This model includes the rolling resistance,

rotational dynamics of a tire, aerodynamic drag, and also simulates accelerating a vehicle through space. The reflected inertia model provided reasonable acceleration results, but the lack of damping and drag made this model less than ideal for control development as shown in Figure 6-3. When tuning the closed loop system it was difficult to obtain adequate input response without unacceptable overshoot or instability. The vehicle modeled on a track with a Pacejka similarity model was easier to tune, provided the desired input response, and did not become unstable. Figure 6-4 shows the control effort in response to the step input. The system did not utilize the full torque available from the motors. As such the controller that works well on the actual moving quarter vehicle model leads to some oscillation in the model with the reflected inertia for a tire model. With the system performing correctly on step inputs, more complex signals were used to simulate the driving input. Since the reflected inertia model displayed some undesirable dynamics, the track based model was used to complete the remainder of the longitudinal control development.

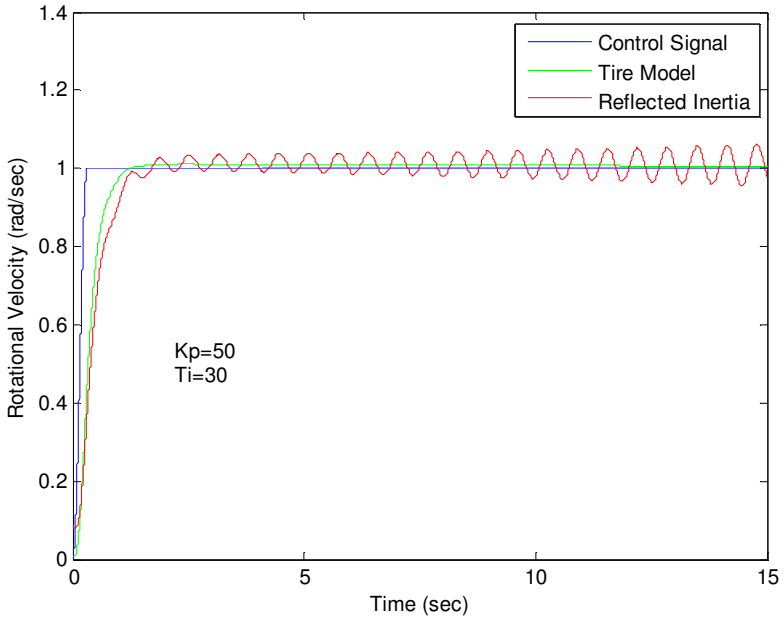

Figure 6-3 Response to a longitudinal velocity step input of the reflected inertia model and Pacejka tire model equipped quarter vehicle software models with the same controller gains.

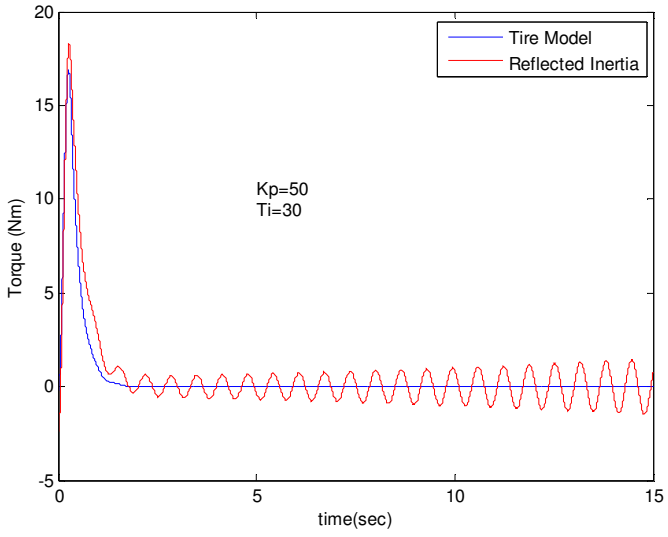

Figure 6-4 Control torque in response to a step input of the quarter vehicle software models with longitudinal control

The driving cycles are defined as a ground velocity vs. time signal. These cycles were simulated by converting the desired vehicle velocity into a desired tire rotational velocity and applying this signal to the controller. These tests were effective at exposing the controller to continuously changing velocity profiles in order to evaluate the system's ability to track the reference signal, but the accelerations are not excessive so they do not test the ability of the controller to operate in extreme driving situations. The UDDS cycle simulates an urban driving cycle which is closer to the intended use of the electric vehicle as shown in Figure 6-5. The FHDS cycle simulates highway conditions, which are more challenging for an electric drive system. The JUDS 10-15 cycle is another urban cycle but consists of more discrete velocity changes so there is inherently more error during the changes. In simulating the three different driving cycles, the system showed an ability to track the desired velocity with minimal error.

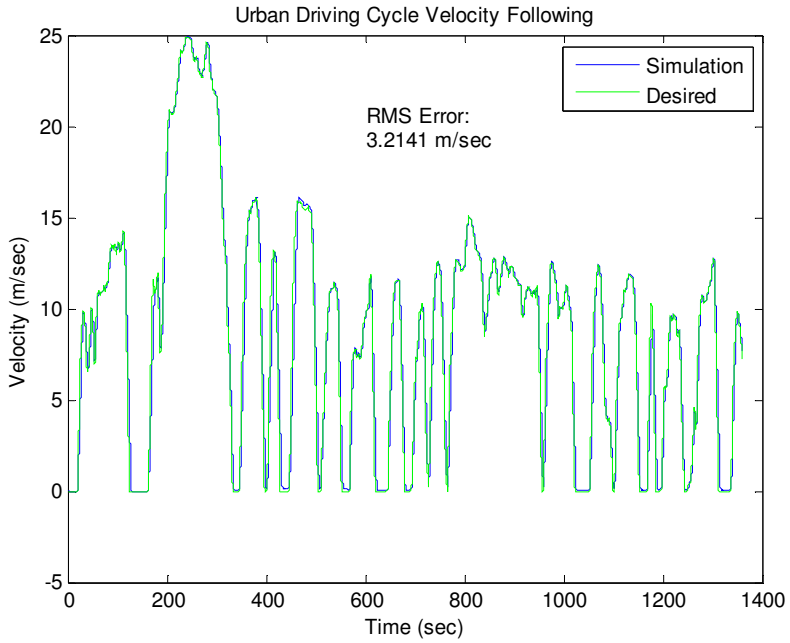

Figure 6-5 UDDS driving cycle with velocity control

The DEDS system has been developed for use in an urban environment. The UDDS cycle represents the start and stop conditions that could be found driving around any city as shown in Figure 6-5. These operating conditions create an ideal market for the use of electrically based vehicles. The longitudinal control for the urban cycle had an RMS error of $3.214^{m}/_{sec}$ over the entirety of the driving cycle. This error is due to the constant changes in velocity, and the detuning of the controller to not saturate the actuators. The system responds slowly and this causes an increased error during velocity changes. Ignoring the electrical drive system efficiency, the DEDS model utilized 904.7kJ of energy in order to propel the vehicle throughout the driving cycle and would have 276.6kJ of energy available for regeneration through braking. This shows the

system's ability to provide 30% regeneration through braking which is in line with what was found in Table 5-2.

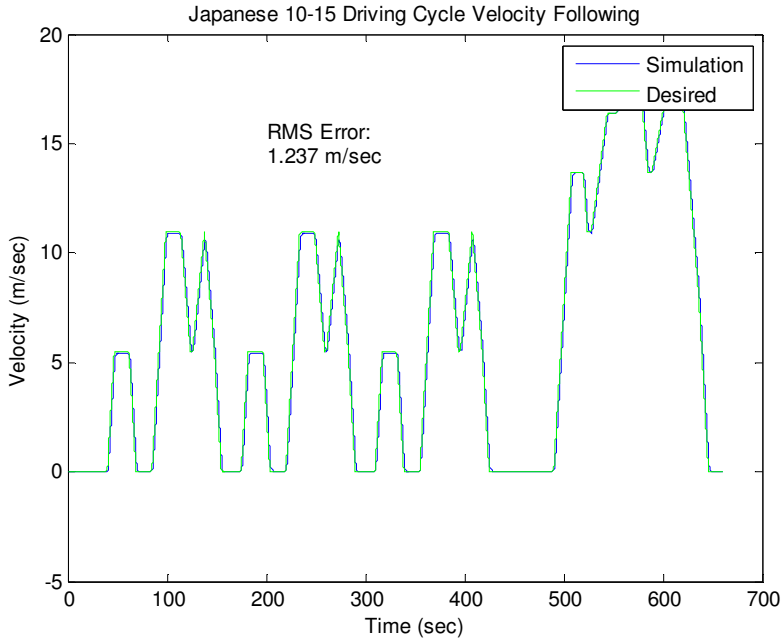

Figure 6-6 JUDS driving cycle with velocity control

The Japanese urban driving cycle model produced similar results. This driving cycle is less ambitious than the UDDS cycle. The velocity changes are more abrupt, which leads to increased control effort, but the maximum velocity of the cycle is reduced. During this cycle the model utilized over 295.8kJ of energy to propel the vehicle and had 96.2kJ of that left for braking regeneration. Again the regeneration potential found for the DEDS system correlates with the results of what is available for the vehicle.

Of course these two driving cycles are suited for the use of braking regeneration and an electric vehicle due to their lower velocities and frequency of acceleration and braking

cycles. The FHDS cycle is based loosely on a highway style driving cycle that consists of higher velocities and very few braking operations as shown in Figure 6-7. The system was able to follow the desired velocity profile very well. There is of course lag in both the initial acceleration and final braking due to the softening of the control gains in an effort to reduce actuator saturation, but overall the desired signal was maintained. Unlike the urban cycles, this cycle did not provide the opportunity for as much braking. In order to follow the desired cycle, the system utilized approximately 1,406.5kJ of energy with only 23.6kJ available for regeneration. The bulk of this regeneration potential comes from the final braking operation.

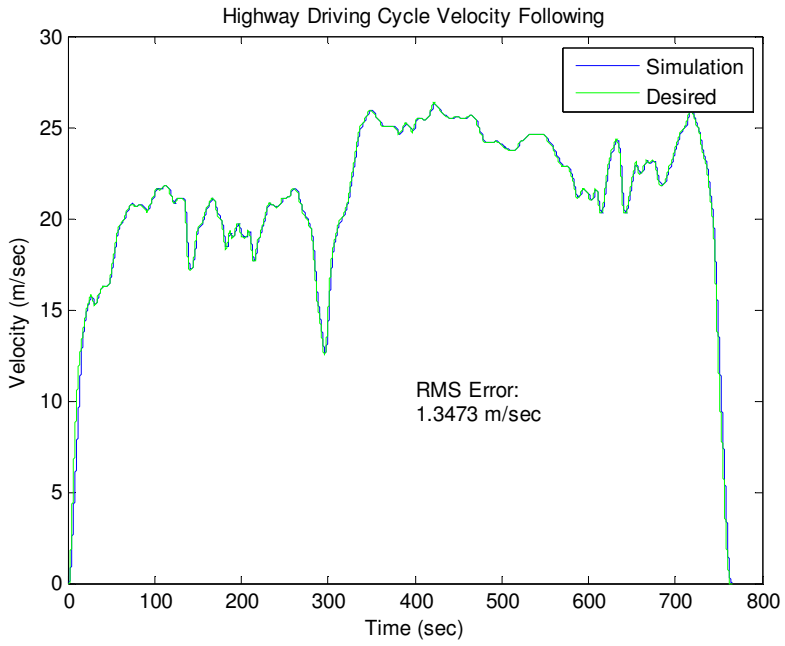

Figure 6-7 FHDS driving cycle with velocity control

Over all three driving cycles the system was operated with identical torques in both magnitude and direction that should result in only longitudinal actuation of the vehicle. However, the system coupled some motion into the system vertically due to the nature of the design. The road surface used for all three driving cycle simulations is completely smooth with no frequency content at all. Figure 6-8 shows the result of the Japanese 10-15 driving cycle and the coupled vertical deflections. During longitudinal accelerations the highest coupling occurs with a peak of less than 2mm of vertical deflection. During braking operations 1mm of vertical deflection occurs. The other two driving cycles also displayed peak vertical deflections of +/- 2mm during changes in velocity.

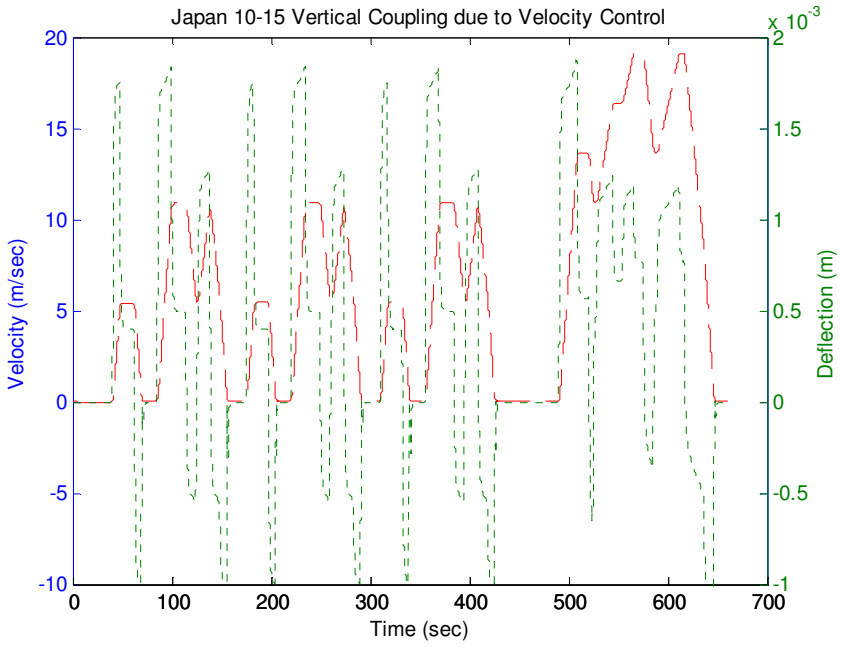

Figure 6-8 Coupling in the vertical degree of freedom during the Japanese 10-15 driving cycle without any vertical control

The longitudinal control showed that the system was capable of providing adequate longitudinal acceleration. Under lighter loads it would be expected that the acceleration performance would improve and the RMS error would be reduced. The system would have better tracking of the driving cycles due to this increased acceleration. Better performance could also be expected if the sensitivity of the controller was increased. This would however require additional utilization of the available torque and would degrade the system's ability to perform both roles of actuation.

6.2 Vertical Control

The idea for controlling the vertical degree of freedom is to adjust the steady state value of the suspension deflection to provide a mechanism for attitude control. The suspension still needs to perform its function, but the DEDS system should be able to force the suspension to a desired nominal value. The vertical degree of freedom is actuated by a difference in torque between the two motors. This can be generated by the torques having opposing torque values or by the motors having a difference in magnitude but with the same direction. As the torque differential between the motors increases, the deflection also increases. The vertical controller is designed with both motors having opposing but equal torques. The idea is that the vertical controller should not be actuating the rotational degree of freedom while still providing sufficient force to actuate the vehicle body vertically. If torques of different magnitudes were utilized the tire would also rotate.

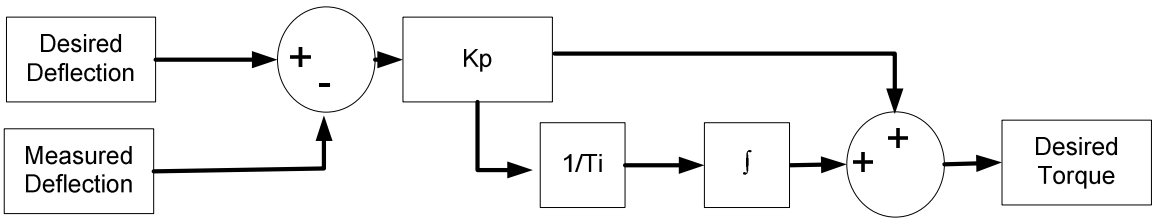

Figure 6-9 Vertical PI controller for the DEDS system

Variable	Value
K_p	25
T_i	0.6

Table 6-1 PI gains for vertical control

Initial control design and development started with the conventional PI structure as shown in Figure 6-9. This controller was exposed to a series of different attitude maneuvers to tune in the tracking. A simple example is shown in Figure 6-10. This example shows the system operating in both extension and compression. The PI controller with a proportional gain of 25 and an integral gain of 0.6 is capable of tracking the desired signal with an RMS error of only 0.22605mm. These simulations were run on the shaker model, which neglects the forces associated with a moving an entire vehicle. While performing these attitude adjustments to the suspension system an equivalent of less than 0.0003 m/s velocity changes would be experienced by the vehicle.

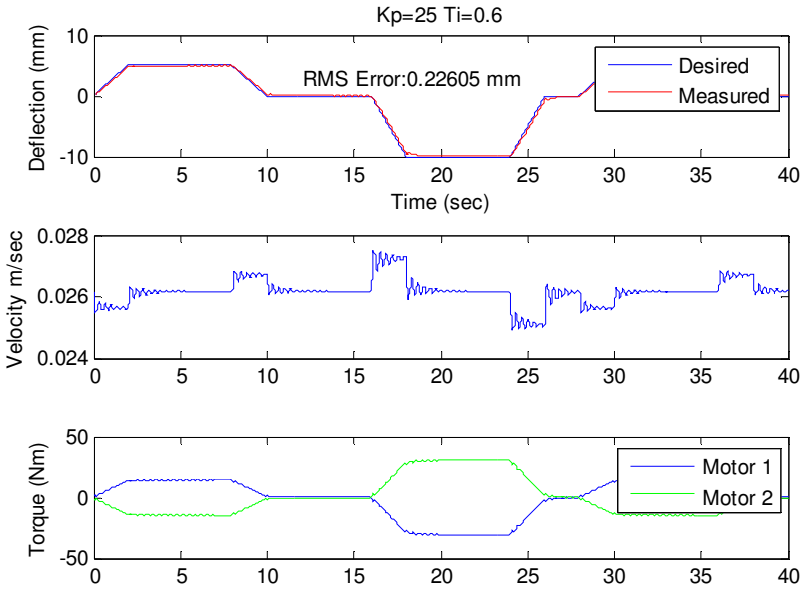

Figure 6-10 PI Controlled DEDS software model's response to amplitude control

If the same system is exposed to a sinusoidal road input that displaces the tire vertically, the RMS error is increased. Figure 6-11 shows the system when a 10rad/sec 20mm peak to peak sinusoidal road disturbance is applied. The RMS tracking error is increased to 0.5461mm. The control effort and velocity coupling are also increased. The additional control effort is being applied by the system to try and reduce the suspension deflection, creating a stiffer system as can be seen in the deflection plot. This could potentially hurt the suspension's physical ability to perform its role in the overall vehicle system. The controller does successfully adjust the operating location of the suspension. The oscillations of the suspension deflection track the desired deflection very well considering the addition of the road disturbance.

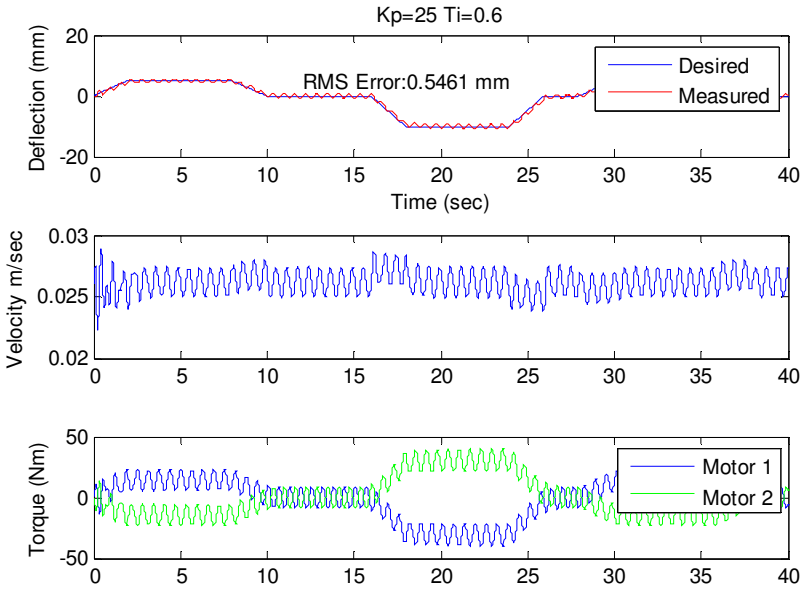

Figure 6-11 PI controlled DEDS with a 10Hz 20 mm peak to peak vertical road input and a commanded deflection signal

When the system is exposed to the same frequency sweeps that were performed earlier to evaluate the suspension's performance, the additional impact of the controller can be evaluated to determine the effect of the suspension's performance. The controller was given a zero mm vertical displacement command, which could be expected during normal steady state driving. A range of frequencies were then utilized to drive the vertical disturbance of the wheel. A 20mm peak to peak signal was utilized to simulate an aggressive road displacement. The addition of the controller driven to zero pushes the body mode back around the passive system frequency and reduces the magnitude of the additional mode that is coupled in around 6Hz. Some power is being consumed due to the controller trying to fight the suspension's natural motion.

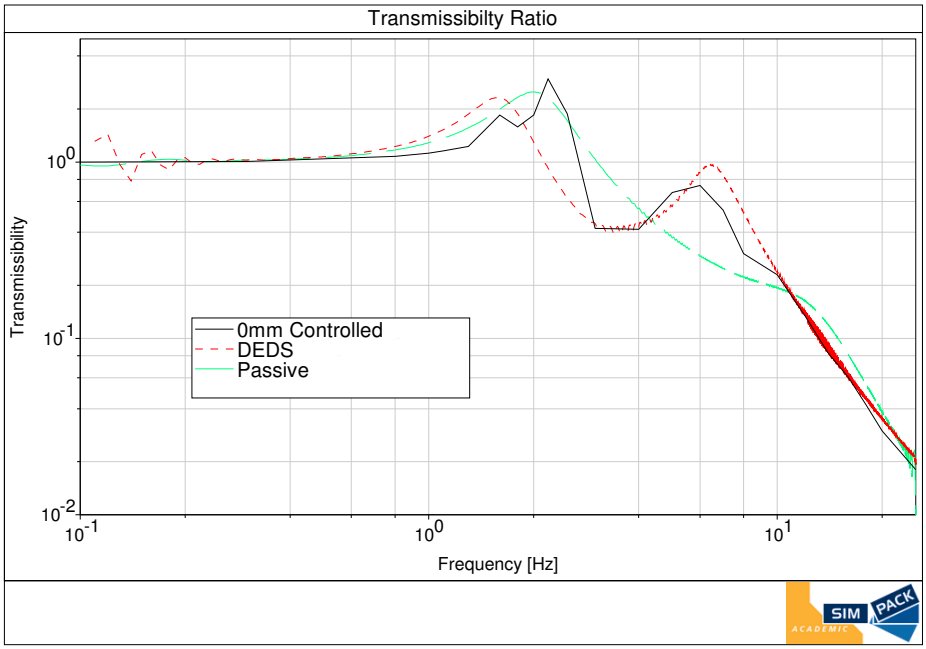

Figure 6-12 Transmissibility ratio of the DEDS system with a controlled deflection of 0mm

The hardware also affects the ability of the suspension to operate within the same rattle space. During lower frequencies, below 1 Hz the DEDS system with the controls enabled has a lower travel ratio. This equates to a stiffer system, which is due to the actuators being utilized to drive the system to combat deflection. The system is able to actuate to prevent the lower frequencies from causing deflection in the system. As the frequency increases the suspension resumes functioning as designed even though the actuators are trying to prevent the deflection. Around the body mode frequency of approximately 2Hz, the actuated system actually deflects more than either the passive system or the non-actuated DEDS configuration. This is due to the lag in the controller brought about by the control gains. Above the body mode the actuated system shows a drop in

suspension travel over the passive system which indicates reduced filtering in the suspension as the frequency is increased.

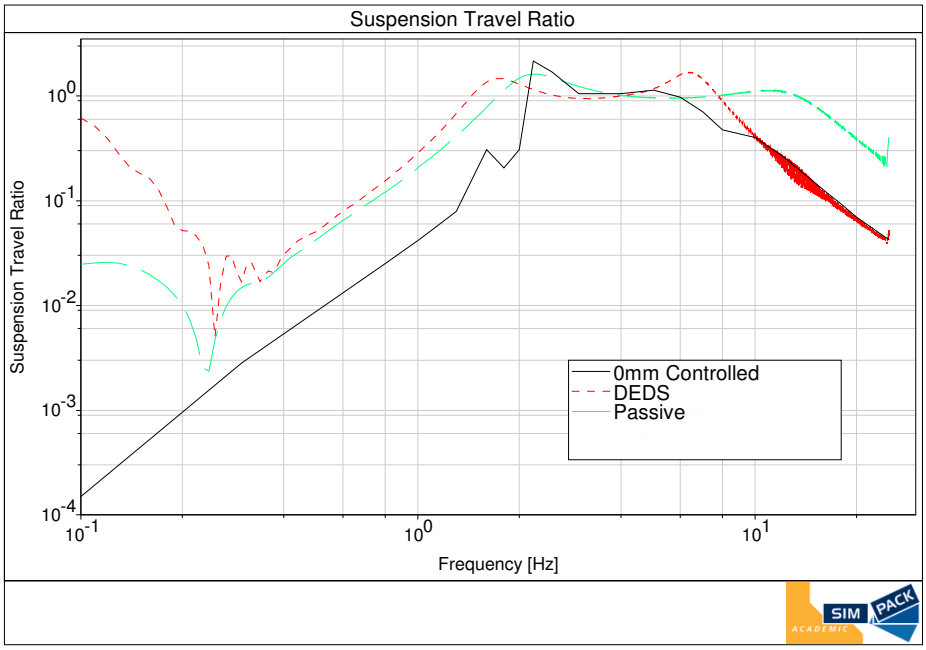

Figure 6-13 Suspension travel ratio of the DEDS system with a desired 0mm deflection signal

When considering the safety of the system, the road holding ability is evaluated by the dynamic tire deflection ratio. The goal is to maintain a constant tire contact force during steady state driving conditions such as the ones evaluated here. The lower the dynamic tire deflection ratio, the better the system is at maintaining a constant tire contact force. Around 2 Hz the actuated DEDS suspension performs worse than its passive counterparts. As the frequency increases towards 10Hz the actuated system performs better than a non-actuated DEDS system, and beyond that it outperforms the equivalent passive system.

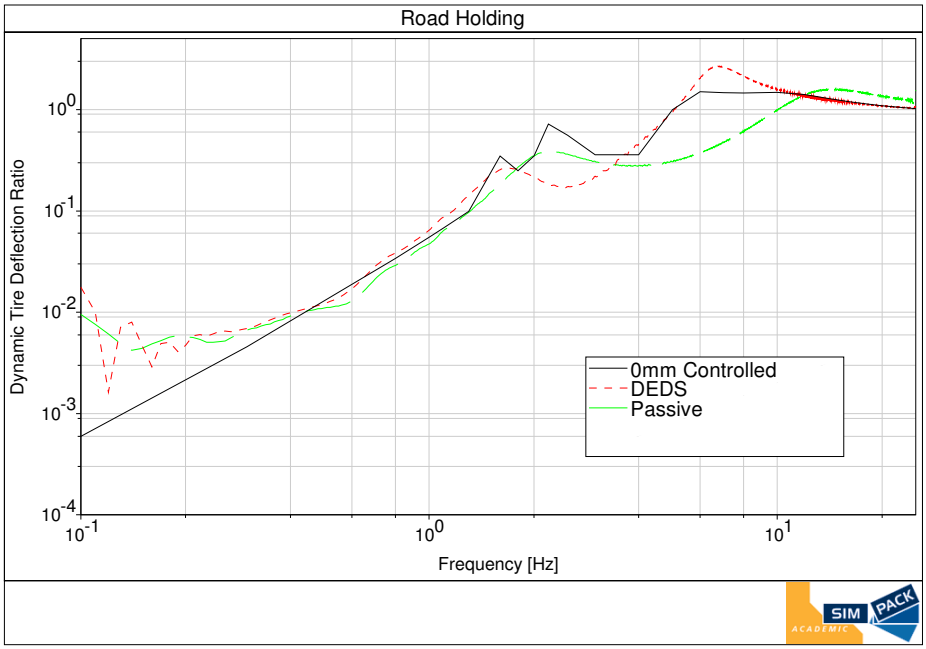

Figure 6-14 Dynamic tire deflection ratio of the DEDS with a desired 0mm deflection signal

These simulations only control the vertical actuation of the system. During the sweep of sinusoidal road actuations, very little of the actuation was coupled into the vehicle velocity. Between the body and wheel hop mode frequencies the system experienced the majority of the coupling into the velocity. During this range the peak velocity coupled was under 0.12m/s. This coupling occurs in the model with an unloaded tire with no drag or increased inertia, so the quarter vehicle model on a road could be expected to perform with even less coupling between the vertical actuation and the longitudinal velocity.

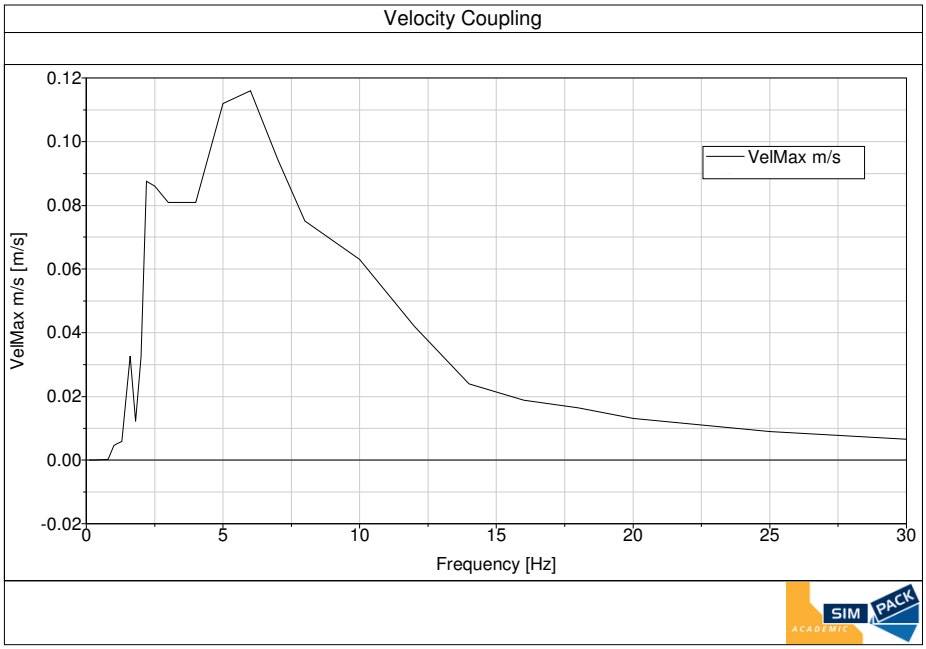

Figure 6-15 Coupled velocity of the vehicle during sinusoidal actuation when controlled around a 0mm desired deflection

Commanding attitude changes from the DEDS system is feasible with a PI control structure. For the controller, the attitude of the vehicle is considered to directly relate to a forced suspension deflection since the tire deflections are negligible. The proportional control path allows the system to respond quickly to any command changes. The integral control path provides a reduction in the steady state error of the commanded deflection. When simulated with a simple jounce and rebound signal, the controller is able to track the desired deflection with minimal error. As noise is added in the form of a road disturbance the system is still able to control the nominal deflection of the suspension with only a small increase in the RMS error over a system without

road disturbances, but the control effort is increased and the vertical dynamics are affected.

6.3 Two Degree of Freedom Control

The overall goal for the control system is to be able to control the wheel rotational velocity and suspension deflection externally and independently. The idea behind controlling a desired deflection is to open up the door for future stability and handling control. The outputs of the two independent degree of freedom controllers are combined in a coupling block that performs the conversion from two independent signals into dual degree of freedom motor actuations. These desired torque signals are then sent to the motor controllers and eventually to the actual hardware system. The two controllers, longitudinal and rotational, have shown the ability to control individual degrees of freedom with minimal cross coupling into the other degree of freedom. These two controllers will be utilized to build the two degree of freedom controller that allows the individual degree of freedom control while sharing actuators.

$$Z_{Vehicle} = C_{lift}(\beta_{M1} - \beta_{M2}) \tag{6.3}$$

$$\omega_{drive} = n\left(\frac{\omega_{M1} + \omega_{M2}}{2}\right) \tag{6.4}$$

Coupling the two control systems considers both the longitudinal and vertical controllers. The longitudinal control system provides a desired combined torque drive signal for the system. This system wants to see both motors providing equal torques in

both magnitude and direction. The vertical control provides a desired torque differential signal. The result is a difference in torque between the two motors. By combining both of these signals algebraically, it is possible to provide actuation of both degrees of freedom as long as the actuators are not driven to saturation. The coupling algorithm is based on equations (6.3) and (6.4) which were derived earlier for a symmetrical mechanism will be applied to join the two controllers as shown in Figure 6-1. The vertical controller was designed and tuned to apply torques to the motors that are equal in magnitude but opposite in direction. As such the torque command signal that is output from the vertical controller is actually a desired torque differential between the two motors. The longitudinal controller was also tuned to provide a torque command that was equal to the sum of the torque between the two motors. The commanded torque for motor 1, T_{motor1}, is described by equation (6.5). The torque for motor 2, T_{motor2}, is described by equation (6.6). $Vel_{Control}$ is the output of the longitudinal controller and acts equally on both motors. $Vert_{Control}$ is the output of the vertical controller and applies a torque differential between the two motors. Both equations have a constant multiplier of 0.5 that divides the actuation between the two motors.

$$T_{motor1} = \frac{1}{2}(Vel_{Control} + Vert_{Control}) \tag{6.5}$$

$$T_{motor2} = \frac{1}{2}(Vel_{Control} - Vert_{Control}) \tag{6.6}$$

Both longitudinal and vertical controllers were tuned for their independent test models. The vertical controller was tuned on a system that used a point follower tire model because of the nature of the systems actuation, and the longitudinal on the actual track model that will be used for the coupled testing. The track model uses a Pacejka similarity tire model, which represents actual tire dynamics much better than a point follower approximation. To test and fine tune the controllers in the coupled environment, two different sets of desired input signals were used. The first set of desired signals commanded independent degree actuation of the system. These were used to verify proper control actuation and to test for any changes in coupling between the degrees of freedom. A 10 rad/sec ramp signal was applied to actuate the rotational degree of freedom, and the vertical deflection was commanded to stay at 0mm as show in Figure 6-16. The coupled controller showed the ability to track the change in velocity, and the torque output shows that the vertical controller was applying a torque to fight any coupling into suspension deflection. The next signal in the set was a 3mm deflection signal applied to actuate the vertical controller, and a 0.01m/s velocity signal was fed to the longitudinal controller as shown in Figure 6-17. In the implementation of the Pacejka similarity tire model in Simpack, the tire must always be moving or the vertical actuation has some non-linearity's, so a small velocity command was applied to during the vertical actuation to avoid any modeling discrepancies.

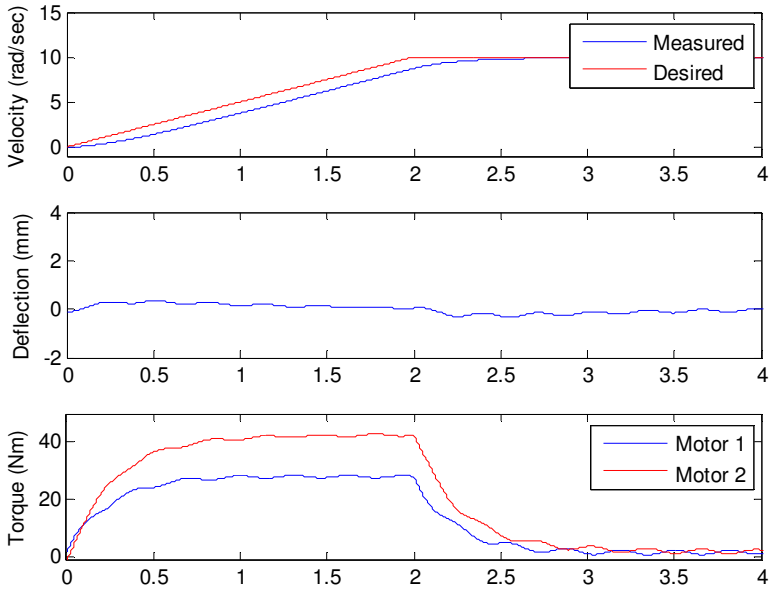

Figure 6-16 Velocity control in the coupled model following a velocity ramp input

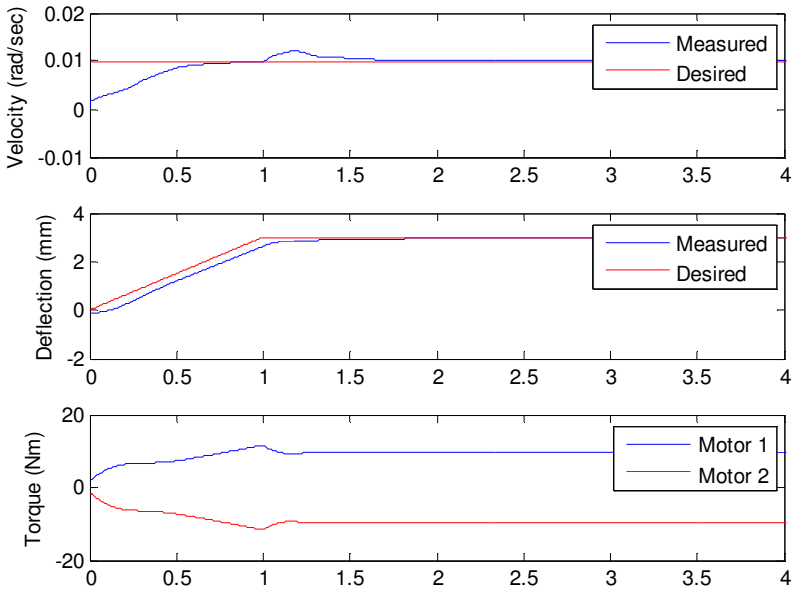

Figure 6-17 Vertical control in the coupled model following a deflection ramp input

These two tests showed that the coupling algorithm was able to control the two degrees of freedom with minimal cross coupling between the two degrees of freedom. The addition of the second degree of freedom controller did reduce the coupling between actuated deflections and velocity in the system. During the 3mm deflection test, the coupled controller reduced the velocity disturbance by 34%. When a 10 rad/sec ramp desired signal was utilized, the coupled control actually increased the vertical disturbance from 0.003mm to 0.03mm. This coupling is still minimal and would not be noticeable by a passenger in the vehicle. The next step was to expose the coupled system to some basic acceleration and deceleration tests.

In a rear suspension application, the DEDS is setup to contribute to fighting squat during acceleration with the appropriate command signal. To accomplish this, during acceleration maneuvers the suspension operating position is extended. During braking, it may or may not be beneficial to compress the rear suspension to try and combat dive. The dynamics of the full vehicle would determine this, but the system needs to be capable of performing both maneuvers. The coupled system was tested using several basic acceleration and deflection adjustments to simulate attitude adjustment for dive and squat. Figure 6-18 shows the system's ability to track both a velocity and deflection signal. During this low velocity and deflection maneuver the controller was able to follow the desired profiles with less than 0.2 rad/sec RMS error in velocity and 0.24 mm

RMS error in deflection. The motor torque and deflection signals show signs of oscillations in the system response. As would be expected, when the desired velocities and deflections are increased as shown in Figure 6-19 the RMS error increases due to the control gains and the motor sizing. The oscillations also increase which could result in the addition of a derivative control path, or the reduction in the vertical gains to reduce the sensitivity of the system to deflection changes and to increase the stability of that control path.

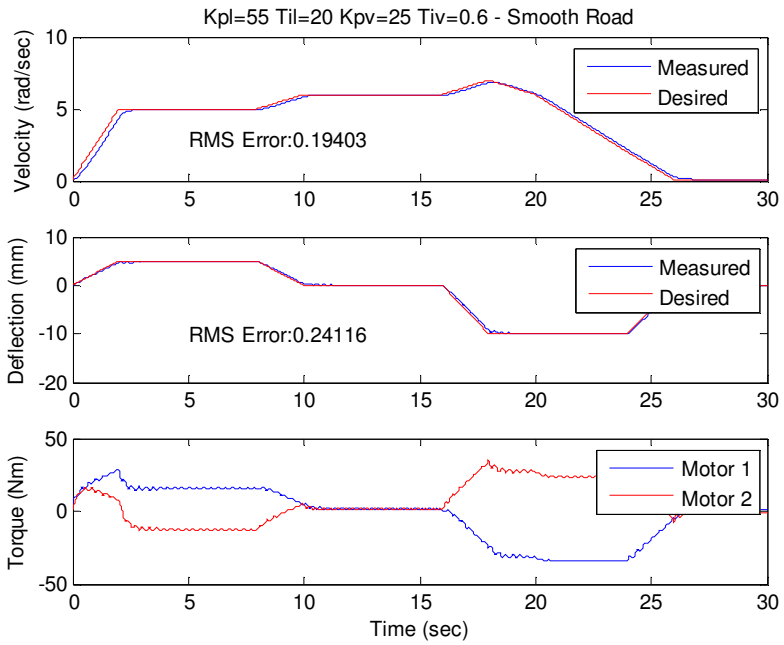

Figure 6-18 Low velocity and deflection acceleration and braking maneuver

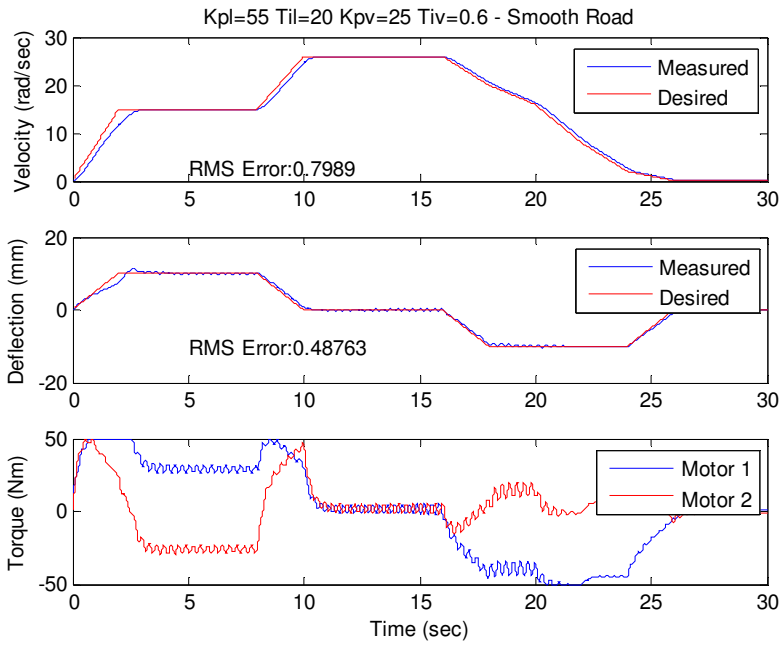

Figure 6-19 Increased velocity and deflection acceleration and braking maneuver

These simulations still neglect an important feature of the system. The suspension system will be in a state of constantly varying deflection due to road disturbances applied to the tire. As these disturbances are reacted throughout the vehicle system, how will the control of the deflection cope with the consistent error and change in position? The next logical step is to utilize the same profiles for velocity and desired deflection, but to add the road disturbance to the simulation. A basic gravel highway road deflection was added to the previous test. The addition of the noise led to a larger error in both the velocity and deflection. Even with the increased error in the deflection, the system tracked the desired deflection and functioned properly. The addition of the road disturbance had a negative effect on control effort, and caused the

actuators to be over burdened with the task of fighting the suspension's designed function. As the desired velocities, deflections, and road disturbances become more aggressive the controller will lose the ability to track the desired low frequency changes in both velocity and deflection because it will saturate trying to fight the higher frequency disturbances. A change in the controller is necessary to prevent the DEDS system from actuating against the higher frequency disturbances that are generated by the tire-road contact.

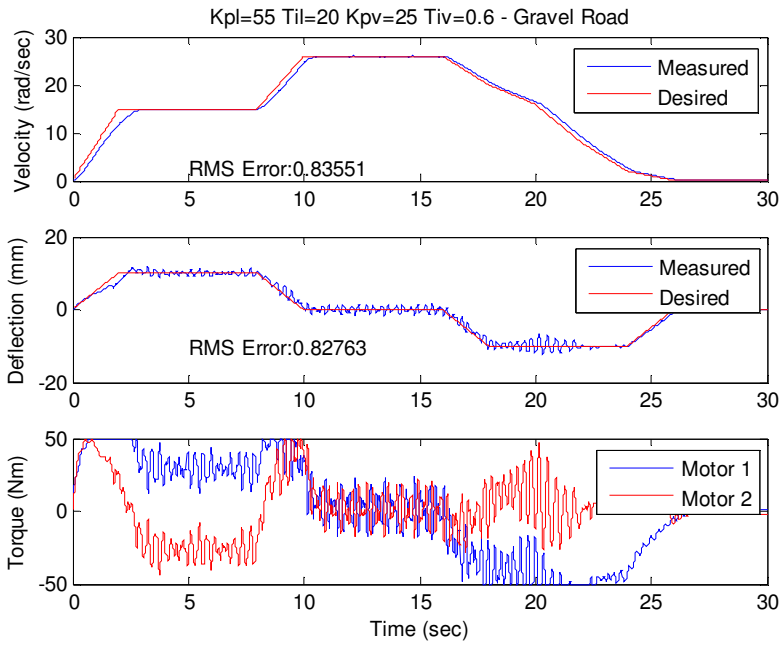

Figure 6-20 Aggressive driving cycle with a gravel road profile

The easiest solution to prevent the saturation of the motors due to the vertical disturbances of the road profile, is to decrease the sensitivity of the vertical controller to soften its response to changes in deflection. Attitude control is a low frequency control

with respect to a suspension system. Detuning the controller to allow adequate attitude control while not reacting to the higher frequency road disturbances will reduce the control effort and allow the actuators to be utilized more efficiently while allowing the suspension to function as designed. The proportional gain provides rapid response to a change in deflection while the integral gain can be a slower system that drives out steady state error. By reducing the proportional gain the DEDS systems control response to the road disturbances can be reduced. The proportional gain will still drive the system to the desired deflection, but the majority of the control effort falls on the integral path to maintain steady-state deflections. Figure 6-21 shows the system response with a reduction in the proportional gain of the vertical controller. The RMS error for the vertical degree of freedom is increased, but the control effort is greatly reduced and this allows for a reduction in the RMS error of the longitudinal degree of freedom.

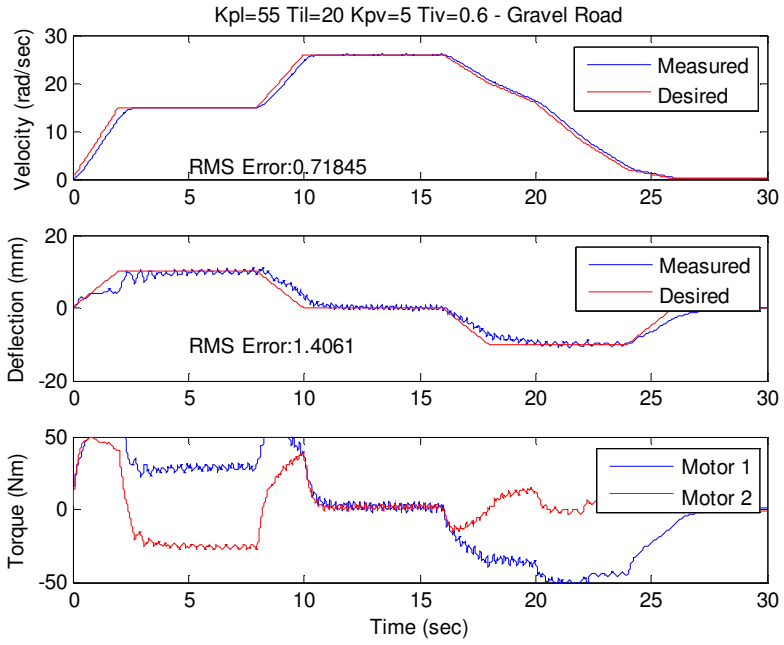

Figure 6-21 Reduced Kp in the vertical controller

If the integral gain is also reduced the system experiences a further increase in the RMS error for the vertical deflection signal, but without a significant reduction in the control effort. Figure 6-22 represents the system with a reduced K_p and T_i. The additional error in the vertical degree of freedom is not justified by the reduction in control effort. The control effort contribution of the proportional gain is directly influenced by the amount of road disturbance noise that is reacted through the suspension. The integral gain's contribution is more towards adjusting the nominal value. As such, higher integral gains can lead the system to track the desired deflection while not penalizing the suspension for performing isolation mechanically. The proportional gain is not without merit however, it provides the initial response to the commanded deflection change and

decreases the systems rise time allowing for more rapidly controlled deflection adjustments. This is paramount if the system is to be utilized to combat squat, dive, roll and heave.

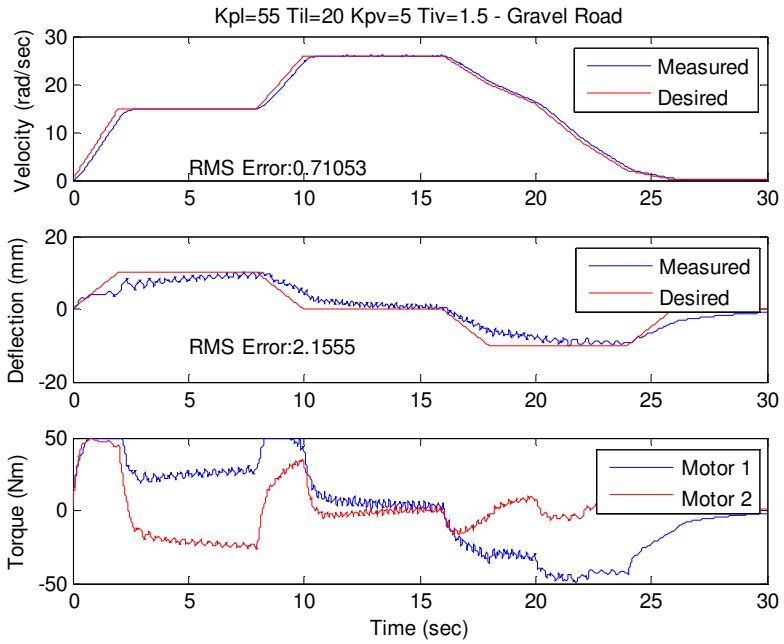

Figure 6-22 Both Kp and Ti are reduced to evaluate the effect of individual gains on performance

Detuning the vertical PI controller allows the system to still follow commanded deflection changes, but reduces the control effort and allows the suspension to function as designed. With the new control gains in place and the system responding to simple velocity and deflection commands; the system can be tested on actual driving cycles over different road surfaces. The driving cycles contain the desired velocity as well as the desired deflection as described earlier to combat squat and dive. The road profiles are the same spatial profiles that were used to test the comfort of the passive system

and the non-actuated DEDS hardware. They are combined together with the driving cycles to test the vertical, longitudinal, and suspension performance of the system.

During low velocity operation, the controller responded as expected. The UDDS driving cycle coupled with a highway with gravel road profile provides the most extreme case that was evaluated. When the wheel speed was below 55 rad/sec the DEDS was able to accurately follow both the velocity profile and the desired deflection that simulates attitude control. Once the velocity exceeded 55 rad/sec the system experienced a degradation in suspension performance. The vertical and velocity control continued to track the desired signals, but the deflection of the suspension was amplified. Figure 6-23 shows the system's response to the UDDS cycle. From approximately 200 seconds to 320 seconds the desired velocity is above 55 rad/sec. The amplification of the suspension deflection is clear as is the additional control effort that drives causes the amplification. In order to validate the results the system was exposed to the highway based driving cycle which consists of velocities in excess of 55rad/sec for the majority of the cycle. Figure 6-24 shows that the system does in fact amplify road disturbances when the velocity is above 55 rad/sec. The cause for the amplification is not the velocity, but the spatial nature of the disturbance signal. As the velocity increases, the frequency of the disturbances increases. This shifts the PSD of the road signal to a higher frequency which excites the coupled wheel hop mode of the system.

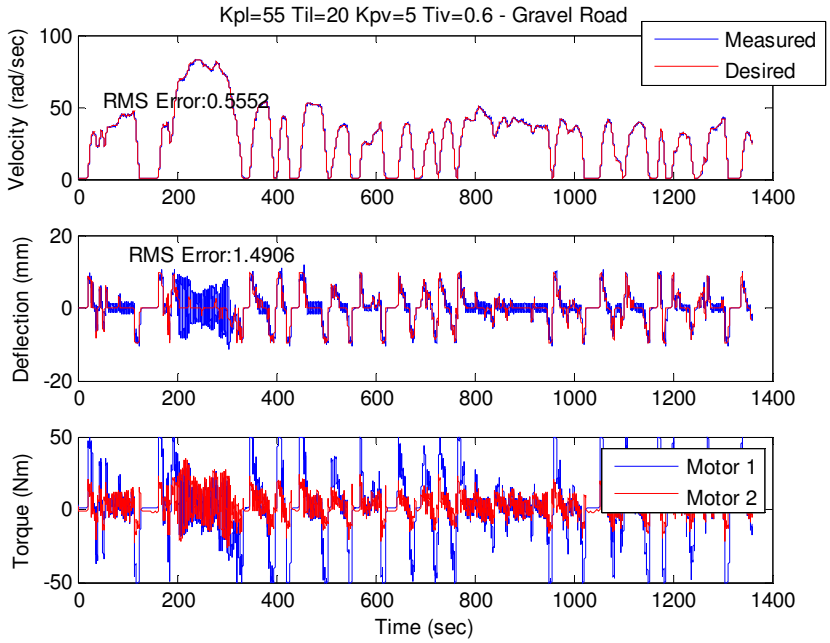

Figure 6-23 Urban driving cycle over a gravel road profile

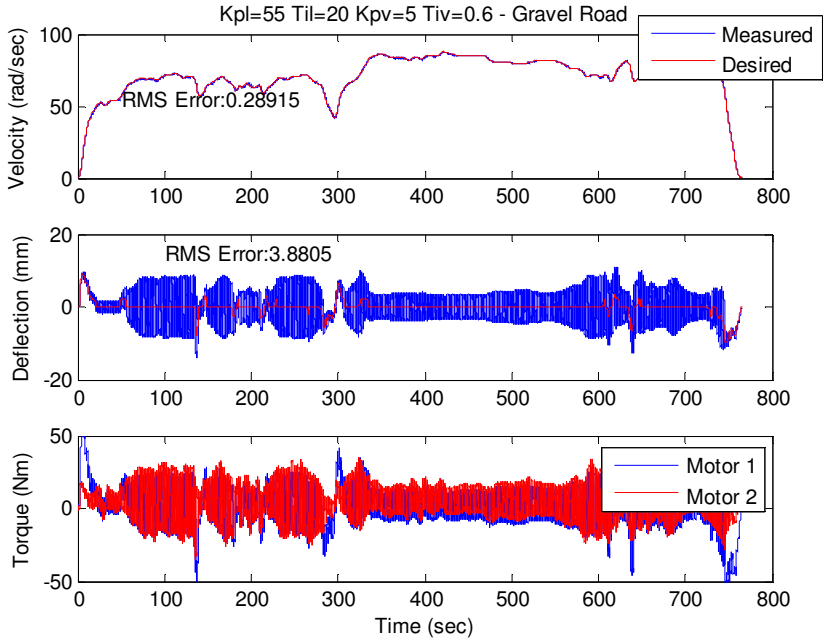

Figure 6-24 Highway driving cycle over a gravel road profile

Of course, this behavior is undesirable as the vehicle suspension performance during higher velocities should not degrade. In order to combat this phenomenon, a variable vertical proportional gain was employed. Since the suspension performance degraded with velocity, the proportional gain was defined as a function of the velocity. During low speed driving the vertical proportional gain is high, providing rapid response to changes in desired deflection. As the velocity increases the gain is reduced, softening the systems response to deflection changes, but not enough to negate the system's ability to track a desired deflection. Figure 6-25 shows the result of the velocity dependent vertical proportional gain. During the period from 200 to 320 seconds there is a remarkable reduction in the amplification of the road disturbance in the suspension deflection, with a negligible effect on the system's ability to track the desired deflection signal. There is still an increase in control effort over this period and a slight amplification of the disturbance, but if the proportional gain is further reduced, there is a significant reduction in the system's ability to follow the desired deflection signal.

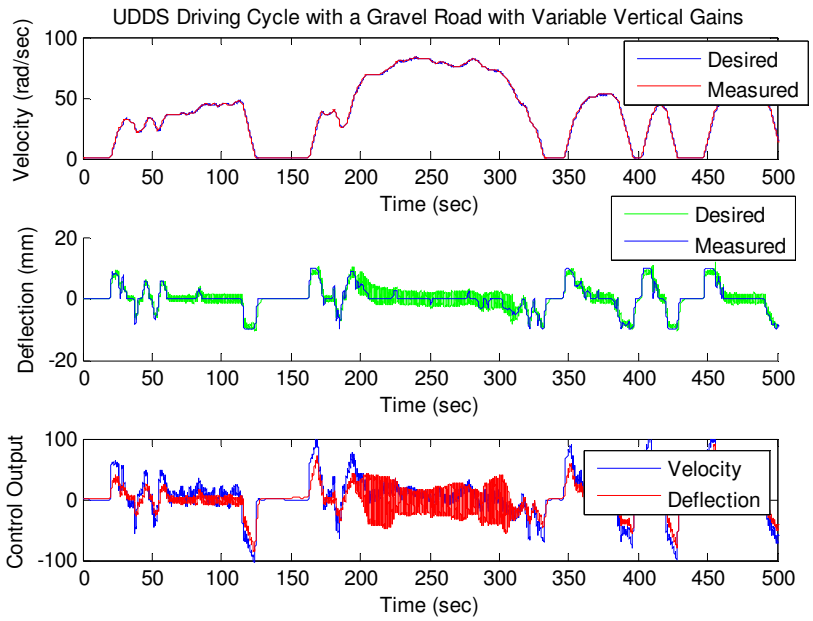

Figure 6-25 UDDS simulation with a variable vertical proportional gain excited by a highway with gravel profile

The highway driving cycle provided similar results with the addition of a velocity dependent vertical proportional gain. The suspension system still experienced additional deflection due to the actuation of the DEDS and the motors are exposed to a wasted control effort. The system with the addition of the velocity dependent proportional gain still saw a reduction in vertical deflection of the suspension relative to the non-variable gain structure.

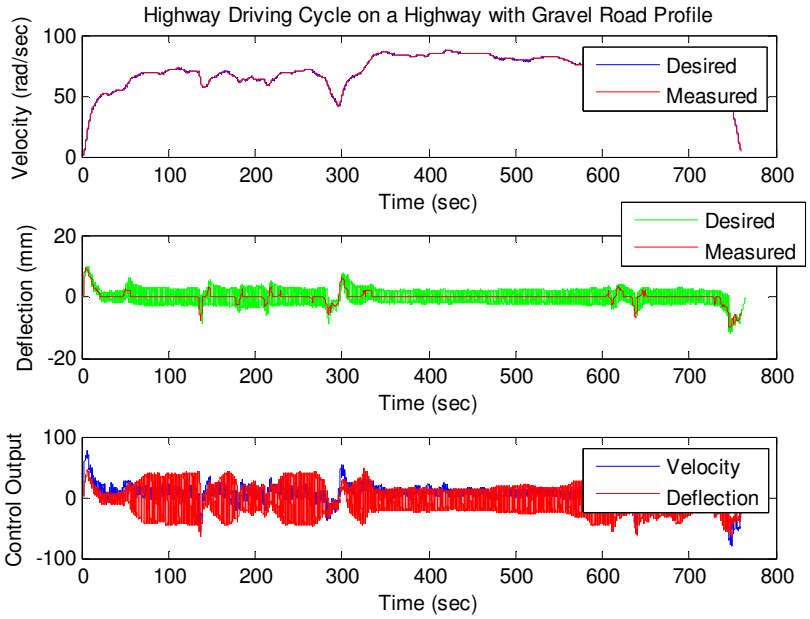

Figure 6-26 FUDS driving cycle with variable vertical proportional gain excited by a highway with gravel road profile

The DEDS system equipped with individual degree of freedom controllers and a coupling algorithm is able to track both velocity and deflection profiles. During high speed driving the system must rely on a variable proportional gain for the vertical controller to reduce its sensitivity to the higher frequency and power signals experienced by the vehicle. With this variable proportional gain the system is able to provide suitable actuation to validate the promise of the design for utilization in further models as a method for providing not only independent wheel longitudinal control, but also suspension deflection control in an effort to adjust the vehicle's attitude parameters.

7 Prototype Hardware

Figure 7-1 DEDS prototype hardware installed on a single post shaker

The system design and modeling were done in parallel with the development of a prototype hardware system. This ensures a more accurate model and also reduces the timeline for deploying the hardware. Any problems found in the design or through modeling can be solved immediately with a large reduction in rework or simulation. The prototype hardware developed to validate this system is a rear passenger side suspension system. The design of the hardware included two test structures that allow the quarter vehicle model to be installed on either a single post shaker or a chassis dynamometer. There is no access to a dynamometer on-top of a shaker, so testing will focus on validating the single degree of freedom actuation with the coupled controller.

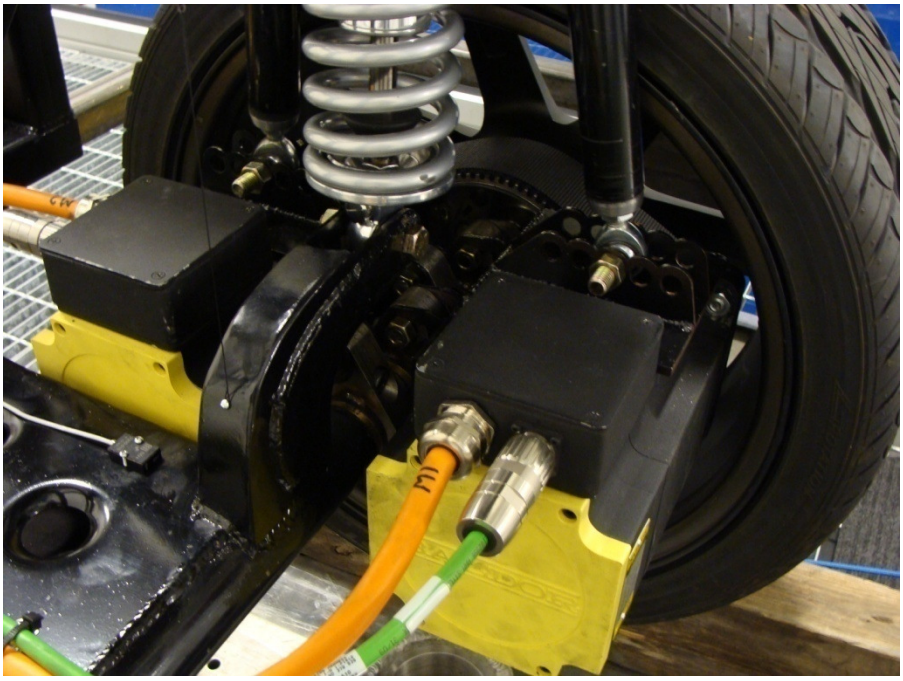

Figure 7-2 Prototype hardware motor mounts, connecting rods, and semi-trailing arm

7.1 Hardware Overview

Figure 7-3 Prototype hardware showing the drive belt setup behind the wheel

The hardware is built up of several different subsystems. The DEDS hardware itself is attached to a vehicle body platform. This can be seen in Figure 7-1 with the weights stacked on top to test with different loading conditions. Figure 7-4 also shows the weight stack directly over the connecting rods and coilover spring and damper assembly. The quarter vehicle model is then attached to the single post shaker via a test fixture. The fixture provides the necessary constraints to maintain the vertical degree of freedom for the quarter vehicle model. The linear guides that constrain the motion can be seen in Figure 7-6. The final piece in the puzzle is the control and drive subsystem.

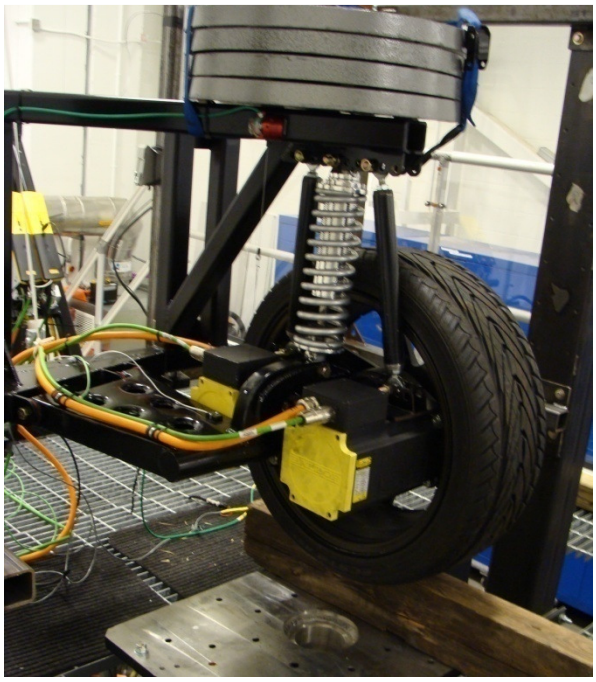

Figure 7-4 Overview of the vehicle side of the DEDS prototype hardware

The control and drive subsystem is configured as shown in Figure 7-5. The two motors are controlled individually by two matched drivers. These drivers provide torque control of the motors by utilizing a PID controller to match a commanded torque. The PID controllers were tuned using an auto-tuning algorithm that is included with the drives. Each PID is tuned specifically for the motor that it is attached to. The drives communicate with the control system which is shown in the grey box. External sensors are also utilized to feedback the sprung and unsprung mass acceleration as well as the suspension deflection and the position of the vehicle body. The control system only utilizes the suspension deflection and motor velocities to perform the control in its current state. The other sensors are used for data logging and analysis. The control block consists of a dSPACE real time system which performs the actual control and analysis of the system. The windows PC functions as a programming terminal, data post processor, and a user interface to monitor the system.

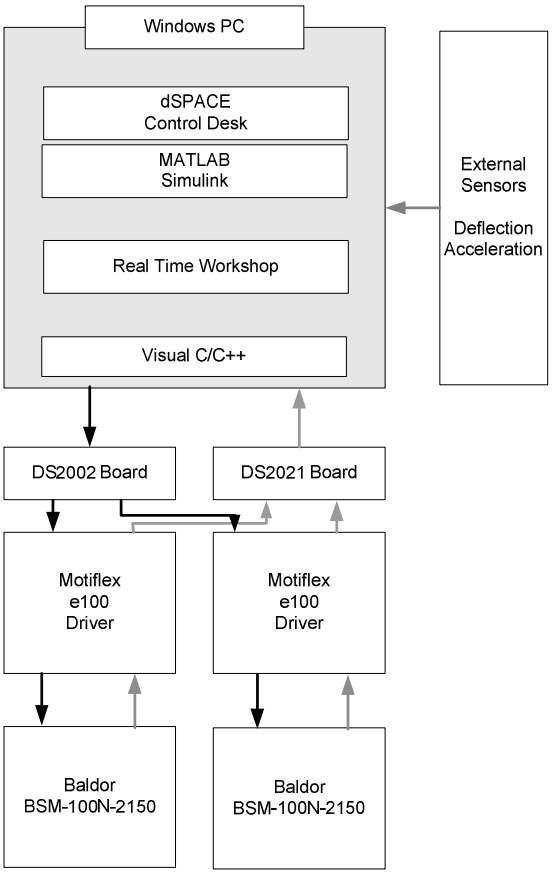

Figure 7-5 Control and Drive subsystem layout

7.2 Single Post Shaker Testing

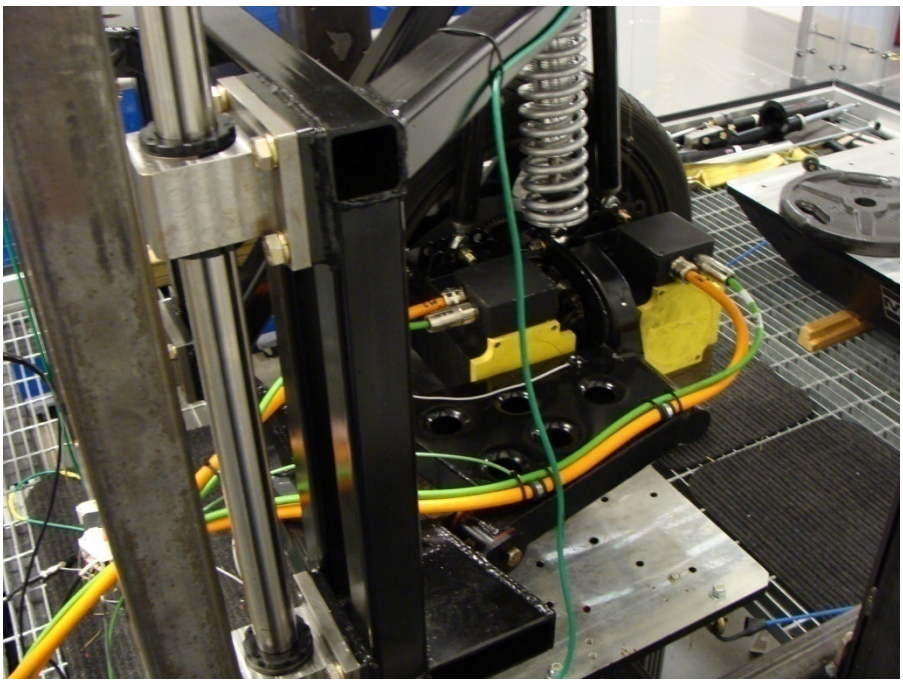

Figure 7-6 Prototype hardware showing the linear guides that constrain system to only vertical motion

Testing the hardware in an environment that allows for the excitation of a road input is paramount to validating the system. Installing the system on a single post shaker allows the system to actuate vertically to test the controller's ability to perform deflection control in the presence of a road disturbance signal. This provides a mechanism for further tuning of the PI controller as well as a method to compare the hardware with the simulation model. Unlike the simulation model for vertical control, the shaker uses a true pneumatic tire and not a massless point follower approximation. The shaker itself also has its own physical limitations and dynamics that affect the system response. The shaker system that is utilized to test the hardware is able to provide high displacement low frequency actuation, but as the frequency increases above 15Hz, the available

displacement is dramatically reduced. Once above 20Hz the shaker with the installed hardware is only able to actuate vertically +/-3mm. For the road profiles that were generated using the Wong approximation [6]; these limits are outside of the bounds of actuation. The same control architecture and gains are used initially on the hardware to determine if there is adequate correlation between the two models. Initial testing of the system showed that the PI gains found in simulation were able to control the system.

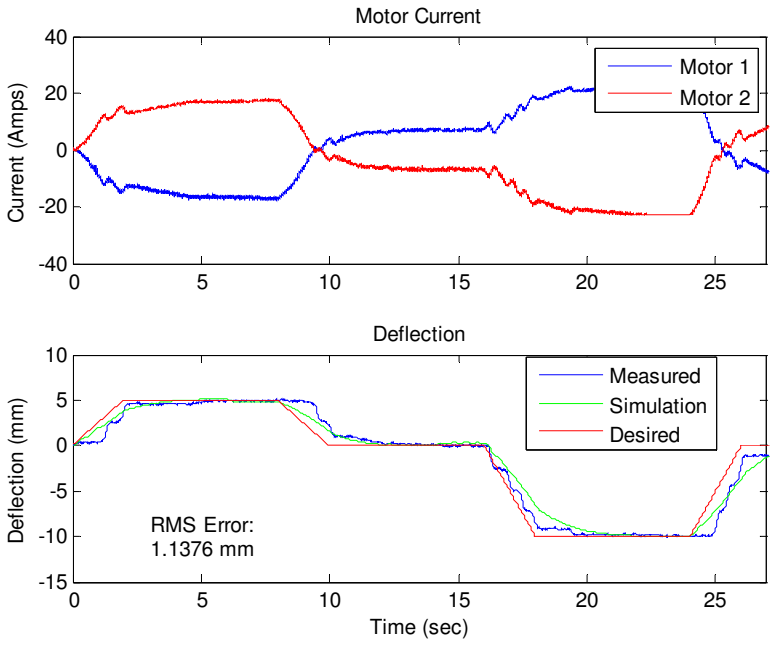

Figure 7-7 Initial control test of the DEDS prototype hardware on the shaker, excited with a simple desired deflection profile and no road disturbances Kp=3 Ti=0.6

Figure 7-7 shows the response of the system to a simple desired deflection signal with no road disturbance signal given to drive the shaker. The response of the hardware to the control inputs is more sluggish than the simulation model. This can be attributed to

the additional friction in the motor mounts and suspension bushings. There are steps to the actuation that are caused by the friction in the polyurethane bushings that locate the semi-trailing arm. The control of the motor torques also sees some higher frequency noise that is a result of noise in the deflection feedback signal. The higher controller gains provide a decreased rise-time, but make the system more susceptible to high frequency noise. This becomes a problem as a road disturbance signal is added to the system.

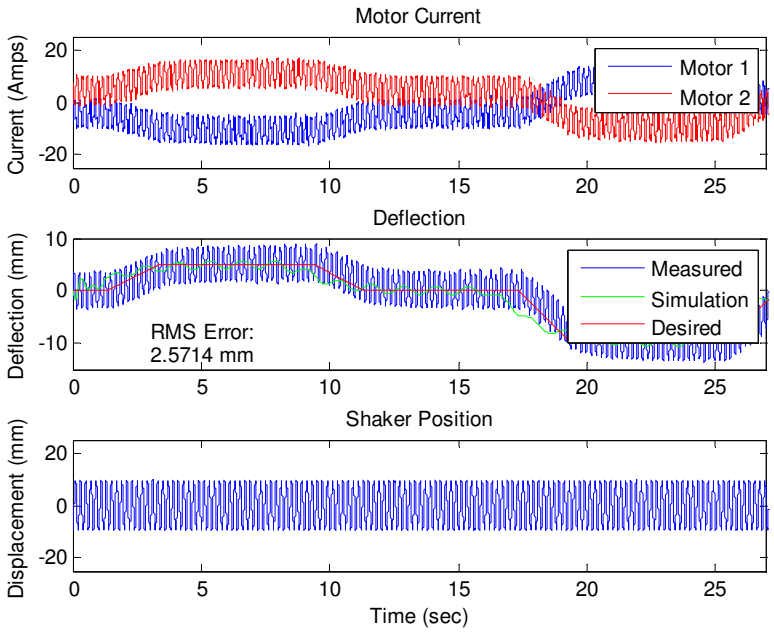

Figure 7-8 Simple controlled deflection with the addition of a 5Hz road disturbance signal Kp=3 Ti=0.6

When a road disturbance is added to the system, the motor torque is significantly increased as the system tries to maintain the desired deflection as shown in Figure 7-8 and Figure 7-9. Testing immediately exposed that the proportional gain was set too

high in the vertical controller causing the system to amplify the road disturbance. Reducing the proportional gain from 5 to 3 resulted in a system that performed very well below 8Hz, but that began to amplify the road disturbance when excited above 8Hz. With a simple 5Hz signal that moves the shaker table +/-10mm, the motors experience a sinusoidal control torque that varies +/-6Nm or just over 25% of the steady state torque available. This additional excitation torque is not efficiently utilized to perform the desired goal of attitude control. When the road excitation frequency is increased to 10Hz, the system with a K_p=3 in the vertical controller begins to amplify the road disturbance and over-actuates the system creating undesired performance (Figure 7-9). It is clear that the controller saturates the actuators and alternates back and forth between their peak actuation currents. Even during these conditions, the attitude control centered the system about the desired deflection without rotating the tire. It was found that if the proportional gain is reduced, reducing the controller's stiffness, that the system would perform as desired without a significant degradation in response time to the desired attitude control signal.

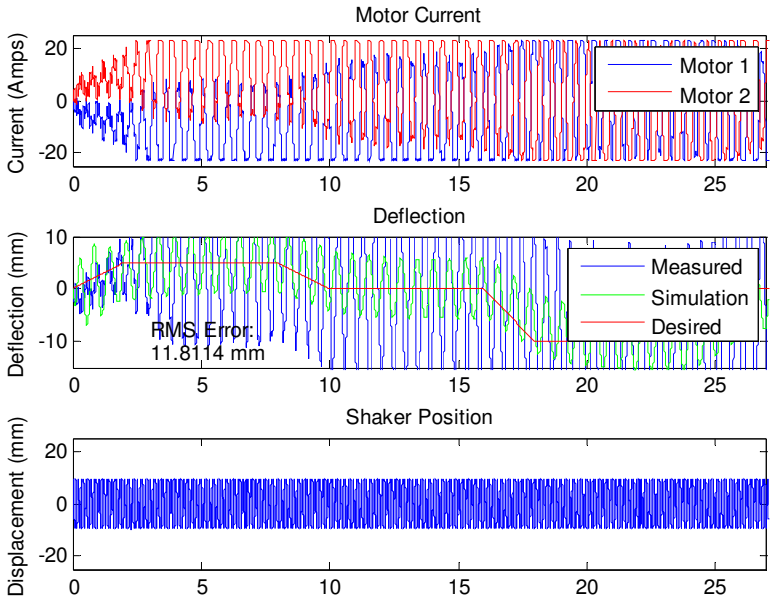

Figure 7-9 Simple attitude control with a 10Hz road excitation signal K_p=3 T_i=0.63

Further testing of the hardware was performed by using the same driving cycles that were used to test the simulation model and controller. The issues with saturation that were present in the simple actuation tests were not found in the road profile testing. The reduced amplitude and lack of sinusoidal oscillations present in the road disturbances did not push the system to oscillate when the proportional gain was left at 3. With the coupled controller, the desired velocity for shaker testing was set to zero to allow the longitudinal controller to prevent excessive wheel movement, although initial tests showed that the coupling during vertical actuation was not enough to overcome the friction between the tire and the shaker table. With the vertical gains set to K_p=5 and T_i=0.6 the highway driving cycle was fed into the system. The larger proportional

gain was utilized to improve the system response time to the attitude control signal and also to evaluate the stability during non-oscillating excitation. Figure 7-10 shows the results of the simulation. The coupled controller with the increased proportional gain was able follow the low effort attitude controls of the highway cycle without any problems. There is an addition of control effort due to the feedback signal noise. In an attempt to reduce the RMS error even more, the proportional gain was increased to 10. This actually caused the RMS error to increase. It was thought that the error would decrease due to the reduction in rise time with the higher proportional gain, but it actually increased the system's sensitivity to the noise in the feedback signal.

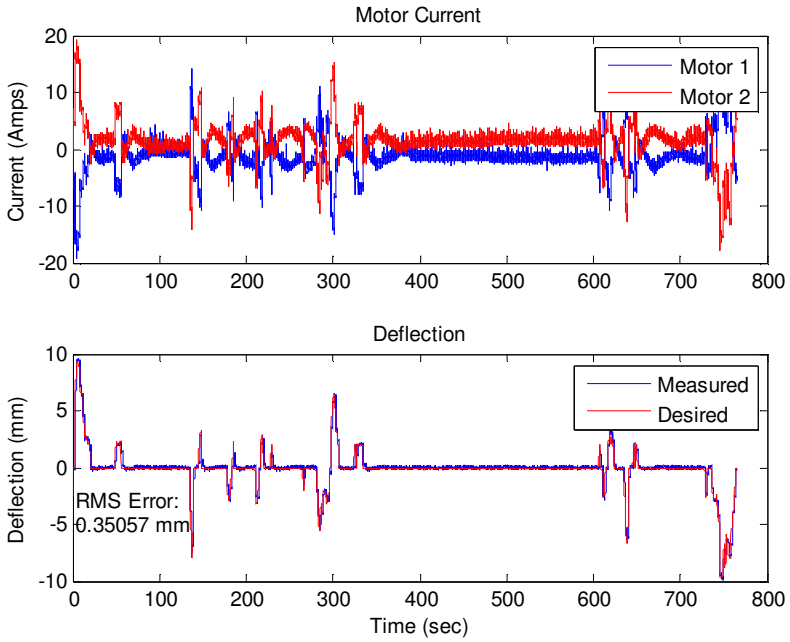

Figure 7-10 Highway driving cycle attitude control on the single post shaker with Kp=5 and Ti=0.6

A more aggressive urban attitude cycle was also used to test the hardware. Using the same gains that were found to work for the simulation model with a road disturbance input, the hardware was tested. Both the simulation model and the hardware were able to follow the desired deflection profile. Over the course of the cycle, the Simpack model of the system had an RMS error of 0.61mm and the hardware was only at 0.9mm. Some of this additional error can be attributed to the reduction in available torque in the hardware system. The model had 50Nm of torque available while the hardware testing was limited to 23Nm. The additional torque in the simulation allowed the system to have a higher single motor average torque and also a higher peak torque.

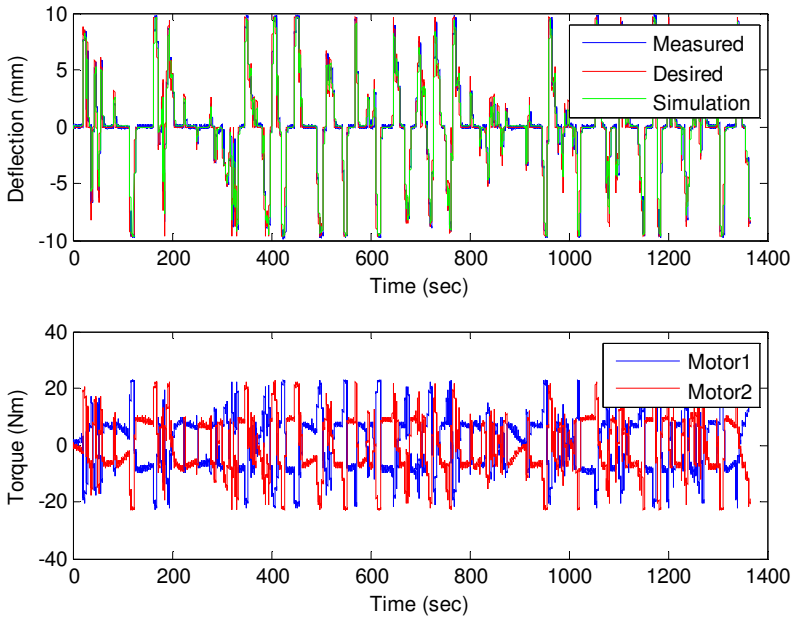

Figure 7-11 Urban driving cycle attitude control on the single post shaker without road noise

During the more aggressive urban conditions that the system was designed to operate in, the DEDS hardware and simulation model utilized very similar amounts of control. The simulation model had a peak torque available of 50Nm and of that during the UDDS cycle approximately 16-17% of the available torque was used throughout the cycle to control the attitude of the vehicle, with up to 77% being utilized to initiate a change in the suspension deflection. During the same cycles and road conditions the hardware system utilized 21% of the available steady state 23Nms of torque for attitude adjustments with a peak of 94% of the torque being used to initiate the change in suspension deflection. The Japanese 10-15 cycle provided similar results, and as expected showed a reduction in the amount of torque utilized as the attitude adjustments are smaller than those required in the modified UDDS cycle.

Simulation		Hardware		
Average Torque Percentage	Peak Torque Percentage	Average Torque Percentage	Peak Torque Percentage	Driving Cycle
16%	73%	21%	94%	Urban
17%	77%	20%	86%	
13%	46%	18%	61%	Japan
14%	49%	16%	54%	

Table 7-1 Simulation versus hardware for urban based driving cycles

Overall the hardware system responded much like its simulation counterpart. This can be attributed to the parallel development of the two systems. The hardware system is

more sensitive to road disturbance inputs and changes in the controller gains. The proportional gain of the vertical controller had to be reduced to prevent the system from progressing into an unstable state during which the actuation of the system oscillates from one extreme to another and the controller's effort continues to grow, only limited by the saturation of the hardware. With a small reduction in the proportional gain the hardware was able to provide very good results in attitude control while experiencing disturbances from a simulated road profile.

8 Conclusions

Over the course of this work, a dual electric drive and suspension system has been explored from conception, through design, and to hardware validation. The impact on vertical dynamics of the hardware and controls, energy regeneration potential, and the application of independent single degree of freedom controls to a coupled system have been evaluated. The results of the system simulation were then validated through hardware testing.

The DEDS hardware directly couples the sprung and unsprung mass. The amount of coupling between the two is design dependent, and can be varied by adjusting physical connection locations of the DEDS system. This direct coupling modifies the vehicle systems vertical response to road disturbances. The addition of the effective unsprung mass created by the DEDS hardware lowers the body frequency and couples some of the wheel hop mode through to the sprung mass. The road holding of the system is improved at the extremes of the frequency spectrum, but reduced between the body and wheel hop modes. Overall, the non-actuated system has a negative effect on the vertical dynamics of the suspension and vehicle as a whole.

Electrically driven vehicles have the opportunity to take advantage of regeneration through braking. The DEDS system is no exception to this, and provides a mechanism for braking regeneration. This provides the potential to recuperate over 30% of the energy consumed to propel the vehicle under the right conditions. The DEDS system also has the potential to recapture energy through the cycling of the suspension. There

is a potential for more than 2% of the energy consumed to be regenerated through damping. The actual regeneration potentials for the DEDS are still unknown as the regeneration hardware and controls were not explored.

Control of the DEDS can be as simple as two PI controllers combined with a coupling algorithm. The vertical and velocity controllers provide adequate excitation of the system in their respective degrees of freedom with minimal coupling into the other degree of freedom. When combined through an algebraic coupling algorithm the two degrees of freedom can be independently controlled within the bounds set by the actuators. They provided excellent following of multiple driving cycles coupled with simulated attitude control and road disturbances. By reducing the magnitude of the proportional gains in the vertical controller, the system's sensitivity to the road disturbances was reduced. Further adjustment of the sensitivity of the vertical controller is necessary to reduce the control effort during higher velocity driving operations.

With the addition of a velocity dependent vertical proportional gain, the system is able to operate at both low and high speeds without excessive interference with the suspensions passive operations. The DEDS is able to shift the operating position of the suspension resulting in what could be considered quarter vehicle attitude control. Even still the vertical PI controller utilizes some of the available power to try and combat the suspension's natural response to road inputs. With a reduction in the proportional gain

of the vertical controller the system utilizes less power, responds to commanded deflection signals slower, and doesn't try to fight the natural deflection of the passive suspension system.

The conversion of the controls to actual hardware required further reduction of the control gains to prevent instability of the system. When a larger proportional vertical gain is utilized the system becomes unstable during road disturbance inputs. As the gains are reduced the systems response becomes more predictable, and it also becomes stable. The hardware was able to track desired deflections while experiencing road disturbances, and also during sinusoidal disturbances as well.

Overall the research led to a system in both simulation and hardware that is capable of actuating two degrees of freedom utilizing coupled actuators. This provides a more flexible architecture than systems with two independent actuators. It also provides a mechanism to incorporate regeneration in not only braking, but also during normal driving conditions through damping regeneration. The end design is suitable for passenger vehicle applications in a small, urban based, electric or hybrid vehicle.

9 Future Work

As with almost all research, this work did not result in a neatly packaged, 100% complete and definite exploration into the system and all of its nuances. There are still a plethora of opportunities for further exploration with this system. What is given here is a small portion of what could possibly be explored and builds the next steps in development of the system into a viable commercial product.

- Application to a bicycle model to explore the ability to combat pitch and the benefits of two systems combined together
- Application to a full vehicle model
    - Exploration in four wheel drive stability control through torque vectoring and attitude control
    - Dynamic braking regeneration of four wheels independently as it pertains to vehicle dynamics and energy capture
    - Regeneration through damping and its effect on ride quality and vehicle range

  Optimal control development that allows for condition varying optimization of the degree of freedom actuation as it pertains to ride, stability, safety, and energy regeneration

Appendices

Appendix A File Structure

During the course of this research a large amount of simulation configurations and data processing files were generated. Due to the utilization of multi-body software, text based code is not available for the majority of the files that were generated. As such the files have been cataloged with the school electronically. They will also be enclosed with an attached CD.

Simpack Files

The Simpack model files and the associated controls are contained in the Simpack folder. There a many files in this folder, but only a few are directly accessed by the user. The remainder are files that configure the model for the multi-body environment.

1. Passive Shaker
   This is the model for the passive suspension configured on top of a shaker. It utilizes vertical road disturbances to excite the system.
2. Shaker
   This is the model for the DEDS system fixture atop a single post shaker. It utilizes vertical road disturbances as well as two motor torque signals to excite the system.
3. Track
   This model represents the DEDS system traveling on a smooth road. The inputs to the system are the two motor torques.
4. Trackv1
   This model uses the same DEDS hardware as the shaker and track models and allows it to travel down a road with vertical disturbances. The inputs are the two motor torques and the vertical road disturbance is defined by a configuration data file that allows for spatial road profiles to be utilized.

This folder also contains the control systems for Simulink that allow co-simulation between Simpack and Simulink. These files require the utilization of the Simat interface and the co-simulation server.

1. ShakerPassive.mdl
   This provides a driving signal for the passive system on the shaker. Multiple profiles from swept sinusoidal signals to road profiles can be utilized.

2. ShakerChirpDrive.mdl
   This system utilizes the shaker model of the DEDS system and applies a swept sinusoidal motor torque differential signal to actuate the hardware. It applies no actuation to the shaker.
3. VerticalControl
   This Simulink system utilizes the shaker model of the DEDS system with PI control to command attitude adjustments. It provides the functionality of the single degree of freedom system and was the development test bed for the controller. The shaker inputs are basic sinusoids and swept signals.
4. VerticalControl_Road
   This model uses the same structure as the VerticalControl system but provides the mechanism to drive the shaker with the road profiles generated by the SAE descriptions of road surface roughness.
5. VelocityControl
   This is the PI control model that uses the Track Simpack model. It applies the appropriate control to the Simpack model to drive the quarter vehicle model down the smooth road to test longitudinal dynamics.
6. CoupledPI
   This is a combination of the VerticalControl and VelocityControl systems with the coupling algorithm in place. It is used on either the Track or Track1 models to drive the system in both the longitudinal direction as well as the vertical direction.
7. CoupledPI_1
   This is the further development of the CoupledPI control algorithm that employees velocity variable gain scheduling for the vertical controller to reduce the sensitivity of the system during higher velocity driving.

Post Processing

The post processing of the data from the above models and controllers is performed through two different methods. The first is through Simpack's built in post processing functionality. These files are completely dependent on the data source of the model. The second is through Matlab analysis of Simulink data. These files are also dependent of the data, and the descriptions of data structure construction are included in the files.

Simpack

1. 0ForcedDeflection.spf
   This performs the post processing of multiple frequency steps to build up regular frequency based analysis of the system without control.
2. 0ForcedDeflectionPIControl.spf
   This performs the post processing of multiple frequency steps to build up regular frequency based analysis of the system with vertical PI control.
3. DataProcess.spf
   This provides a lot of the general data analysis from multiple simulations. Comfort curves, bandwidth, torque versus deflection, and many others. It served as a catch all for small, rapid analysis.
4. DrivingCycles.spf
   This performs the analysis on the hardware for the driving cycles without any vertical road disturbances.
5. DrivingCyclesWRoad.spf
   This performs the analysis that DrivingCycles.spf does, but with the addition of vertical road disturbances. Power consumption, tracking, and error
6. Regeneration.spf
   This provides the analysis of the system for potential regeneration through braking and damping.
7. VerticalDataProcessing.spf
   This provides the basic analysis for the shaker data processing.
8. WongAnalysis.spf
   This performs the analysis for the passive and hardware equipped system for ride comfort, suspension travel, ISO comfort curves, and tire to road contact forces.
9. WongAnalysisControlled.spf
   This performs the same analysis as WongAnalysis, but with the addition of control to the DEDS hardware.

Matlab

These files provide basic processing of data collected from Simulink.

1. VelPIRoadCycleDataProcessing
   This file provides the basic analysis of the driving cycles and the system's ability to follow the desired profile with only velocity control.

2. VertSimple
   This system analyzes the coupled system with simple attitude and velocity curves as well as with comples driving cycles that include attitude control.
3. RegenPotential
   This calculates the power consumption for the UDDS, HTFS, and Japanese 10-15 driving cycles and figures out how much could be recaptured through braking. It includes a small vehicle model for aerodynamic drag and rolling resistance.
4. VerticalControlAnalysis
   This provides basic analysis for vertical actuation, including the simple vertical profiles and sinusoidal disturbance additions.
5. CoupledCycleAnalysis
   This processes data from the coupled controller to determine the system's ability to track reference velocity profiles and perform attitude adjustments.
6. CoupledCycleWRoadAnalysis
   This performs the same analysis as the CoupledCycleAnalysis software, but the data has the addition of road disturbance profiles as defined by SAE.
7. SimpleVertProcess
   This provides the basic analysis of the PI based vertical controller including some of the gain analysis of the controller.
8. CoupledAnalysis
   This file provides the analysis of how much coupling is introduced through vertical or velocity control without the addition of the second degree of freedom controller or the coupling algorithm.
9. HardwareProcess
   This provides the basic processing of the shaker data with the actual hardware in place. It analyzes the basic curve following with and without simplistic road disturbances.
10. HardwareProcessWRoad
    This software includes processing of hardware data that was collected utilizing dSPACE. It provides the analysis of the road profiles while simulating attitude control of the system, and includes the comparison of the hardware to the simulation of the same disturbances.

Appendix B Kinematic Modeling

The planar kinematic modeling is performed by breaking the system into separate bodies and performing free body analysis to determine a set of equations that describe the system.

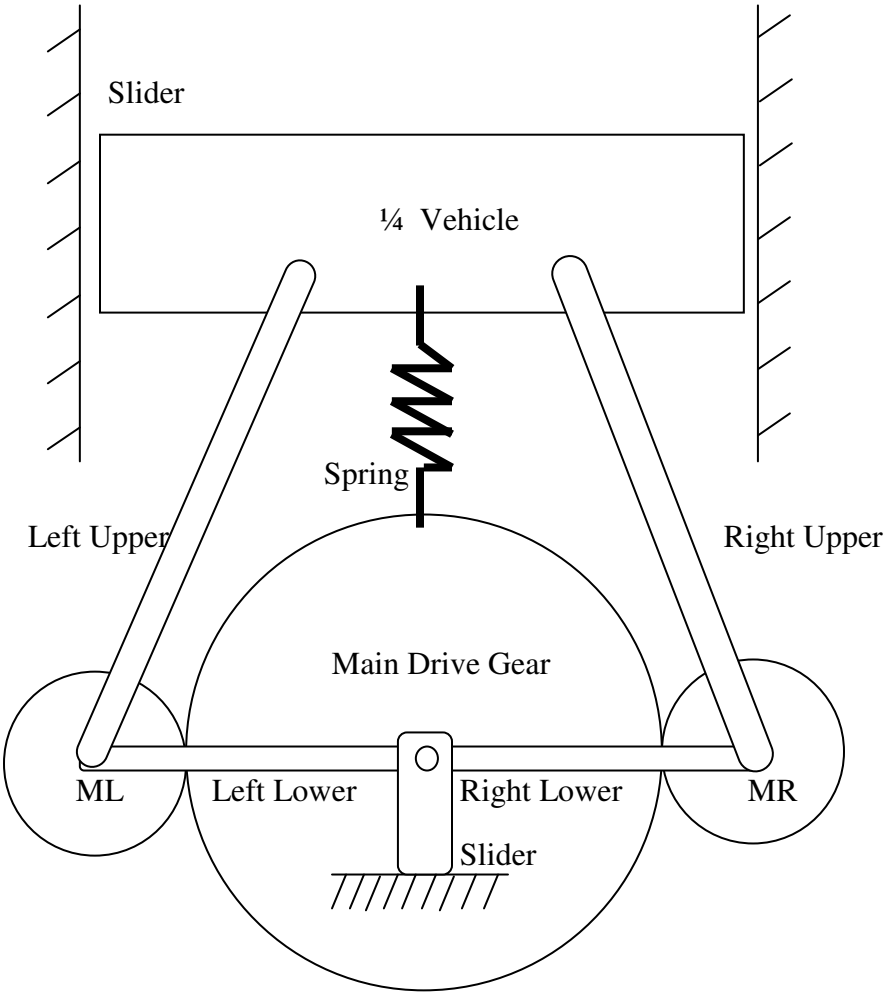

Vehicle

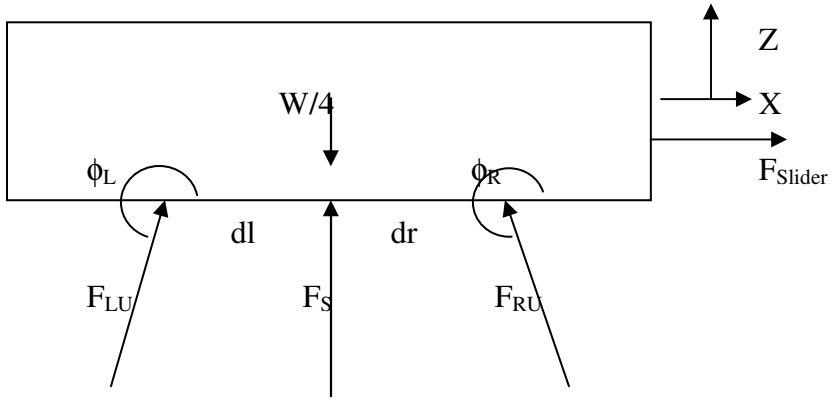

$$\sum M = 0 -> slider$$

$$\sum F_X = F_{Slider} + F_{LU} \sin\phi_L - F_{RU} \sin\phi_R$$

$$\sum F_Z = F_S - \frac{W}{4} + F_{LU} \cos\phi_L + F_{RU} \cos\phi_R$$

$$= kz + F_{LU} \cos\phi_L + F_{RU} \cos\phi_R$$

Linkage and slide is treated like an offset slider.

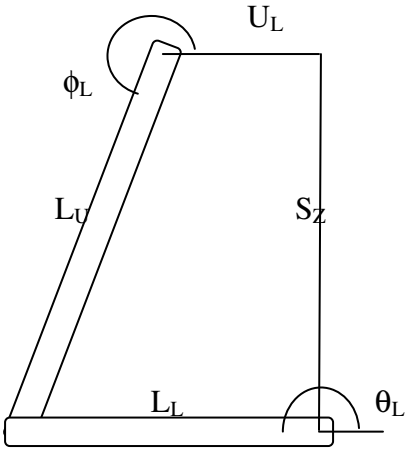

$$\vec{U}_L + \vec{L}_U + \vec{L}_L = \vec{S}_Z$$
$$L_U \cos\phi_L + L_L \sin\theta_L = S_Z$$
$$U_L + L_U \sin\phi_L + L_L \cos\theta_L = 0$$

$$\dot{\vec{U}}_L + \dot{\vec{L}}_U + \dot{\vec{L}}_L = \dot{\vec{S}}_Z$$

$$L_U \omega_{LU} \cos\phi_L + L_L \omega_{LL} \sin\theta_L = \dot{S}_Z$$

$$\cancel{V}_L^0 + L_U \omega_{LU} \sin\phi_L + L_L \omega_{LL} \cos\theta_L = 0$$

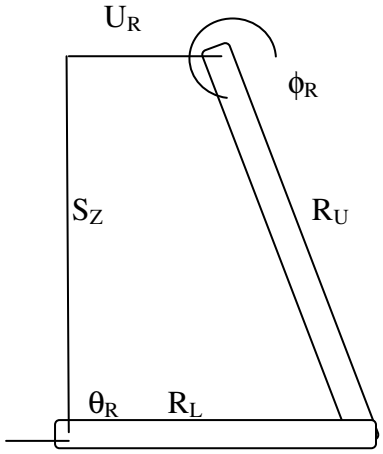

$$\vec{U}_R + \vec{R}_U + \vec{R}_L = \vec{S}_Z$$

$$R_U \cos\phi_R + R_L \sin\theta_R = S_Z$$

$$U_R + R_U \sin\phi_R + R_L \cos\theta_R = 0$$

$$\dot{\vec{U}}_R + \dot{\vec{R}}_U + \dot{\vec{R}}_L = \dot{\vec{S}}_Z$$

$$\cancel{V}_R^0 + R_U \omega_{RU} \sin\phi_R + R_L \omega_{RL} \cos\theta_R = 0$$

$$R_U \omega_{RU} \cos\phi_R + R_L \omega_{RL} \sin\theta_R = \dot{S}_Z$$

Main Drive Gear and Tire

Treat as static and let the vehicle move. Modify later to include a basic tire model.

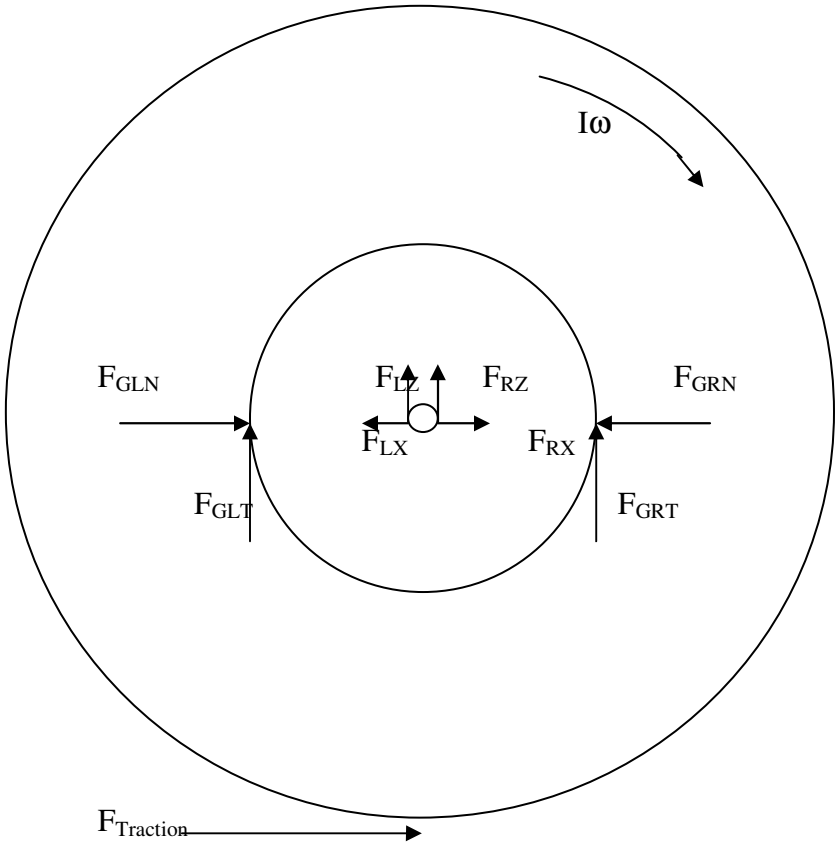

Equations

$$\sum M_o = F_{Traction} \times r_{tire} + \left(F_{GLT} - F_{GRT}\right) r_{Gear}$$

$$\sum F_X = ma_X = F_{RX} - F_{LX} - F_{GR}\sin\theta_{CR} + F_{GL}\sin\theta_{CL} - F_{Traction}$$

$$\sum F_Z = -F_{Spring} + F_{LZ} + F_{RZ} + F_{GL}\cos\theta_{CL} + F_{GR}\cos\theta_{CR}$$

Right Motor Pinion and Gear

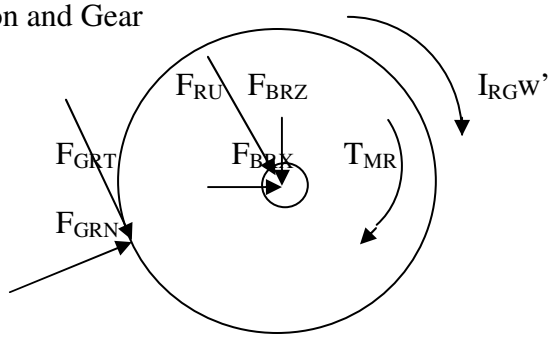

Equations

$$\sum M = F_{GRT} \times r_{PinionGear} + T_{MR}$$
$$\sum F_x = F_{GRT} \cos\theta_{CR} + F_{BRX} + F_{RU} \sin\phi_R$$
$$\sum F_Z = F_{GRT} \sin\theta_{CR} - F_{BRZ} - F_{RU} \cos\phi_R$$

Right Lower Link

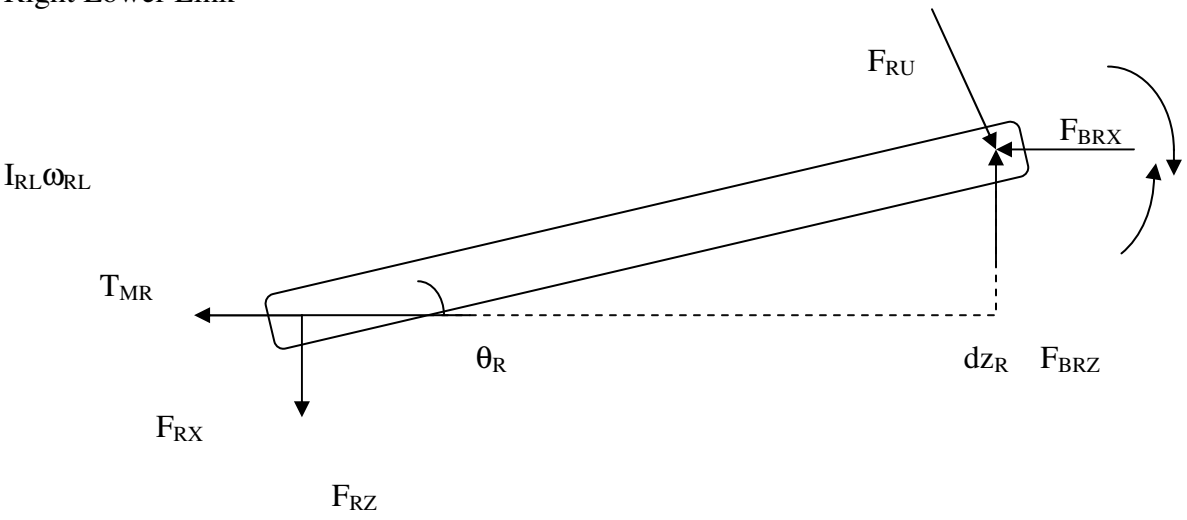

Equations

$$\sum M = F_{RU} L_L - F_{BRX} dz_R - F_{BRZ} dx_R - T_{MR}$$
$$\sum F_x = F_{RU} \sin\phi_R - F_{RX} - F_{BRX}$$
$$\sum F_Z = F_{BRZ} - F_{RU} \cos\phi_R - F_{RZ}$$

Left Motor Pinion and Gear

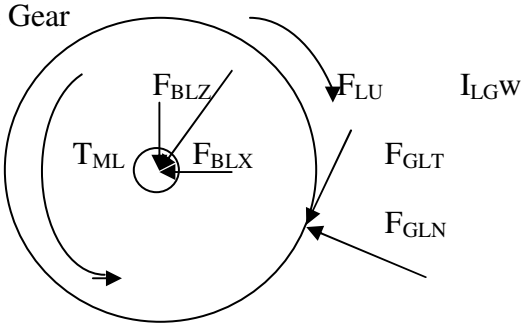

Equations

$$\sum M = F_{GLT} \times r_{PinionGear} - T_{ML}$$

$$\sum F_x = -F_{GLT} \cos\theta_{CL} - F_{BLX} - F_{LU} \sin\phi_L$$

$$\sum F_Z = F_{GLT} \sin\theta_{CL} - F_{BLZ} - F_{LU} \cos\phi_L$$

Left Lower Link

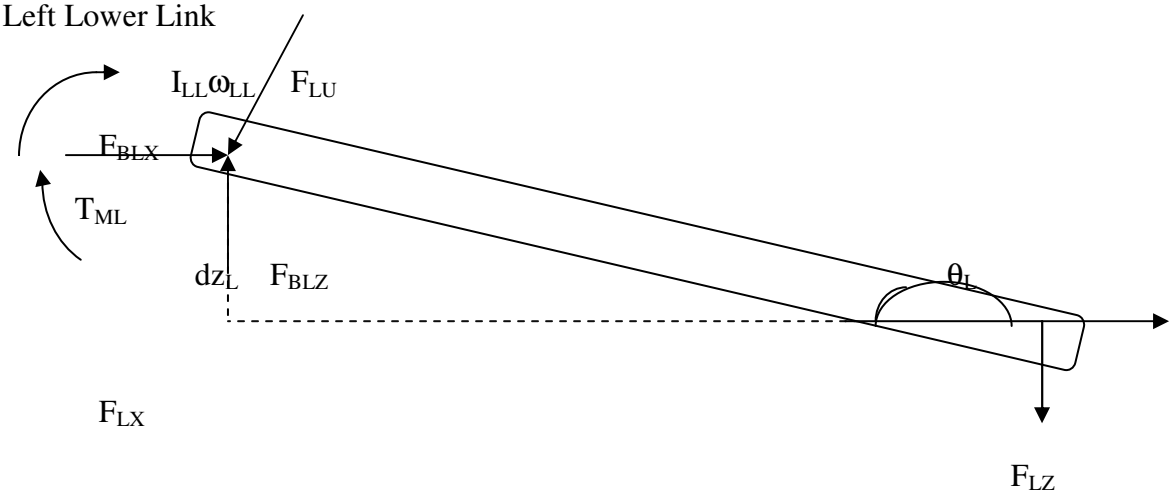

Equations

$$\sum M = F_{BLX} dz_L + F_{BLZ} dx_L + T_{ML} - F_{LU} L_L$$

$$\sum F_x = F_{LX} + F_{BLX} - F_{LU} \sin\phi_L$$

$$\sum F_Z = F_{BLZ} - F_{LU} \cos\phi_L - F_{LZ}$$

$$\sum F_X = F_{Slider} + F_{LU}\sin\phi_L - F_{RU}\sin\phi_R$$

$$\sum F_Z = m_V a_Z = F_S - \frac{W}{4} + F_{LU}\cos\phi_L + F_{RU}\cos\phi_R$$

$$= kz + F_{LU}\cos\phi_L + F_{RU}\cos\phi_R$$

$$\sum M_o = F_{Traction}\times r_{tire} + \left(F_{GLT} - F_{GRT}\right) r_{Gear}$$

$$\sum M = F_{GRT}\times r_{PinionGear} + T_{MR}$$

$$\sum F_x = F_{GRT}\cos\theta_{CR} + F_{BRX} + F_{RU}\sin\phi_R$$

$$\sum F_Z = F_{GRT}\sin\theta_{CR} - F_{BRZ} - F_{RU}\cos\phi_R$$

$$\sum M = F_{RU}L_L - F_{BRX}dz_R - F_{BRZ}dx_R - T_{MR} \quad \sum F_x = F_{RU}\sin\phi_R - F_{RX} - F_{BRX}$$

$$\sum F_Z = F_{BRZ} - F_{RU}\cos\phi_R - F_{RZ}$$

$$\sum M = F_{GLT}\times r_{PinionGear} - T_{ML}$$

$$\sum F_x = -F_{GLT}\cos\theta_{CL} - F_{BLX} - F_{LU}\sin\phi_L$$

$$\sum F_Z = F_{GLT}\sin\theta_{CL} - F_{BLZ} - F_{LU}\cos\phi_L$$

$$\sum M = F_{BLX}dz_L + F_{BLZ}dx_L + T_{ML} - F_{LU}L_L \quad \sum F_x = F_{LX} + F_{BLX} - F_{LU}\sin\phi_L$$

$$\sum F_Z = F_{BLZ} - F_{LU}\cos\phi_L - F_{LZ}$$

For use when T_{MR} and T_{ML} are the system inputs
Unknowns

F_{Slider}
F_{LU}
F_{RU}
F_{Spring} =kz+w/4
$F_{Traction}$
F_{GLT}
F_{GRT}
F_{BRX}
F_{BRZ}
F_{BLX}
F_{BLZ}
F_{LX}
F_{LZ}
F_{RX}
F_{RZ}
T_{MR}
T_{ML}
17 Unknowns, 2 Inputs, 2 Outputs

$$\begin{bmatrix} 1 & \sin\phi_L & -\sin\phi_R & 0 & 0 & 0 & 0 & 0 & 0 & 0 & 0 & 0 & 0 & 0 & 0 \\ 0 & \cos\phi_L & \cos\phi_R & k & 0 & 0 & 0 & 0 & 0 & 0 & 0 & 0 & 0 & 0 & 0 \\ 0 & 0 & 0 & 0 & r_{Tire} & r_{Gear} & -r_{Gear} & 0 & 0 & 0 & 0 & 0 & 0 & 0 & 0 \\ 0 & 0 & 0 & 0 & 0 & 0 & r_{PG} & 0 & 0 & 0 & 0 & 0 & 0 & 0 & 0 \\ 0 & 0 & \sin\phi_R & 0 & 0 & 0 & \cos\theta_{CR} & 1 & 0 & 0 & 0 & 0 & 0 & 0 & 0 \\ 0 & 0 & -\cos\phi_R & 0 & 0 & 0 & \sin\theta_{CR} & 0 & -1 & 0 & 0 & 0 & 0 & 0 & 0 \\ 0 & 0 & L_L & 0 & 0 & 0 & 0 & -dz_R & -dx_R & 0 & 0 & 0 & 0 & 0 & 0 \\ 0 & 0 & \sin\phi_R & 0 & 0 & 0 & 0 & -1 & 0 & 0 & 0 & 0 & 0 & -1 & 0 \\ 0 & 0 & -\cos\phi_R & 0 & 0 & 0 & 0 & 0 & 1 & 0 & 0 & 0 & 0 & 0 & -1 \\ 0 & 0 & 0 & 0 & 0 & r_{PG} & 0 & 0 & 0 & 0 & 0 & 0 & 0 & 0 & 0 \\ 0 & -\sin\phi_L & 0 & 0 & 0 & -\cos\theta_{CL} & 0 & 0 & 0 & -1 & 0 & 0 & 0 & 0 & 0 \\ 0 & -\cos\phi_L & 0 & 0 & 0 & \sin\theta_{CL} & 0 & 0 & 0 & 0 & -1 & 0 & 0 & 0 & 0 \\ 0 & -L_L & 0 & 0 & 0 & 0 & 0 & 0 & 0 & dz_L & dx_L & 0 & 0 & 0 & 0 \\ 0 & -\sin\phi_L & 0 & 0 & 0 & 0 & 0 & 0 & 0 & 1 & 0 & 1 & 0 & 0 & 0 \\ 0 & -\cos\phi_L & 0 & 0 & 0 & 0 & 0 & 0 & 0 & 0 & 1 & 0 & -1 & 0 & 0 \end{bmatrix} \begin{bmatrix} F_{Slider} \\ F_{LU} \\ F_{RU} \\ Z \\ F_{Traction} \\ F_{GLT} \\ F_{GRT} \\ F_{BRX} \\ F_{BRZ} \\ F_{BLX} \\ F_{BLZ} \\ F_{LX} \\ F_{LZ} \\ F_{RX} \\ F_{RZ} \end{bmatrix} = \begin{bmatrix} 0 \\ 0 \\ 0 \\ -T_{MR} \\ 0 \\ 0 \\ T_{MR} \\ 0 \\ 0 \\ T_{ML} \\ 0 \\ 0 \\ -T_{ML} \\ 0 \\ 0 \end{bmatrix}$$

For use when Z and $F_{Traction}$ are the inputs

$$\begin{bmatrix} 1 & \sin\phi_L & -\sin\phi_R & 0 & 0 & 0 & 0 & 0 & 0 & 0 & 0 & 0 & 0 & 0 & 0 \\ 0 & -\frac{\cos\phi_L}{k} & -\frac{\cos\phi_R}{k} & 0 & 0 & 0 & 0 & 0 & 0 & 0 & 0 & 0 & 0 & 0 & 0 \\ 0 & 0 & 0 & 0 & 0 & \frac{r_{Gear}}{r_{Tire}} & \frac{-r_{Gear}}{r_{Tire}} & 0 & 0 & 0 & 0 & 0 & 0 & 0 & 0 \\ 0 & 0 & 0 & 1 & 0 & 0 & r_{PG} & 0 & 0 & 0 & 0 & 0 & 0 & 0 & 0 \\ 0 & 0 & \sin\phi_R & 0 & 0 & 0 & \cos\theta_{CR} & 1 & 0 & 0 & 0 & 0 & 0 & 0 & 0 \\ 0 & 0 & -\cos\phi_R & 0 & 0 & 0 & \sin\theta_{CR} & 0 & -1 & 0 & 0 & 0 & 0 & 0 & 0 \\ 0 & 0 & L_L & -1 & 0 & 0 & 0 & -dz_R & -dx_R & 0 & 0 & 0 & 0 & 0 & 0 \\ 0 & 0 & \sin\phi_R & 0 & 0 & 0 & 0 & -1 & 0 & 0 & 0 & 0 & 0 & -1 & 0 \\ 0 & 0 & -\cos\phi_R & 0 & 0 & 0 & 0 & 0 & 1 & 0 & 0 & 0 & 0 & 0 & -1 \\ 0 & 0 & 0 & 0 & -1 & r_{PG} & 0 & 0 & 0 & 0 & 0 & 0 & 0 & 0 & 0 \\ 0 & -\sin\phi_L & 0 & 0 & 0 & -\cos\theta_{CL} & 0 & 0 & 0 & -1 & 0 & 0 & 0 & 0 & 0 \\ 0 & -\cos\phi_L & 0 & 0 & 0 & \sin\theta_{CL} & 0 & 0 & 0 & 0 & -1 & 0 & 0 & 0 & 0 \\ 0 & -L_L & 0 & 0 & 1 & 0 & 0 & 0 & 0 & dz_L & dx_L & 0 & 0 & 0 & 0 \\ 0 & -\sin\phi_L & 0 & 0 & 0 & 0 & 0 & 0 & 0 & 1 & 0 & 1 & 0 & 0 & 0 \\ 0 & -\cos\phi_L & 0 & 0 & 0 & 0 & 0 & 0 & 0 & 0 & 1 & 0 & -1 & 0 & 0 \end{bmatrix} \begin{bmatrix} F_{Slider} \\ F_{LU} \\ F_{RU} \\ T_{MR} \\ T_{ML} \\ F_{GLT} \\ F_{GRT} \\ F_{BRX} \\ F_{BRZ} \\ F_{BLX} \\ F_{BLZ} \\ F_{LX} \\ F_{LZ} \\ F_{RX} \\ F_{RZ} \end{bmatrix} = \begin{bmatrix} 0 \\ Z \\ -F_{Traction} \\ 0 \\ 0 \\ 0 \\ 0 \\ 0 \\ 0 \\ 0 \\ 0 \\ 0 \\ 0 \\ 0 \\ 0 \end{bmatrix}$$

References

[1] Adams, H., 1993, "Chassis engineering: chassis design, building, and tuning for high performance handling," The Berkley Publishing Group, New York, New York, .

[2] Gillespie, T.D., 1992, "Fundamentals of Vehicle Dynamics," Society of Automotive Engineers, Warrendale, PA, .

[3] Milliken, W.F., and Milliken, D.L., 1995, "Race Car Vehicle Dynamics," SAE International, Warrendale, PA, .

[4] Milliken, D.L., and Milliken, W.F., 2003, "Companion to Race Car Vehicle Dynamics," SAE International, Warrendale, PA, .

[5] Popp, K., and Schiehlen, W., 1993, "Ground Vehicle Dynamics," Spring-Verlang, Berlin, .

[6] Wong, J.Y., 2001, "Theory of Ground Vehicles," John Wiley & Sons, Inc., New Yory, NY, .

[7] Fischer, D., and Isermann, R., 2004, "Mechatronic Semi-Active and Active Vehicle Suspensions," Control Engineering Practice, **12**(11) pp. 1353-67.

[8] Evangelou, S. A., 2010, "Control of motorcycles by variable geometry rear suspension," 2010 IEEE International Conference on Control Applications (CCA) part of the IEEE Multi-Conference on Systems & Control (MSC), Anonymous IEEE, Piscataway, NJ, USA, pp. 148-54.

[9] Noh, T., Yoo, W., Kim, M., 2006, "Analysis and design of a multi-wheeled vehicle with variable geometry suspension," Sensors, and Command, Control, Communications, and Intelligence (C3I) Technologies for Homeland Security and Homeland Defense V, April 17, 2006 - April 21, Anonymous SPIE, Kissimmee, FL, United states, **6201,** .

[10] Li, R., Chen, W., Yu, M., 2006, "Research on vehicle magneto-rheological suspensions vibration control and test," 2006 IEEE International Conference on Robotics and Biomimetics, ROBIO 2006, December 17, 2006 - December 20, Anonymous Inst. of Elec. and Elec. Eng. Computer Society, Kunming, China, pp. 902-907.

[11] Fang Zi-fan, Deng Zhao-xiang, and Yi, C., 2004, "Study on Control Strategy of Magnetorheological Semi-Active Suspension for Ground Vehicle," Journal of System Simulation, **16**(6) pp. 1139-42.

[12] Sharp, R. S., and Hassan, S. A., 1987, "ON THE PERFORMANCE CAPABILITIES OF ACTIVE AUTOMOBILE SUSPENSION SYSTEMS OF LIMITED BANDWIDTH," Vehicle System Dynamics, **16**(4) pp. 213-225.

[13] Sharp, R. S., and Hassan, S. A., 1987, "PERFORMANCE AND DESIGN CONSIDERATIONS FOR DISSIPATIVE SEMI-ACTIVE SUSPENSION SYSTEMS FOR AUTOMOBILES," Proceedings of the Institution of Mechanical Engineers.Part D, Transport Engineering, **201**pp. 149-153.

[14] Toti, G., and Marinoni, F., 1984, "Design of active suspensions," International Symposium on Automotive Technology and Automation, Anonymous ISATA, Croydon, Surrey, UK, pp. 185-207.

[15] Hrovat, D., 1997, "Survey of Advanced Suspension Developments and Related Optimal Control Applications," Automatica, **33**(10) pp. 1781-817.

[16] Venhovens, P. J. T., 1994, "Optimal Control of Vehicle Suspensions," .

[17] Sharp, R. S., 1998, "Variable Geometry Active Suspension for Cars," Computing & Control Engineering Journal, **9**(5) pp. 217-22.

[18] Watanabe, Y., and Sharp, R. S., 1999, "Mechanical and control design of a variable geometry active suspension system," Advanced Vehicle Control (AVEC) 1998, Anonymous Swets & Zeitlinger, Netherlands, **32,** pp. 217-35.

[19] Appleyard, M., and Wellstead, P. E., 1995, "Active Suspensions: Some Background," IEE Proceedings-Control Theory and Applications, **142**(2) pp. 123-8.

[20] Anonymous "Michelin Active Wheel: 2008 Paris Motor show October 2008 Press Kit," .

[21] Farazandeh, A., and Kazemi, R., 2006, "Fuzzy control for active suspension in ADAMS/car full vehicle," 2006 Chinese Control Conference, Anonymous IEEE, Piscataway, NJ, USA, pp. 6.

[22] Elmadany, M. M., Abduljabbar, Z., and Foda, M., 2003, "Optimal Preview Control of Active Suspensions with Integral Constraint," Journal of Vibration and Control, **9**(12) pp. 1377-400.

[23] Marzbanrad, J., Ahmadi, G., Hojjat, Y., 2002, "Optimal Active Control of Vehicle Suspension System Including Time = Delay and Preview for Rough Roads," Journal of Vibration and Control, **8**(7) pp. 967-991.

[24] Youn, I., and Hac, A., 1993, "Active preview suspension with integral action," Proceedings of the 1993 ASME Winter Annual Meeting, November 28, 1993 - December 3, Anonymous Publ by ASME, New Orleans, LA, USA, **52,** pp. 1-6.

[25] ElMadany, M. M., Al Bassam, B. A., and Fayed, A. A., "Preview Control of Slow-Active Suspension Systems," Journal of Vibration and Control, .

[26] Cech, I., 2000, "Anti-Roll and Active Roll Suspensions," Vehicle System Dynamics: International Journal of Vehicle Mechanics and Mobility, **33**(2) pp. 91.

[27] Rui, L., Weimin, C., Changrong, L., 2010, "Fuzzy Hybrid Control of Vibration Attitude of Full Car Via Magneto-Rheological Suspensions," Chinese Journal of Mechanical Engineering, **23**(1) pp. 72-9.

[28] Li, J., Wu, Y., Yang, Z., 2006, "Suspension Damping Control Strategy for Vehicle Attitude Control System," Jilin Daxue Xuebao (Gongxueban)/Journal of Jilin University (Engineering and Technology Edition), **36**pp. 24-28.

[29] Jiangtao, C., Honghai, L., Ping, L., 2007, "An improved active suspension model for attitude control of electric vehicles," 2007 IEEE International Conference on Mechatronics and Automation, ICMA 2007, August 5, 2007 - August 8, Anonymous Inst. of Elec. and Elec. Eng. Computer Society, Harbin, China, pp. 147-152.

[30] Venhovens, P. J. T., van, d. K., Savkoor, A. R., 1994, "Semi-Active Control of Vibration and Attitude of Vehicles," Vehicle System Dynamics, **23**pp. 522-540.

[31] Venhovens, P. J. T., Van, d. k., and Pacejka, H. B., 1993, "Semi-Active Attitude and Vibration Control," Vehicle System Dynamics, **22**(5-6) pp. 359-381.

[32] Youn, I., Im, J., and Tomizuka, M., 2006, "Level and Attitude Control of the Active Suspension System with Integral and Derivative Action," Vehicle System Dynamics, **44**(9) pp. 659-674.

[33] Zhang, Y., Zhao, L., Cong, H., 2004, "Study on control of vehicle attitude and ride comfort based on full-car model," Fifth World Congress on Intelligent Control and Automation, Anonymous IEEE, Piscataway, NJ, USA, **4,** pp. 3514-19.

[34] Ade, M., Binder, A., and Ove, H. N., 2004, "Modeling the Parallel Powertrain for a Hybrid Electric Vehicle (HEV) of "Hybrid through the Road" Type," Elektrotechnik Und Informationstechnik, **121**(4) pp. 144-9.

[35] Asaei, B., and Habibidoost, M., 2010, "A new energy control strategy for a through the road parallel hybrid electric motorcycle," 2010 IEEE Vehicle Power and Propulsion Conference (VPPC), Anonymous IEEE, Piscataway, NJ, USA, pp. 5.

[36] Young, M., Molen, G. M., Oglesby, D., 2007, "The design and development of a through-the-road parallel diesel electric hybrid," VPPC 2007 - 2007 IEEE Vehicle Power and Propulsion Conference, September 9, 2007 - September 12, Anonymous Inst. of Elec. and Elec. Eng. Computer Society, Arlington, TX, United states, pp. 511-518.

[37] Momoh, O. D., and Omoigui, M. O., 2009, "An overview of hybrid electric vehicle technology," 5th IEEE Vehicle Power and Propulsion Conference, VPPC '09, September 7, 2009 - September 10, Anonymous IEEE Computer Society, Dearborn, MI, United states, pp. 1286-1292.

[38] Zhifu, W., and Chengning, Z., 2009, "Control strategy of energy distribution on hybrid electric vehicle," 2009 Asia-Pacific Power and Energy Engineering Conference, APPEEC 2009, March 27, 2009 - March 31, Anonymous Inst. of Elec. and Elec. Eng. Computer Society, Wuhan, China, pp. Wuhan University; IEEE Power and Energy Society; Chinese Society for Electrical Engineering; Scientific Research Publishing.

[39] Singh, B., and Goyal, D., 2006, "Computer aided design of permanent magnet brushless DC motor for hybrid electric vehicle application," 2006 International Conference on Power Electronics, Drives and Energy Systems, PEDES '06, December 12, 2006 - December 15, Anonymous Inst. of Elec. and Elec. Eng. Computer Society, New Delhi, India, .

[40] Sen, C., and Kar, N. C., 2009, "Battery pack modeling for the analysis of battery management system of a hybrid electric vehicle," 2009 IEEE Vehicle Power and Propulsion Conference (VPPC), Anonymous IEEE, Piscataway, NJ, USA, pp. 207-12.

[41] Williamson, S. S., 2007, "Electric drive train efficiency analysis based on varied energy storage system usage for plug-in hybrid electric vehicle applications," PESC 07 - IEEE 38th Annual Power Electronics Specialists Conference, June 17, 2007 - June 21, Anonymous Institute of Electrical and Electronics Engineers Inc, Orlando, FL, United states, pp. 1515-1520.

[42] Imai, S., Takeda, N., and Horii, Y., 1997, "Total efficiency of a hybrid electric vehicle," Proceedings of Power Conversion Conference - PCC '97, Anonymous IEEE, New York, NY, USA, **2,** pp. 947-50.

[43] Wen, L., Chengning, Z., Zhifu, W., 2010, "Compilation of dynamic efficiency test cycle for motor propulsion system on hybrid electric vehicle," 2010 IEEE International Conference on Intelligent Computing and Intelligent Systems (ICIS 2010), Anonymous IEEE, Piscataway, NJ, USA, **1,** pp. 86-90.

[44] Kim, T., and Yang, J., 2009, "Control of a brushless DC motor/generator in a fuel cell hybrid electric vehicle," IEEE International Symposium on Industrial Electronics, IEEE ISIE 2009, July 5, 2009 - July 8, Anonymous Institute of Electrical and Electronics Engineers Inc, Seoul, Korea, Republic of, pp. 1973-1977.

[45] Kim, D., Hwang, S., and Kim, H., 2008, "Vehicle Stability Enhancement of Four-Wheel-Drive Hybrid Electric Vehicle using Rear Motor Control," IEEE Transactions on Vehicular Technology, **57**(2) pp. 727-735.

[46] Guo, H., Wang, W., Xing, W., 2008, "Design and research on electrical/mechanical hybrid four-redundancy brushless DC motor system," 2008 IEEE Vehicle Power and Propulsion Conference (VPPC), Anonymous IEEE, Piscataway, NJ, USA, pp. 4.

[47] Diego-Ayala, U., Martinez-Gonzalez, P., McGlashan, N., 2008, "The Mechanical Hybrid Vehicle: An Investigation of a Flywheel-Based Vehicular Regenerative Energy Capture System," Proceedings of the Institution of Mechanical Engineers, Part D (Journal of Automobile Engineering), **222**pp. 2087-101.

[48] Jefferson, C. M., 1984, "CONTROL OF POWER TRANSMISSION IN A FLYWHEEL ENERGY STORAGE UNIT." Real Time Control of Electromechanical Systems. Anonymous IERE, London, Engl, pp. 127-132.

[49] Lustenader, E. L., Edelfelt, I. H., Jones, D. W., 1979, "Regenerative flywheel energy storage system," Proceedings of the 14th Intersociety Energy Conversion Engineering Conference, Anonymous IEEE, New York, NY, USA, **I,** pp. 343-51.

[50] Montazeri-Gh, M., and Soleymani, M., 2010, "Investigation of the Energy Regeneration of Active Suspension System in Hybrid Electric Vehicles," IEEE Transactions on Industrial Electronics, **57**(3) pp. 918-925.

[51] Apter, R., and Prathaler, M., 2002, "Regeneration of power in hybrid vehicles," VTC Spring 2002, Anonymous IEEE, Piscataway, NJ, USA, **4,** pp. 2063-9.

[52] Kawamoto, Y., Suda, Y., Inoue, H., 2008, "Electro-Mechanical Suspension System Considering Energy Consumption and Vehicle Manoeuvre," Vehicle System Dynamics, pp. 1053-63.

[53] Ming-Ji Yang, Hong-Lin Jhou, Bin-Yen Ma, 2009, "A Cost-Effective Method of Electric Brake with Energy Regeneration for Electric Vehicles," IEEE Transactions on Industrial Electronics, **56**(6) pp. 2203-12.

[54] Chen, J., Zhu, J., Guo, Y., 2007, "Performance analysis of energy regeneration system of electric vehicle with two wheels under the mode of constant braking torque," 2007 2nd IEEE Conference on Industrial Electronics and Applications, ICIEA 2007, May 23, 2007 - May 25, Anonymous Inst. of Elec. and Elec. Eng. Computer Society, Harbin, China, pp. 891-895.

[55] Eghbali, A. H., and Asaei, B., 2010, "Effects of using ultracapacitors on acceleration and regenerative braking performances in hybrid electric vehicle," 2010 IEEE 72nd Vehicular Technology Conference Fall, VTC2010-Fall, September 6, 2010 - September 9, Anonymous Institute of Electrical and Electronics Engineers Inc, Ottawa, ON, Canada, .

[56] Caceres Delgado, A., Solaque, L., Gutierrez, R., 2010, "Proposal of an energy management architecture applied into a regenerative braking system," 2010 IEEE ANDESCON, Anonymous IEEE, Piscataway, NJ, USA, pp. 6.

[57] Guo, J., Wang, J., and Cao, B., 2009, "Regenerative braking strategy for electric vehicles," 2009 IEEE Intelligent Vehicles Symposium (IV), Anonymous IEEE, Piscataway, NJ, USA, pp. 864-8.

[58] Simpack AG, "Simpack 8904," **8904**.

[59] Faria, L. O., Oden, J. T., Yavari, B., 1992, "Tire Modeling by Finite Elements," Tire Science and Technology, **20**(1) pp. 33-56.

[60] Hall, W., Mottram, J. T., and Jones, R. P., 2004, "Tire Modeling Methodology with the Explicit Finite Element Code LS-DYNA," Tire Science and Technology, **32**(4) pp. 236-261.

[61] Husemann, T., and Wohrmann, M., 2010, "The Impact of Tire Measurement Data on Tire Modeling and Vehicle Dynamics Analysis," Tire Science & Technology, **38**(2) pp. 155-80.

[62] Van Oosten, J. J. M., 2007, "TMPT Tire Modeling in ADAMS," Vehicle System Dynamics, pp. 191-8.

[63] Van Deusen, B. D., 1967, "Analytical techniques for designing riding quality into automotive vehicles," SAE Meeting, Anonymous Society of Automotive Engineers (SAE), New York, NY, United States, pp. 11.

[64] Anonymous 1995, "NiMH and NiCd Battery Management," Microprocessors and Microsystems, **19**(3) pp. 165-74.

[65] Alahmad, M. A., and Hess, H. L., 2008, "Evaluation and Analysis of a New Solid-State Rechargeable Microscale Lithium Battery," IEEE Transactions on Industrial Electronics, **55**(9) pp. 3391-401.

[66] Bei Shao-yi, Long, C., Chen Bai-lin, 2008, "On fuzzy-PID integrated control of automotive electric power steering and semi-active suspension," 2008 Second International Symposium on Intelligent Information Technology Application, Anonymous IEEE, Piscataway, NJ, USA, **1,** pp. 847-51.

[67] Brogan, W.L., 1991, "Modern Control Theory," Prentice-Hall, Inc., .

[68] Buma, S., Kajino, H., Takahashi, T., 2008, "Consideration of a human dynamic characteristic and performance evaluation of an electric active suspension," 2008 IEEE/ASME International Conference on Advanced Intelligent Mechatronics, AIM 2008, August 2, 2008 - August 5, Anonymous Institute of Electrical and Electronics Engineers Inc, Xi'an, China, pp. 1030-1036.

[69] Cameron, D. S., and Kheir, N. A., 1996, "On the modeling of ground vehicle attitude control," Part 3 (of 4), December 11, 1996 - December 13, Anonymous Kobe, Jpn, **3,** pp. 2355-3592.

[70] Cao, J., Liu, H., Li, P., 2007, "A Study of Electric Vehicle Suspension Control System Based on an Improved Half-Vehicle Model," International Journal of Automation and Computing, **4**(3) pp. 236-242.

[71] Carter, R., and Cruden, A., 2008, "Strategies for control of a battery/supercapacitor system in an electric vehicle," 2008 International Symposium on Power Electronics, Electrical Drives, Automation and Motion (SPEEDAM), Anonymous IEEE, Piscataway, NJ, USA, pp. 727-32.

[72] Chan, C. C., Jiang, J. Z., Xia, W., 1996, "A novel wide speed range permanent magnet brushless DC motor drive for electric vehicles," PEDS 95, Anonymous Taylor & Francis, UK, **80,** pp. 235-48.

[73] Chen, Y., and Lu, Z., 2010, "Study on control of an two hub-motor electric vehicle," 2010 International Conference on Information and Automation (ICIA 2010), Anonymous IEEE, Piscataway, NJ, USA, pp. 627-32.

[74] Ching, T. W., and Chan, K. U., 2008, "Soft-switching converter for brushless DC motor drives," 2008 IEEE Vehicle Power and Propulsion Conference (VPPC), Anonymous IEEE, Piscataway, NJ, USA, pp. 5.

[75] Crolla, D. A., Horton, D. N. L., Pitcher, R. H., 1987, "ACTIVE SUSPENSION CONTROL FOR AN OFF-ROAD VEHICLE," Proceedings of the Institution of Mechanical Engineers.Part D, Transport Engineering, **201**pp. 1-10.

[76] El-Demerdash, S., 2004, "Performance tradeoffs in control design for automotive active suspensions," Proceedings of the 3rd IMechE Automobile Division Southern Centre Conference on: Total Vehicle Technology; Finding the Radical, Implementing the Practical, April 26, 2004 - April 27, Anonymous Professional Engineering Publishing, Brighton, United kingdom, pp. 275-285.

[77] Eller, B., Hetet, J. F., Andre, S., 2010, "Electric Vehicle Platform for Drivability Analysis," 2010 8th IEEE International Conference on Control and Automation (ICCA 2010), Anonymous IEEE, Piscataway, NJ, USA, pp. 2251-7.

[78] ElMadany, M. M., and Yigit, A. S., 1993, "Robust Control of Linear Active Suspensions," Transactions of the Canadian Society for Mechanical Engineering, **17**(4) pp. 759-773.

[79] Evers, W. -., Besselink, I., Teerhuis, A., 2009, "Controlling active cabin suspensions in commercial vehicles," 2009 American Control Conference (ACC-09), Anonymous IEEE, Piscataway, NJ, USA, pp. 683-8.

[80] Feriancik, M., and Liska, O., 2010, "Application for battery monitoring," 2010 IEEE 8th International Symposium on Applied Machine Intelligence and Informatics (SAMI 2010), Anonymous IEEE, Piscataway, NJ, USA, pp. 253-4.

[81] Gordon, T. J., 1996, "An integrated strategy for the control of a full vehicle active suspension system," 14th IAVSD Symposium on the Dynamics of Vehicles on Roads and Tracks, Anonymous Swets & Zeitlinger, Netherlands, **25,** pp. 229-42.

[82] Hegel, R., 1973, "VEHICLE ATTITUDE CONTROL METHODS," SAE Preprints, (730166) .

[83] Horton, D. N. L., and Crolla, D. A., 1986, "THEORETICAL ANALYSIS OF A SEMI-ACTIVE SUSPENSION FITTED TO AN OFF-ROAD VEHICLE," Vehicle System Dynamics, **15**(6) pp. 351-374.

[84] Karnopp, D., and Sang-Gyun So, 1998, "Energy Flow in Active Attitude Control Suspensions: A Bond Graph Analysis," Vehicle System Dynamics, **29**(2) pp. 69-81.

[85] Li, G., Wang, H., and Yu, Z., 2009, "New method for estimation modeling of SOC of battery," WCSE 2009, Anonymous IEEE, Piscataway, NJ, USA, **2,** pp. 387-90.

[86] Liberzon, A., Rubinstein, D., and Gutman, P. O., 2001, "Active Suspension for Single Wheel Station of Off-Road Track Vehicle," International Journal of Robust and Nonlinear Control, **11**(10) pp. 977-999.

[87] Malek, K. M., and Hedrick, J. K., 1985, "DECOUPLED ACTIVE SUSPENSION DESIGN FOR IMPROVED AUTOMOTIVE RIDE QUALITY/HANDLING PERFORMANCE," Vehicle System Dynamics, **14**(1-3) pp. 78-81.

[88] Metz, D., and Maddock, J., 1986, "Optimal Ride Height and Pitch Control for Championship Race Cars," Automatica, **22**(5) pp. 509-20.

[89] Michelberger, P., Gaspar, P., Palkovics, L., 1996, "Iterative Design of Active Suspension System," Proceedings of the Mini Conference on Vehicle System Dynamics, Identification and Anomalies, pp. 335-344.

[90] Myung-Jin Chung, 2008, "Development of in-wheel motor system using blushless DC motor of Hall sensor type," 2008 International Conference on Control, Automation and Systems (ICCAS), Anonymous IEEE, Piscataway, NJ, USA, pp. 1508-11.

[91] Nagiri, S., Doi, S., Shoh-no, S., 1992, "Improvement of ride comfort by preview vehicle-suspension system," International Congress and Exposition, Febrary 24, 1992 - Febrary 28, Anonymous Publ by SAE, Detroit, MI, USA, pp. 81-87.

[92] Nelson, J. P., and Bolin, W., 1993, "Basics and advances in battery systems," Proceedings of IEEE Petroleum and Chemical Industry Technical Conference (PCIC '93), Anonymous IEEE, New York, NY, USA, pp. 259-69.

[93] Ogata, K., 1997, "Modern Control Engineering," Prentice-Hall, Inc., .

[94] Poussot, C., Sename, O., Dugard, L., 2008, "Attitude and handling improvements through gain-scheduled suspensions and brakes control," 17th World Congress, International Federation of Automatic Control, IFAC, July 6, 2008 - July 11, Anonymous Elsevier, Seoul, Korea, Republic of, **17,** .

[95] Poussot-Vassal, C., Sename, O., Dugard, L., 2010, "Attitude and Handling Improvements through Gain-Scheduled Suspensions and Brakes Control," .

[96] Raghavan, M., 1991, "Suspension Kinematic Structure for Passive Control of Vehicle Attitude," International Journal of Vehicle Design, **12**(5-6) pp. 525-547.

[97] Rahman, K. M., Patel, N. R., Ward, T. G., 2006, "Application of Direct-Drive Wheel Motor for Fuel Cell Electric and Hybrid Electric Vehicle Propulsion System," IEEE Transactions on Industry Applications, **42**(5) pp. 1185-1192.

[98] Sharp, R. S., 2002, "Wheelbase filtering and automobile suspension tuning for minimizing motions in pitch," Anonymous Professional Engineering Publishing, **216,** pp. 933-946.

[99] Terashima, M., Ashikagi, T., Mizuno, T., 1996, "Novel motors and controllers for high performance electric vehicle with 4 in-wheel motors," 22nd International Conference on Industrial Electronics, Control, and Instrumentation, Anonymous IEEE, New York, NY, USA, **1,** pp. 20-7.

[100] Todd, K. B., and Kulakowski, B. T., 1990, "Handling performance of road vehicles with different active suspensions," Winter Annual Meeting of the American Society of Mechanical Engineers, November 25, 1990 - November 30, Anonymous Publ by ASME, Dallas, TX, USA, **108,** pp. 19-26.

[101] Uygan, I. M. C., Hartavi, A. E., Guvenc, L., 2010, "Propulsion System Design of a Hybrid Electric Vehicle," International Journal of Vehicle Design, **52**(1-4) pp. 96-118.

[102] Vahidi, A., and Eskandarian, A., 2001, "Predictive Time-Delay Control of Vehicle Suspensions," Journal of Vibration and Control, .

[103] Yu, H., and Huang, M., 2008, "Potential energy analysis and limit cycle control for dynamics stability of in-wheel driving electric vehicle," 2008 IEEE Vehicle Power and Propulsion Conference (VPPC), Anonymous IEEE, Piscataway, NJ, USA, pp. 5.

[104] Zhu, X., and Gao, F., 2008, "Simulation and Analysis on Semi-Active Control Technology of Multi-Axle Vehicle Suspension," Nongye Jixie Xuebao/Transactions of the Chinese Society of Agricultural Machinery, **39**(8) pp. 33-37+61.